Quantifying the Effect of Vitamin D Deficiency and Alcohol Exposure on Immune Response to Mycobacterium Infection

A Dissertation

Presented to

the Faculty of the Department of Biomedical Engineering

University of Houston

In Partial Fulfillment

of the Requirements for the Degree

Doctor of Philosophy

in Biomedical Engineering

by

Maya Gough

May 2019

Quantifying the Effect of Vitamin D Deficiency and Alcohol Exposure on Immune Response to Mycobacterium Infection

_____
Maya Gough

Approved:

_____
Chair of the Committee
Dr. Elebeoba E. May, Associate Professor, Department of Biomedical Engineering

Committee Members:

_____
Dr. Edward A. Graviss, Associate Professor, Pathology and Genomic Medicine, Houston Methodist Research Institute

_____
Dr. Ezemenari M. Obasi, Professor, Department of Psychological, Health, & Learning Sciences

_____
Dr. Chandra Mohan, Vice Chair, Hugh Roy and Lillie Cranz Cullen Endowed Professor, Department of Biomedical Engineering

_____
Dr. Yingchun Zhang, Associate Professor, Department of Biomedical Engineering

_____
Dr. Suresh K. Khator, Associate Dean, Cullen College of Engineering

_____
Dr. Metin Akay, Founding Chair, John S. Dunn Cullen Endowed Professor, Department of Biomedical Engineering

Acknowledgements

I would like to thank my family and friends, which supported me through this process. Most of all I would like to thank my mother, brother, and grandmother which never doubted me, they believed I could move mountains and so I did. I would like to thank my lab mates and my mentor Dr.Elebeoba May, without whom all of this would have been impossible. Thanks and gratitude go out to Dr.Edward Graviss and his lab for all their support and guidance. Dr. Metin Akay, has been instrumental at critical points in my career and I am thankful for his continued support throughout the years. I would like to thank our sources of funding, DTRA, UH/HMRI Fellowship, NSF, and UH HEALTH Institute. I would like to thank Dr. Ann Chen for her expertise with linear mixed models. Special thanks go to Dr.Chandra Mohan, Dr. Ezemenari Obasi; and any others that have provided assistance during this incredible experience. I would also like to thank my committee members for their advice and insight.

Quantifying the Effect of Vitamin D Deficiency and Alcohol Exposure on Immune Response to Mycobacterium Infection

An Abstract of

A Dissertation

Presented to

the Faculty of the Department of Biomedical Engineering

University of Houston

In Partial Fulfillment

of the Requirements for the Degree

Doctor of Philosophy

in Biomedical Engineering

by

Maya Gough

May 2019

Abstract

The goal of the May Multiscale Immunobiology Design, Algorithms, & Simulation (MIDAS) Lab is to develop dynamic empirical and simulation-based models of host-pathogen interactions to further our understanding of the mechanisms guiding immunologic response. Previous studies on the role of vitamin D3 and its modulation of host response have shown increased anti-inflammatory cytokines and effector substrates during innate immune response; however, many of these studies investigated only single, often dissimilar, levels of infection[1]–[8]. There is currently not a well-established model of macrophage immune modulation by vitamin D3 and the data regarding the kinetics of this process are scarce. There remains a need for more quantitative data on the dynamic impact of vitamin D3 on host response to infection [3], [5]. The majority of studies collected samples and investigate the host response at a single, usually end-stage, time point versus quantifying vitamin D3's modulation of the host response throughout the study. Furthermore, minimal consideration has been given to the potential immune modulatory effects of the vehicle and biochemical process through which vitamin D3 is delivered [3], [9]. This results in a lack of empirical dynamic data that takes into consideration state of host prior to and during infection/treatment. The objective of our lab's research is to develop in vitro, ex vivo, and in silico models that can capture host state, quantifying and expounding on the mechanistic differences in immunologic response due to host state. The focus of my doctoral research is the investigation of host vitamin D3 deficiency in conjunction with adolescent immune response and alcohol exposure. This research will provide insight into the ramifications of age-related vitamin D3 deficiency and its effect on the outcome of mycobacterium infection, as well as, the combined effects of vitamin D3 deficiency and alcohol exposure on infection outcome. This platform can be expanded upon in the future to aid in the identification of immunomodulator associated therapies to enhance host immune response to TB.

Table of Contents

List of Figures

List of Tables

……..

Chapter 1- Introduction

TB and BCG general background

Tuberculosis (TB), caused by the bacterium *Mycobacterium tuberculosis (Mtb)*, is a global health crisis affecting over 10 million people worldwide and causing over one million deaths per year[1]. *M. tuberculosis* is a highly infectious airborne bacterium which has a myriad of pathogen associated molecular patterns (PAMPs) that can be recognized by macrophage internal and external pattern recognition receptors (PRRs), resulting in the activation of an innate immune response. One of the first responders to *Mtb* respiratory infection are alveolar macrophages, which identify the bacterium as foreign through complement mediated opsonization, mannose receptors, pulmonary surfactant proteins, phosphatidylinositol glycan-linked membrane protein CD14 and many other methods [2], [3]. Bacteria are then phagocytosed by alveolar macrophages and exposed to effector molecules and harmful enzymes within the phagosome[4], [5]. Depending on the effectiveness of the host immune response, bacterium may be cleared following the formation of the phagolysosome, production of antimicrobial proteins, and the subsequent activation of an adaptive response to infection. The alternative outcome is that the bacterium resist elimination, replicate within host cells, eventually causing host cells to burst and allow for further spreading of the infection [5]. Current therapeutic regimens aim to control active disease through the use of antibiotics such as, isoniazid (INH) and rifampin (RIF) [4], [6], [7].

The Bacillus of Calmette and Guerin (BCG) vaccine is an attenuated strain of *Mycobacterium bovis. M. bovis* BCG, which was isolated from virulent *M. bovis* after 239 passage; this is the most widely used TB vaccine in the world [8], [9]. Meta-analysis studies have confirmed that BCG vaccination protects children, providing >80% efficacy against severe forms of TB, such as tuberculous meningitis and miliary TB[10]–[12]. In contrast, evidence for protection against pulmonary TB in adolescents and adults remains contentious as efficacy estimates from clinical trials, observational case control studies and contact studies range from 0 to 80%[13], [14]. We will utilize BCG as an analog for Mtb, which is commonly used as a model organism for the study of *Mtb,* as the bacterium for our experimental protocol [15]. While BCG does not capture all aspects of TB disease, it has been used in other studies to capture multiple features of disease, such as macrophage function and bacterial performance under stress [16], [17]. The genomes of BCG and *M. tuberculosis* exhibit a high degree of homology, sharing 99.9% of their DNA and similar

surface proteins [18], [19]. BCG is typically non harmful to humans when compared to *M. tuberculosis*, it acts pathogenically in mice in a similar behavior to Mtb and shares similar cell structure and metabolic characteristics including a mycolic acid cell wall and relatively low response to antibiotics [20]. We chose to utilize the inbred laboratory strain C57BL/6 mice as our animal model to enable the development of an *in vivo* deficiency model with minute genetic variation in host [18], [21], [22].

Vitamin D3 and immune system/TB

Previous studies dating back over a century have found a positive correlation between vitamin D_3 supplementation and overall health of TB infected patient [4], [23]. Vitamin D_3 has been found to have a profound effect on the production of several key immune regulating cytokines, including tumor necrosis factor alpha (TNF-a), interferon gamma (IFN-g)[24], [25], interleukin-10 [26], as well as interleukin-1b [5], [27], [28]. Vitamin D_3 is thought to reduce the production of proinflammatory cytokines such as TNF-a, IL-6, IL-1b and increase the production of anti-inflammatory cytokines like IL-10. Vitamin D_3 encourages activation of macrophage cells and the formation of multinucleated giant cells, commonly present in TB granulomas [29]. Previous studies, as well as our current study, have found that exposing host cells to vitamin D_3 results in enhanced immune response to infection and greater host cell preservation (Table 1) [4], [5], [24], [26], [29].

Classically, vitamin D_3 is commonly associated with the absorption of calcium and phosphorous, however interest in its non-classical role in immune regulation has become increasingly important, particularly given the high rates of vitamin D_3 deficiency in the adult population [30]–[33]. Macrophages are known to express vitamin D_3 receptors (VDR) and are able to produce the enzyme Cyp27B1 (1α-hydroxylase), which converts 25-hydroxyvitamin D_3 to biologically active 1α,25-dihydroxyvitamin D_3 [31], [34]. The inactive form, 25-hydroxyvitamin D_3, accounts for the majority of vitamin D_3 circulating throughout the host body, though the active form incites a much more acute response. The modulation of the immune response by vitamin D_3, leads to a more effective innate and adaptive response, equipping the host to deal with infection while preserving host cells. While it is known that vitamin D_3 is able to modulate macrophage effector response and influence the production of several chemokines and cytokines, the mechanism through which this modulation occurs is not well understood. Some studies have concluded

that vitamin D_3 can act as a transcription factor, binding to vitamin D response elements (VDRE) on the promoter of the gene of interest, however further immune mechanisms concomitant with VDRE activation have not been extensively investigated.

An effective innate immune response is critical to disease outcome upon infection. Macrophages, specifically alveolar macrophages, are an integral part of the innate response and are an important line of defense in *Mycobacterium* infection. Macrophages are known to express vitamin D_3 receptors (VDR) and are able to produce the enzyme Cyp27B1 (1α-hydroxylase), which converts 25-hydroxyvitamin D_3 to biologically active 1α,25-dihydroxyvitamin D_3 [31], [34]. The inactive form, 25-hydroxyvitamin D_3, accounts for the majority of vitamin D_3 circulating throughout the host body, though the active form incites a much more acute response. Classically, vitamin D_3 is commonly associated with the absorption of calcium and phosphorous, however interest in its non-classical role in immune regulation has become increasingly important, particularly given the high rates of vitamin D_3 deficiency in the adult population [30]–[33]. The modulation of the immune response by vitamin D_3, leads to a more effective innate and adaptive response, equipping the host to deal with infection while preserving host cells. While it is known that vitamin D_3 is able to modulate macrophage effector response and influence the production of several chemokines and cytokines, the mechanism through which this modulation occurs is not well understood. Some studies have concluded that vitamin D_3 can act as a transcription factor, binding to vitamin D response elements (VDRE) on the promoter of the gene of interest, however further immune mechanisms concomitant with VDRE activation have not been extensively investigated.

Vitamin D_3 is a well-accepted immune modulator of several macrophage products and is commonly thought to downregulate proinflammatory cytokines such as IL-12 [35] and TNF- α [36] and upregulate anti-inflammatory cytokines such as IL-10 [32] and antimicrobial peptides like cathelicidin (LL-37) [37] and human beta defensin-4 (DEFB4) [34]. Though LL-37 and DEFB4 production is heavily dependent on vitamin D_3 in humans, in murine that is not the case; while mice do produce a murine cathelicidin called CRAMP it is not regulated by vitamin D_3[38]. IL-12 plays an important part in the development of cell-mediated immune response to intracellular bacterial infections. It is released primarily by antigen-presenting cells and acts as a link between innate and acquired immunological responses by

inducing the differentiation of antigen specific T cells of Th1 phenotype and the release of interferon-γ (IFN-γ) from activated T cells and natural killer (NK) cells [39]. TNF-α is primarily produced by macrophages. TNF-α is induced in response to infection, and is involved in fever, apoptotic cell death, cachexia, and inflammation. TNF-α is critical to the Th1 cell mediated response and its dysregulation can cause serious harm to the host [39]. IL-12 and TNF- α are believed to be down regulated in the presence of vitamin D3, as are most Th1 responses [31]. The primary function of IL-10 is to limit inflammatory response, skewing the host cell to a Th-2 anti-inflammatory response and thus aiding in the preservation of host cells. In addition IL-10 is able to regulate growth and differentiation of immune cells, along with several other functions of immune maturation and regulation, and is thought to be upregulated in the presences of vitamin D_3 [40]–[42].

In addition to cytokine modulation, vitamin D3 is believed to modulate phagocytic products and effectors such as NO (nitric oxide) and H_2O_2 (hydrogen peroxide) [43], which aid in the destruction of the pathogen. H_2O_2 and its metabolic precursor superoxide (O_2^-) are produced by the macrophage and mainly sequestered inside of the *Mtb*-containing phagosome. These reactive oxygen species (ROS) are produced in response to phagocytic stimuli or certain soluble agents, such as lipoarabinomannan (LAM). LAM, a primary virulence factor for mycobacterium, enables the bacteria to infect macrophage cells. It also plays a role in mycobacterium's ability to evade host immune response by preventing apoptosis of host cell, and the fusion of the phago-lysosome [44]. H_2O_2 , along with NO acts inside the phagocyte to break down the consumed intracellular bacteria. NO is a diffusible radical gas produced by the transcription of inducible nitric oxide synthase (iNOS - murine) or NOS2/NOS3 (human), and the subsequent activity of nitric oxide synthase. Reactive nitrogen species (RNS) are generated by nitric oxide synthase (NOS), and these species act as antimicrobials protecting the host against a myriad of pathogens. Previous studies revealed that NO production is elevated in surgically resected tuberculosis infected human lungs, though the effects of this increased production remain unclear [45]. H2O2 and NO are believed to be upregulated in the presence of vitamin D_3 [43], [44].

Alcoholism and immune system and response to Mtb

Malnutrition and alcoholism have long been associated with suboptimal immune function and efficacy. Alcohol has commonly been associated with a detrimentally upregulated inflammatory response. Alcohol disrupts ciliary function in the upper airways, impairs the function of immune cells, and weakens the barrier function of the epithelia in the lower airways [46]. Often, the alcohol-provoked lung damage goes undetected until a secondary challenge, such as a respiratory infection, leads to more severe lung diseases than those seen in nondrinkers. Alcohol consumption does not have to be chronic to have negative health consequences. Previous studies have shown that acute binge drinking, as well as moderate drinking affects the immune system [47]. Both short and long term alcohol usage has been shown to decrease phagocytosis and alveolar macrophages in rats have shown decreased superoxide burst, as well as decrease efficacy of vaccination [48]–[50].

Cytokines, chemokines and their modulation by vitamin D_3 and alcohol exposure.

Vitamin D_3 is a well-accepted immune modulator of several macrophage products and is commonly thought to downregulate proinflammatory cytokines such as IL-12 [35] and TNF- α [36] and upregulate anti-inflammatory cytokines such as IL-10 [32] and antimicrobial peptides like cathelicidin (LL-37) [37] and human beta defensin-4 (DEFB4) [34] (Table 1). In addition to cytokine modulation, vitamin D_3 is believed to modulate phagocytic products and effectors such as NO (nitric oxide) and H_2O_2 (hydrogen peroxide) [43], which aid in the destruction of the pathogen. H_2O_2 , along with NO act inside the phagocyte to break down the consumed intracellular bacteria (Table 1).

Table 1. Common effects of vitamin D_3 deficiency and alcohol exposure.

Cytokines and Effectors	Function	Effect of Vitamin D_3	Effect of Alcohol
NO	a diffusible radical gas produced by the transcription of inducible nitric oxide synthase (iNOS) , this reactive nitrogen species acts as an antimicrobial	Increase[45], [51], [52]	Decrease and Increase[27], [53], [54]
IFN-γ	proinflammatory, macrophage activation [39]	Decrease [24], [25], [55]–[59]	Decrease [60][61]
IL-10	limits inflammatory response, skewing the host cell to a Th-2 anti-inflammatory response [40]–[42].	Decrease and Increase [27], [55], [62]	Decrease and Increase [26][63][59][64] [65]
IL-12p70	inducing the differentiation of antigen-specific T cells of Th1 phenotype and the	Decrease and Increase [27],	Decrease and Increase [27],

Table 1. continued

	release of IFN-γ from activated T cells and NK cells [39]	[31], [55]	[66]
IL-1β	Inflammatory cytokine involved in apoptosis, cell differentiation and proliferation.	Decrease and Increase [55], [62], [67], [68];	Decrease [69]
IL-2	Stimulates and differentiates host cells.	Decrease [55], [70]–[74]	Decrease [75]
IL-4	Involved in cell differentiation and activation.	Increase [55], [76]–[78]	Increase [67]
IL-5	Increases host cell replication and immunoglobulin production.	Increase [77]–[79]	Decrease [80]
IL-6	Fever inducer, participates in energy mobilization, immune regulator that increases production of neutrophils and B cells.	Decrease [55], [62], [81], [82]	Decrease and Increase [69][83]
KC/GRO/CXCL1	Neutrophil chemoattractant.	Increase [55] [84],	Decrease [85]
TNF-α	Induced in response to infection, and is involved in fever, apoptotic cell death, cachexia and inflammation. TNF-α is critical to the Th1 cell-mediated response [39]	Decrease [24], [26], [31], [55], [81]	Decrease [48], [60], [69], [83], [86]
Cytotoxicity	Host cell death measured by lactate dehydrogenase (LDH)	Decrease and Increase [27], [55], [68];	Increase [87]
H2O2	acts inside the phagocyte to break down the consumed intracellular bacteria.	Increase [27], [43], [44]	Increase [27]

Previous studies have revealed that the role of vitamin D_3 and its modulation of host response have shown increased anti-inflammatory cytokines and effector substrates during innate immune response, however many of these studies neglected to investigate common comorbidities associated with malnutrition [5], [16], [24]–[26], [44], [45], [88], [89]. Studies have shown that chronic alcohol exposure interferes with the functions of essential vitamins and nutrients, including folic acid and vitamins D, C, and E but these studies are few and fail to investigate the compounding effect of alcohol exposure, impaired vitamin function, and infection [90]–[93]. Proper controls in our previous study necessitated the use of alcohol as a vehicle control. Previous studies had implied that the effect of alcohol was negligent, but we found the opposite to be true. Our study found that alcohol, even at small concentrations had a noticeable effect on macrophage behavior and cytokine production, resulting in increased H_2O_2, NO, and cytotoxicity, as well as negative correlation between bacterial load and IL-12 production [27].

Pediatric Tuberculosis

Age of the host during initial infection plays an important role in disease outcome. Children represent 10-11% of all TB cases. In 2017, 230,000 children died from TB[1]. In children cell-mediated immunity is incomplete. They are predisposed to an anti-inflammatory response to infection, which puts emphasis on a reduction of pro-inflammatory enzymes and a decrease in acidic bacterial clearance. They rely heavily on underdeveloped innate immune responses. Children depend mostly on impaired innate immunity and maternal antibodies. Their adaptive immunity is skewed to a helper T cell 2 type response, as a way to reduce proinflammatory reactions, decrease an allo-immune response against the mother, and promote tolerance of harmless new antigens (gut flora, food). This puts them at a high risk for intracellular organisms, such as Mtb, which defense against depends on a Th1 response

Previous studies have found that young children experience reduced function in antigen-presenting cells, neutrophils, toll-like receptors (TLRs), and decreased blood complement levels [94]. Children with TB are often asymptomatic in comparison to adults and succumb quickly to disease, making diagnosis and treatment very difficult. They commonly present as false negatives for the most common forms of TB testing, IFN-g release assay, skin and sputum test. For these reasons childhood TB infection is easy to overlook or misdiagnose. It is common practice for young children with TB to be given a treatment plan that is very similar to adults but in a smaller dose. This approach can often be ineffective because a child's immune response can differ so drastically from that of an adult's. Children are much more susceptible to disease and their immune system has a much harder time clearing bacteria; thus those children that survive the infection often enter into a latent state [95]. At a later stage in life, when the immune system is weakened by age, cancer, HIV, or some other occurrence, the disease then reemerges as active TB.

It is well acknowledged that alcohol exposure decreases the efficacy of vitamin D_3 but most studies fail to extend beyond alcohol uses' effects on classical vitamin D_3 functions[90], [91], [93], [96]. Our studies address several of the limitations of previous vitamin D_3 studies. We have developed quantitative in vitro, ex vivo, and in silico models which can capture host state and elucidate mechanistic differences in response due to that health state. Specifically, we have investigated the role of vitamin D_3

modulation on macrophage response to infection and the ramifications of alcohol exposure in conjunction with vitamin D_3 deficiency during the infection process. Our studies have found that the generally accepted supposition of down-regulation of pro-inflammatory and up-regulation of anti-inflammatory in the presence of vitamin D_3 may be an over simplification of the effects of vitamin D_3, rather we observed a modulatory pattern dependent on the level of bacterial infection and vitamin D_3 availability. Our study determined that vitamin D_3's modulation of the immune system is much more complex and protean than originally accepted, notably observing that variations in infection level, host conditioning effected response greatly. Our hope is that this research will provide insight into the ramifications of host vitamin deficiency, alcohol exposure, and other host immune states during mycobacterium infection, and aid in the identification of immunomodulator associated therapies to enhance host immune response to TB.

In chapter 2 we developed our methodology and performed preliminary experimentation to validate that methodology. There we discovered that the modulation of the immune system by vitamin D3 is infection level dependent. We also learned that given a, once considered, negligible amount of ethanol the host cells react strongly to its presence, differentially modulating their response. In chapter 3 we sought to isolate the alcohol response during infection from that of vitamin D3. We also explored the systematic metabolic processing of vitamin D3 and how that would compare to the outcomes of chapter 2. We found that alcohol greatly effected vitamin D3 deficient cell immune modulation and that vitamin D3 sufficient cells that were not conditioned exogenously had the least cytotoxicity and less bacterial load than other conditions. In chapter 4 we expanded our empirical data into a computational model. In the first subsection we modeled the uptake and metabolic use of vitamin D3 and its ability to act as a gene transcription modulator. In the second subsection of chapter 4 we expanded the first subsection and modeled vitamin D3 modulated effector molecule production through NADPH oxidase complex assembly. In the final subsection of chapter 4 we assembled a fully integrated model of vitamin D3 immunomodulation. We combined the previous models of vitamin D3 metabolic processing and gene modulation, as well as its modulation of effector molecule production through the addition of the Salim et.al model [97]. We also added cytokine production and signaling. In chapter 5 we built upon chapter 3 experimentation and moved to a fully in vivo conditioning methodology. Utilizing liquid diet we are able to administer alcohol and incite vitamin D3 deficiency in vivo, concurrently. This allowed for the

examination of a fully systemic response to alcohol and vitamin D3 deficiency, both together and separately. In chapter 6 we have quantified differences in growth between strains of mycobacteria. We were able to develop methodology for the generation of in utero vitamin D3 deficient host cells to better understand the nature of deficiency, immunologic response, and mycobacterium infection in a prepubescent host. In chapter 7 we have discussed the future directions of our work and our major conclusions.

Chapter 2: *In vitro* conditioning of J774 murine macrophage cells with vitamin D3 during M.smegmatis infection results in bacterial load dependent immune modulation

Introduction

Previous studies on the role of vitamin D_3 and its modulation of host response have shown increased anti-inflammatory cytokines and effector substrates during innate immune response, however many of these studies investigated only single, often dissimilar, levels of infection [5], [16], [24]–[26], [44], [88], [89]. There is currently not a well-established *in vitro* model of macrophage immune modulation by vitamin D_3 and the data regarding the kinetics of this process is scarce. Studies have provided a better understanding of the activation potential of vitamin D3 for host cell as well as the cytokine response vitamin D3 is able to induce in the presence of *Mycobacterium* infection. However there remains a need for more quantitative data on the dynamic impact of vitamin D3 on host response to infection [25], [26]. While the immunomodulatory effects of vitamin D3 and its production of cytokines through effector immune cells is generally accepted to be dependent on the presence of infection, prior studies overlooked the possible ramifications that severity of infection could have on vitamin D3's ability to enact response. Additionally the majority of studies collected samples and investigate the host response at a single, usually end-stage, time point versus quantifying vitamin D_3's modulation of the host response throughout the study. Furthermore, minimal consideration has been given to the potential immune modulatory effects of the vehicle and biochemical process through which vitamin D_3 is delivered [26], [34].

The current study addresses several of the limitations of current vitamin D_3 studies and develops an *in vitro Mycobacterium* murine infection model to quantify the role of vitamin D_3 in dynamic modulation of the macrophage response to infection and investigates the possible mechanisms through which immunomodulation occurs. We utilized *Mycobacterium smegmatis*, a less virulent homologue of *Mtb* which is commonly used as a model organism for the study of *Mtb,* as the bacterium for our experimental protocol [15]. While *M.smegmatis* typically is non-pathogenic compared to *M. tuberculosis* or *M. bovis,* it shares similar cell structure and metabolic characteristics including a mycolic acid cell wall and relatively low response to antibiotics[20]. Although typically the virulence of *M. smegmatis* is minimal compared to *Mtb* or *M. bovis* BCG, the infection level used in this study compounded with the use of the J774 cell line resulted in a pathogenic model of infection, with uncontrolled bacterial growth and cell death

in our *in vitro* model. As such, we were able to use this model to investigate the role of vitamin D_3 in modulating host response to mycobacterial infection. Results of the study demonstrate that modulation of immune cell behavior by vitamin D_3 correlated directly to level of infection. We found that the generally accepted supposition of downregulation of IL-12 and upregulation of IL-10 in the presence of vitamin D_3 may be an over simplification of the effects of vitamin D_3, rather we observed a modulatory pattern dependent on the level of bacterial infection and vitamin D_3 availability. In prior studies vitamin D_3 was thought to bias immune response towards Th2 and hinder Th1 response [31]. We have found in our studies that this is not always the case, and that vitamin D_3's modulation of the immune system is much more complex and protean than originally accepted, notably observing that variations in TNF-α production was in response to the level of infection only, irrespective of conditioning with ethanol or vitamin D3. Overall our observations support the hypothesis that vitamin D_3 modulates the production of immunologically relevant cytokines and effector molecules in response to level of *Mycobacterium* infection in a manner that consistently results in increased clearance of bacterial load in cells conditioned with vitamin D_3, as well as decreased host cell cytotoxicity. Our study allows for a broader view of the interconnected effects of vitamin D_3 on immune response. Elucidating the mechanism through which vitamin D_3 is able to dynamically modulate the immune response of host cells will provide insight into the ramifications of host vitamin deficiency during infection, and aid in the identification of vitamin D associated therapies to enhance host immune response to TB. (Table 1)

Materials and Methods

Host cell adherence, vitamin D3 conditioning, and infection

Murine J774A.1 cell line (TIB-67 ATCC) was maintained at 37˚C and 5% CO_2 in DMEM (Dulbecco's Modified Eagle Medium) containing 10% fetal bovine serum, 1% penicillin-streptomycin (pen/strep), and 1% L-glutamine. Cells were passed every 5 days at 1:20 ratio of cells to media into 100 x 20mm treated cell culture plates. J774A.1 cells were dislodged from plate by gentle pipetting and centrifuged at 1500rpm for 10 minutes and then resuspended to a concentration of $5x10^5$ cells/ml in DMEM complete without pen/strep. Cells were distributed to 24-well plates (for colony forming unit

counts and imaging on Olympus CKX41 microscope) and 6-well plates (for sample collection) and incubated for 2 hours to allow adherence.

Bacterial culture

M. smegmatis (gifted from Graviss Lab, Houston Methodist Research Institute, TX) was grown from frozen stock in Middlebrook 7H9 media using Hardy Diagnostics 7H9 dehydrated culture media (C6301), containing 0.2% glycerol, 10% OADC and 0.05% Tween-80. After undergoing one subculture bacteria was grown to late growth phase and used to infect host cells.

Host cell infection and vitamin D_3 conditioning

DMEM complete without pen/strep was prepared containing either (1) 4ng/ml of 1,25-dihydroxyvitamin D_3, (2) an equivalent amount of 1,25-dihydroxyvitamin D_3 solvent, ethanol, or (3) unconditioned media (Figure 1). Molecular biological grade ethanol was used as a control for the vitamin D_3 solvent, to determine any effect ethanol might inadvertently be having on the system. J774A.1 murine were infected at an MOI of 1:10 and 1:100 host cells to bacteria, respectively, achieving the prerequisite high and low infection condition states . Both and high and low infections were performed in duplicate, creating biological replicates. *M. smegmatis* was centrifuged at 1500rpm for 10 minutes and then resuspended to a desired concentration in the DMEM complete media without pen/strep conditioned and non-conditioned media. The supernatant was removed from 6-well and 24-well plates and replaced with conditioned and non-conditioned media containing bacteria. Cells were then incubated at 37˚C and 5% CO_2 for an hour. After infection was complete supernatant was removed and host cells were washed twice with phosphate buffer saline solution (PBS), then conditioned and unconditioned media containing 50µg/ml of gentamicin was added to wells followed by one hour of incubation. After incubation with gentamicin plates were washed with PBS twice and fresh conditioned and non-conditioned DMEM complete was added to appropriate cells. Cells were then incubated for 74 hours, with samples collected at hour 0, 8, 16, 24, 34, 44, 54, 64, and 74 post infection.

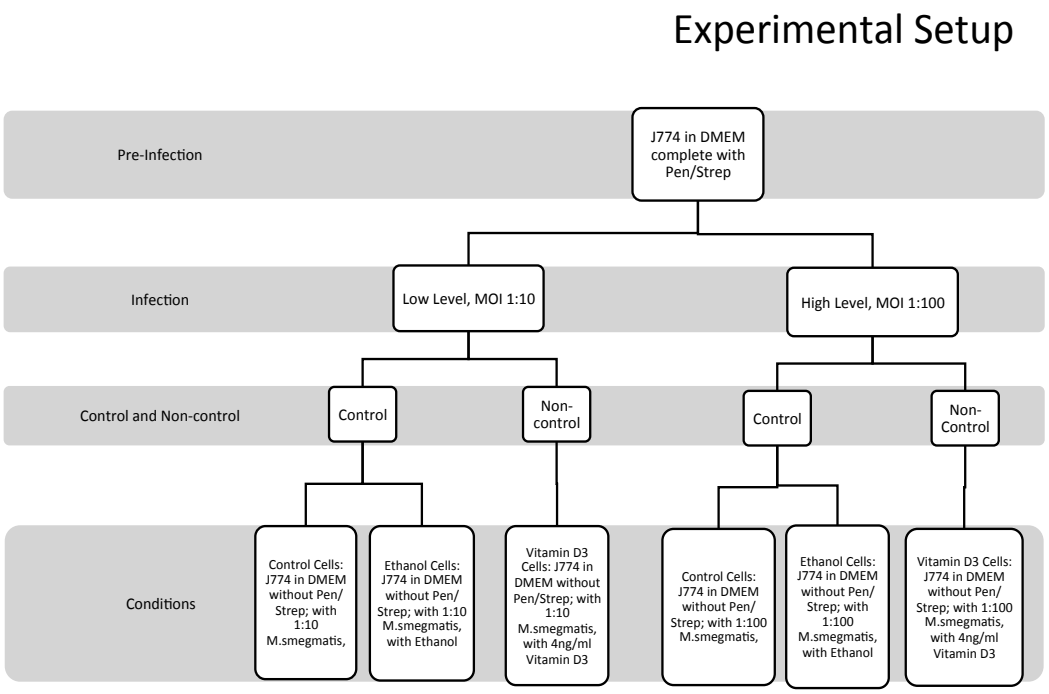

Figure 1. .Experimental Setup.

Sample collection and preparation

At hours 0, 8, 16, 24, 34, 44, 54, 64, and 74 post infection, supernatant from 24-well plate was collected and serially diluted 10-fold. Dilutions were then plated on 7H11 agar plates (C6292, Hardy Diagnostics) to quantify the extracellular bacterial load. After 72 hours incubation, countable colony forming units (CFU) were enumerated to determine extracellular and intracellular bacterial load. It should be noted that at hour 0 extracellular counts were present; this is caused by a delay between incubation of cells with gentamicin and hour 0 sample collection. This delay is due to the time required to process all wells, thus allowing the infection time to progress; hence the hour 0 time point is relative, and represents the first time point sampled and evaluated. Wells were washed once with PBS then incubated with 1% Triton X-100 for 10 minutes, to allow cells to lyse. The lysate was then collected, serially diluted 10-fold, and plated on 7H11 agar plates to quantify intracellular bacterial load. 7H11 plates were counted 3 days after plating the sample to quantify intracellular and extracellular loads. From the 6-well plates we collected supernatant, which was stored in -80˚C and later used for cytokine and reactive species

quantification. After collection of supernatant from 6-well plates, trizol was added to wells. Trizol lysate was collected from from 6 well plates and chloroform extraction for the purification of mRNA (Qiagen, 74104) was performed. Samples were frozen in -80C for short term storage. Purified mRNA samples were further process using iScript cDNA kit (#1708891, Bio-Rad), SYBR green universal mix (#1725275, Bio-Rad), and primers (Bio-Rad) to quantify mRNA.

Assays

Using supernatant collected from the 6-well plates, ELISA assays for TNF-α, IL-10, and IL-12(p70) (BOSTER bio. tech. EK0527, EK0417, EK0422) were performed in accordance with manufacturers instructions with a sensitivity of less than 15 pg/ml. Griess reagent (Promega, G2930) was utilized to quantify NO_2^- concentrations. LDH cytotoxicity assay (Pierce, 88954), performed in accordance with manufacturers instructions, was used to quantify cell death; known concentrations of host cells were lysed and subsequent linear regression applied to assay readings to determine amount of cell death. Hydrogen Peroxide Assay Kit (Abcam, ab102500) was utilized to quantify H_2O_2 concentrations. All assay concentrations values were obtained by averaging duplicate wells.

Statistical Analysis

All statistical analysis was performed using Matlab (MathWorks, R2016b) [98]. Biological replicate trials for high infection and trials for low infection were averaged together. The data for high and low infection conditions were independently normalized using a median normalization scheme (Table 2). To enable comparison of the immune response across experimental conditions (unconditioned control, vitamin D3 conditioned, and ethanol conditioned) the grand median was determined for each assay across all experimental conditions, and used as the common normalization factor [99]. Grand median normalized data was used to perform Welch's *t* test for overlapping time intervals of 0-16, 8-24, 16-34, 24-44, 34-54, 44-64, 54-74 hours to identify variations in immune response between experimental conditions. These sliding intervals allow us to elucidate differences that otherwise may be minimized due to grouping. Pearson correlation analysis was utilized on non-normalized data to calculate correlation coefficients and associated p-values. All p-values were determined to be statistically significant at a value of less than 0.05.

To determine the effect of conditioning on the immune response, the rate of change (velocities) of response were calculated as change in concentration over change in time using non-normalized data. Welch's *t* test and Pearson correlation was used to analyze velocities. Heat maps of grand median normalized assay concentrations were generated using Matlab. For each time period represented in the heat maps, the relative magnitudes of the assays shown were compared to the average value of all assays for that time period and the degree of variation from the average was captured graphically by the heatmap. The heat maps depict higher than average concentrations as red and lower than average values as green, with values falling within the average shaded in black. This pictorial representation of the data provided a visualization-based comparison of the system-scale response for all conditions in the study.

Table 2. Statistical Analysis Chart.

Explanation of the statistical analysis performed on data and which figures utilize that data.

Data Processing	Analysis
Non-normalized Data	Average of trials Pearson Correlation Analysis Rate of change
Rate of Change	Concentration Ratio Analysis Overlapping Interval Welch's t Test Pearson Correlation
Grand Median Normalized Data	Overlapping Interval Welch's t Test/ Concentration Ratio Analysis System Wide Heatmap Analysis

Results

Comparing the temporally changing ratios of vitamin D_3 conditioned cells to control cells suggest vitamin D_3 not only modulates bioavailability but also the potential rate of cytokine and effector molecule production. This variation in the availability and dynamics of immune mediators results consequentially in lower cytotoxicity and higher clearance of intracellular and extracellular bacterial load for vitamin D_3 conditioned cells.

Vitamin D_3 conditioning promotes increased bacterial clearance during low-level infection, intracellular containment during high-level infection, and minimizes host cytotoxicity.

We found that in low-level infection extracellular load and cytotoxicity for vitamin D_3 cells was less than that of control and ethanol conditioned cells (Figure 2). Vitamin D_3 extracellular load ranged from 0.7% to 90% of the control cells, and 0.19% to 78% of ethanol conditioned cells, except at 0-16 and 34-54 hours during which vitamin D_3 loads were greater than that of ethanol. Intracellularly, vitamin D_3 conditioned cells carried a smaller load than control (1.8% to 53% that of control cells) for all intervals except 0-16 hours (110% of control cells) but carried a higher bacterial load than ethanol conditioned cells (105% to 313% of ethanol cells) for all time intervals except 44-64 hours (17% of ethanol cells). Cytotoxicity for vitamin D_3 conditioned cells was less than the control cells and the ethanol conditioned cells throughout, with vitamin D_3 having only 23% to 56% cell death levels of control and 73% to 93% that of ethanol cells. Vitamin D_3 cells cytotoxicity was statistically significantly different from control at several intervals, 0-16, 8-24, 24-44, 34-54, 44-64; (Table 3) and maintained a positive rate of change 0.7 times (0.7x) that of control consistently over time (Table 6). Though vitamin D_3 cells maintained a much larger intracellular load than control and ethanol cells it was able to clear that load more effectively, evidenced by the lower extracellular load, while still keeping a lowered amount of cell death.

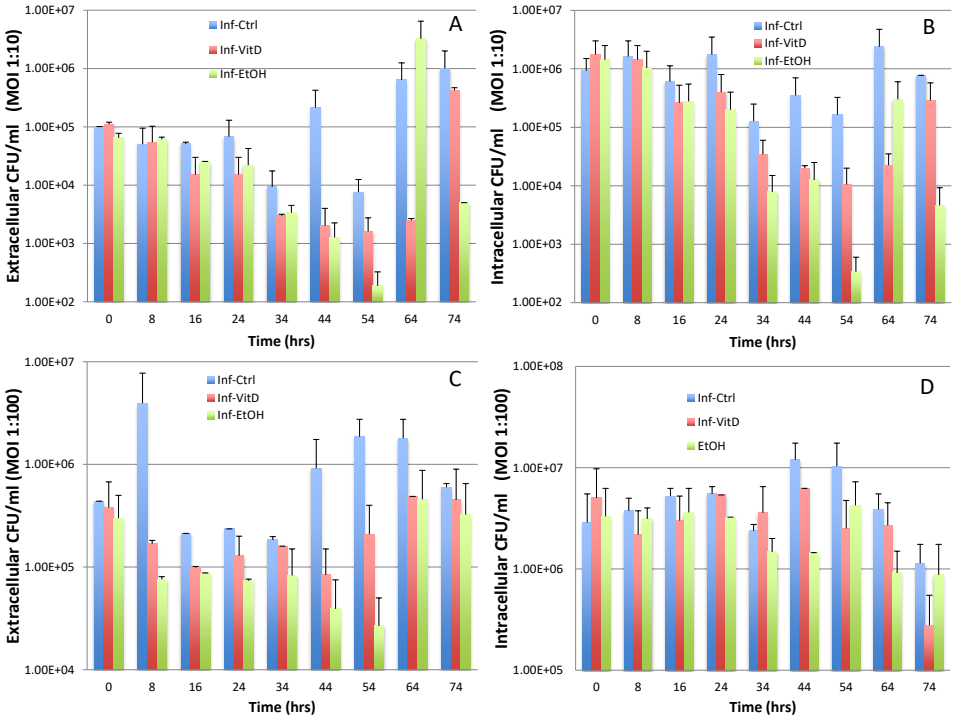

Figure 2. Extracellular and intracellular CFU counts at MOI of 1:10 (A,B) and 1:100 (C,D).

In high-level infection we found that vitamin D_3 cells maintained lower extracellular and intracellular bacterial load than the control but had higher bacterial loads than ethanol conditioned cells (Fig. 2C-D). Extracellular load of vitamin D_3 cells ranged from 9% to 61% that of control but were 140% to 340% that of ethanol. Extracellular load of vitamin D_3 cells were significantly different from control at 16-34, 44-64 hours (Table 3). A similar pattern was seen in the intracellular load carried, in which vitamin D_3 cells were 36% to 91% that of control but 91% to 246% that of ethanol cells. Vitamin D_3 cells had a bacterial load that consistently fell between that of control and ethanol. Vitamin D_3 cells cytotoxicity ranged from 41% to 150% that of control, with only the first two intervals of 0-16, 8-24 hours, falling below 100% (Figure 3). Given that our studies use cell lines, we expect that host cells replicated under all conditions during the 74 hour experiment. However, the significant amount of host cell death experienced early on by control cells during high-level infection would likely result in a significantly reduced quantity of replicating cells and lower cell numbers at later time points in comparison to non-control conditions. The discrepancy in cell numbers may account for cell death in vitamin D_3 and ethanol conditioned cells appearing higher at later time points in comparison to control conditions. This possibility is further

supported by the significant number of viable host cells observed in non-control samples using bright-field microscopy (Figure 3). Due to the high amounts of cytotoxicity experienced by control cells in earlier time points (hour 0-16) there was a resulting decrease in host cells leading to decreased measurement of LDH throughout the rest of the study (hour 24-74) for the control condition, in comparison to other conditions which had a higher quantity of cells. This effect can also be seen when comparing hour 64 to 74 in high level infection, in which high amounts of cytotoxicity at hour 64 resulted in the death of the majority of host cells, leading to a lower amounts of LDH produced at hour 74. Vitamin D_3 cells ranged from 79% to 112% that of ethanol, with vitamin D3 cells having less cytotoxicity than ethanol at the majority of time intervals, except 24-44 and 34-54 hours (Figure 3). This shift resulted due to the large variances in the amount of living host cells present at the given time periods within each condition, evidenced by the significant difference observed between vitamin D_3 conditioned cells and control, as well as control and ethanol conditioned cells at the initial rate of change (Table 6).

Table . 3. Rate of Change Welch's t test Table.

Low		**08-024**	**16-34**	**24-44**	**34-54**	**44-64**	**54-74**
il10_ic.l	il10_id.l					0.018	
il10_ic.l	il10_ie.l		0.050			0.021	
High		**08-024**	**16-34**	**24-44**	**34-54**	**44-64**	**54-74**
ldh_ic.h	ldh_id.h	0.033					
ldh_ic.h	ldh_ie.h	0.039					
High vs. Low		**08-024**	**16-34**	**24-44**	**34-54**	**44-64**	**54-74**
h2o2_id.h	h2o2_id.l		0.031				
il10_ic.h	il10_ic.l		0.029			0.000	
il10_id.h	il10_id.l			0.009	0.006	0.035	
il10_ie.h	il10_ie.l			0.018	0.028		
tnfa_id.h	tnfa_id.l						0.026

Table 4. Welch's t Test.

Conc.1	Conc.2							
Low		**0-16**	**08-024**	**16-34**	**24-44**	**34-54**	**44-64**	**54-74**
h2o2_ic.l	h2o2_ie.l		0.91 *			0.92 *	0.87 *	0.89 *
h2o2_id.l	h2o2_ie.l		0.92 *			0.93 *		0.89 *
il10_ic.l	il10_id.l		3.05 *	2.98 **	2.54 ***	1.98 **		
il10_ic.l	il10_ie.l		3.74 *	3.63 **	2.97 ***	2.37 ***	1.87 **	1.55 *
il12_ic.l	il12_id.l		1.45 **	1.45 **	1.34 *	1.35 *		
il12_id.l	il12_ie.l				0.71 *	0.72 *		
ldh_ic.l	ldh_id.l	4.43 ***	3.82 **		2.46 *	1.97 *	1.89 *	
ldh_ic.l	ldh_ie.l	3.56 ***	3.51 *					
no_ic.l	no_id.l				1.34 *	1.32 *		
High		**0-16**	**08-024**	**16-34**	**24-44**	**34-54**	**44-64**	**54-74**
extra_c.h	extra_d.h			1.63 *			5.87 *	
extra_c.h	extra_e.h			2.58 **			8.73 *	
h2o2_ic.h	h2o2_id.h	0.93 **						
h2o2_ic.h	h2o2_ie.h	0.89 ***	0.89 ***					
h2o2_id.h	h2o2_ie.h	0.95 **						
il10_ic.h	il10_id.h		1.57 *	1.49 *				
il10_ic.h	il10_ie.h		1.58 ***	1.51 *				
il12_ic.h	il12_id.h	0.54 *						
intra_d.h	intra_e.h				2.46 *			
ldh_id.h	ldh_ie.h	0.79 *						
no_ic.h	no_id.h	0.88 **	0.87 **	0.88 **	0.90 **	0.89 **	0.90 **	
no_ic.h	no_ie.h		0.86 *	0.84 ***	0.84 *	0.82 ***	0.82 ***	
no_id.h	no_ie.h					0.92 *	0.91 **	
tnfa_ic.h	tnfa_ie.h		1.16 *	1.19 *	1.14 *			
tnfa_id.h	tnfa_ie.h		1.15 *	1.15 *	1.11 *			
High vs. Low		**0-16**	**08-024**	**16-34**	**24-44**	**34-54**	**44-64**	**54-74**
h2o2_ic.h	h2o2_ic.l	1.10 ***	1.10 ***	1.10 ***	1.10 *	1.12 *	1.16 *	
h2o2_id.h	h2o2_id.l	1.18 ***	1.16 **	1.11 *	1.09 **	1.12 **	1.14 **	
h2o2_ie.h	h2o2_ie.l		1.13 *					
il10_ic.h	il10_ic.l		0.14 *	0.13 **	0.12 ***	0.13 **	0.12 **	0.12 **
il10_id.h	il10_id.l		0.28 *	0.26 *	0.25 *	0.19 *	0.14 *	0.13 **
il10_ie.h	il10_ie.l	0.35 *	0.34 *	0.32 *	0.29 *	0.25 *	0.21 **	0.20 *
il12_ic.h	il12_ic.l	0.51 *	0.48 **					
il12_id.h	il12_id.l					1.46 *		
il12_ie.h	il12_ie.l			0.61 *	0.68 *			
ldh_ic.h	ldh_ic.l	0.37 **	0.22 **		0.11 *	0.11 ***	0.16 **	0.11 *
ldh_id.h	ldh_id.l	0.66 *				0.30 *	0.41 *	0.30 *
ldh_ie.h	ldh_ie.l					0.21 *		0.33 *
no_ic.h	no_ic.l					0.72 *		0.53 *
no_id.h	no_id.l	1.15 **	1.19 **					
no_ie.h	no_ie.l						1.08 *	
tnfa_ic.h	tnfa_ic.l		0.87 ***	0.90 **	0.89 *		0.82 *	
tnfa_id.h	tnfa_id.l		0.86 **	0.87 **	0.87 **	0.85 ***	0.82 **	0.79 **
tnfa_ie.h	tnfa_ie.l		0.75 **	0.75 **	0.78 **	0.80 *	0.79 *	0.75 *

When comparing low and high-level infections we observed a distinct shift in behavior of all cells, most assuredly in vitamin D_3 conditioned cells. During low-level infection vitamin D_3 cells had a much lower extracellular load than both control and ethanol cells, but at high-level of infection vitamin D_3 maintained a lower load than control but a much higher load than ethanol conditioned cells (Figure 2). Intracellularly, at low and high-level infection vitamin D_3 cells carried a lower load than control but a higher load than ethanol (Figure 2). For all intervals in low-level infection and most intervals during high-level of infection vitamin D_3 cells cytotoxicity was lower than that of control and ethanol, with the

exception of the massive cell death experienced during high infection in control which resulted in skewed cell death at later intervals. Vitamin D_3 was able to modify host cell behavior in such a way that host cell death was minimized and bacterial containment intracellularly and subsequent bacterial death was maximized. In the case of low-level infection vitamin D3 is able to perform this task with minimal host cell death, while still clearing the most bacteria extracellularly of all conditions, yet carrying an intracellular load that exceeds that of ethanol and is cleared more quickly than that of control. During high-level of infection this was not the case and, we postulate, to minimize host cell damage and minimize cytotoxicity, infection was allowed to persist at a slightly higher level than that of ethanol conditioned cells but a lower level than that of control for both extracellular and intracellular load.

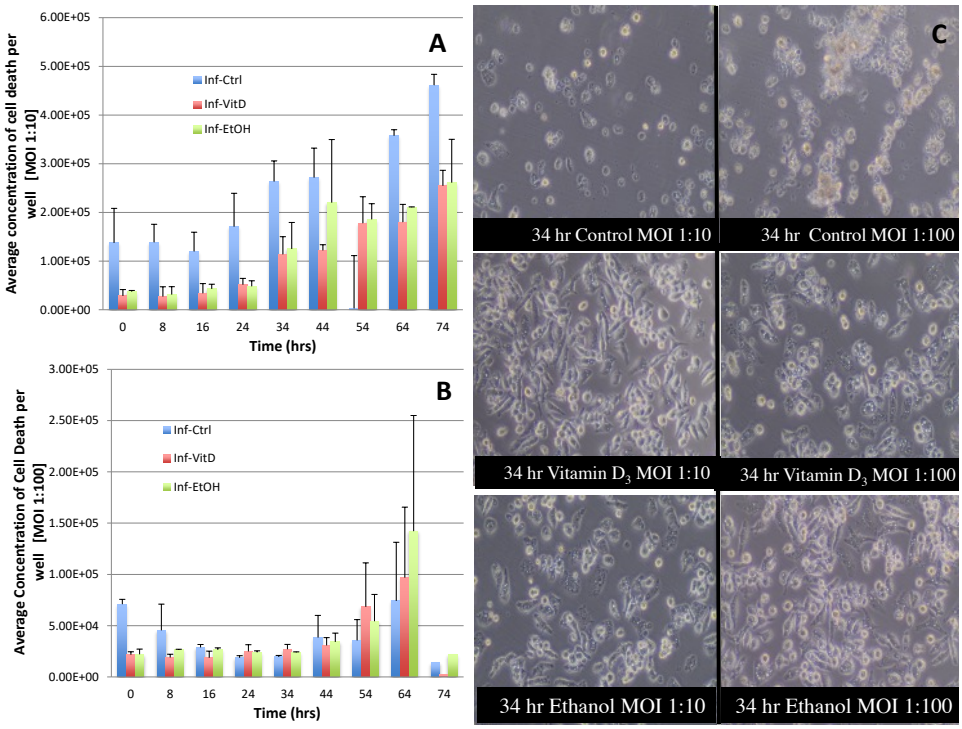

Figure 3. Cytotoxicity determined by LDH production.

<u>Vitamin D_3 differentially modulates host effector molecules based on level of infection</u>

Vitamin D_3 response elements have been found on several genes involved in the production of NO and H_2O_2 though few studies have been conducted quantifying the effect of vitamin D_3 availability on the production of these phagocytic effector molecules.

We found vitamin D_3 cells at low-level of infection had initially high concentrations of NO and low concentrations of H_2O_2 (Figure 4). Vitamin D_3 cells' NO concentrations ranged from 61% to 101% that of control with concentrations consistently decreasing over time and is statistically significant different at time intervals 24-44 and 34-54 hours (Table 3). When comparing vitamin D_3 cells to ethanol, we observed that vitamin D_3 conditioned cells produced less NO throughout, with vitamin D_3 cells production ranging from 89% to 97% that of ethanol conditioned cells. The H_2O_2 concentrations of vitamin D_3 cells were comparable to control, ranging from 100% to 103% that of control during low-level infection. However, compared to the H_2O_2 concentration of ethanol exposed cells, we found that vitamin D_3 cells produced 89% to 95% that of ethanol cells, significantly differing at intervals 8-24, 34-54, 54-74 (Table 3). Vitamin D_3 independent of ethanol produced a decreased amount of H_2O_2 when compared to ethanol conditioned cells, the amount produced was most similar to that of control.

During high-level infection vitamin D_3 conditioned cells maintained higher concentrations of NO than control (Figure 4), producing between 106% to 114% that of control, significantly differing at several intervals, 0-16, 8-24, 16-34, 24-44, 34-54, 44-64 (Table 3). When comparing vitamin D_3 to ethanol conditioned cells we observed that similar to low-level of infection, vitamin D_3 cells produce 91% to 98% the amount of NO produced by ethanol conditioned cells, with the percentage decreasing over time and significantly differing during two intervals, 34-54 and 44-64 hours (Table 2). H_2O_2 production was slightly elevated compared to control, with vitamin D_3 initially producing 107% the concentration of control and decreasing to 100% over time, with significance difference for the interval during 0-16 hours (Table 3). Throughout all time intervals the H_2O_2 concentration of vitamin D_3 cells was lower than that of ethanol exposed cells, ranging between 85% and 95% that of ethanol.

When comparing high and low vitamin D_3 conditioned cells both levels of infection produced their maximum percentage of NO relative to control during the initial time interval following infection (0-16 hrs; Figure 4), after which the concentration decreased over time. In low-level infection vitamin D_3 conditioned cells' NO concentrations never exceeded that of control but in high-level infection vitamin D_3 initially did exceed control but reduced to a concentration lower than control cells at a later interval (Figure 4). Ethanol conditioned cells consistently produced more NO compared to vitamin D_3 and control cells regardless of level of infection (Figure 4). In both low and high-levels of *Mycobacterium* infection, the concentration of

H_2O_2 in vitamin D_3 conditioned cells was nearly equivalent to that of control for most time intervals, exceeding that of control only during a few time periods (Figure 4). During low-level infection vitamin D_3 exceeded control by 3% for one interval (44-64) and in high-level infection it exceeded control from 1-7% for all intervals except 34-54 and 54-74. In low and high-level infections, vitamin $D_3$3 cells consistently produced 10%±5% less H2O2 than that of ethanol conditioned cells. In the case of NO and H_2O_2 production ethanol consistently produced a higher concentration of both when compared to vitamin D_3 and control cells, with vitamin D_3 producing concentrations at times more similar to control cells than that of ethanol cells. Considering the higher levels of reactive species observed for ethanol conditioned cells, conditioning with vitamin D_3 actively reduced the production of NO and H_2O_2 during high-levels of infection. We see this modulation best displayed when vitamin D_3 cells produced greater concentrations of NO than control during high-level infections but much lower concentrations during lower level infection. Our observations suggest that vitamin D_3 differentially modulates H_2O_2 and NO based on bacterial load, by reducing the production of reactive species during low-level infection, irrespective of the ethanol vector, to a level comparable to that of control in the case of H_2O_2 or lower than control in the case of NO. However during high-levels of infection, the presence of vitamin D_3 lead to increased concentrations of H_2O_2 and NO higher than that of control cells but still lower than that of ethanol cells, potentially modulating the level of reactive species to circumvent host cell damage during increased bacterial load.

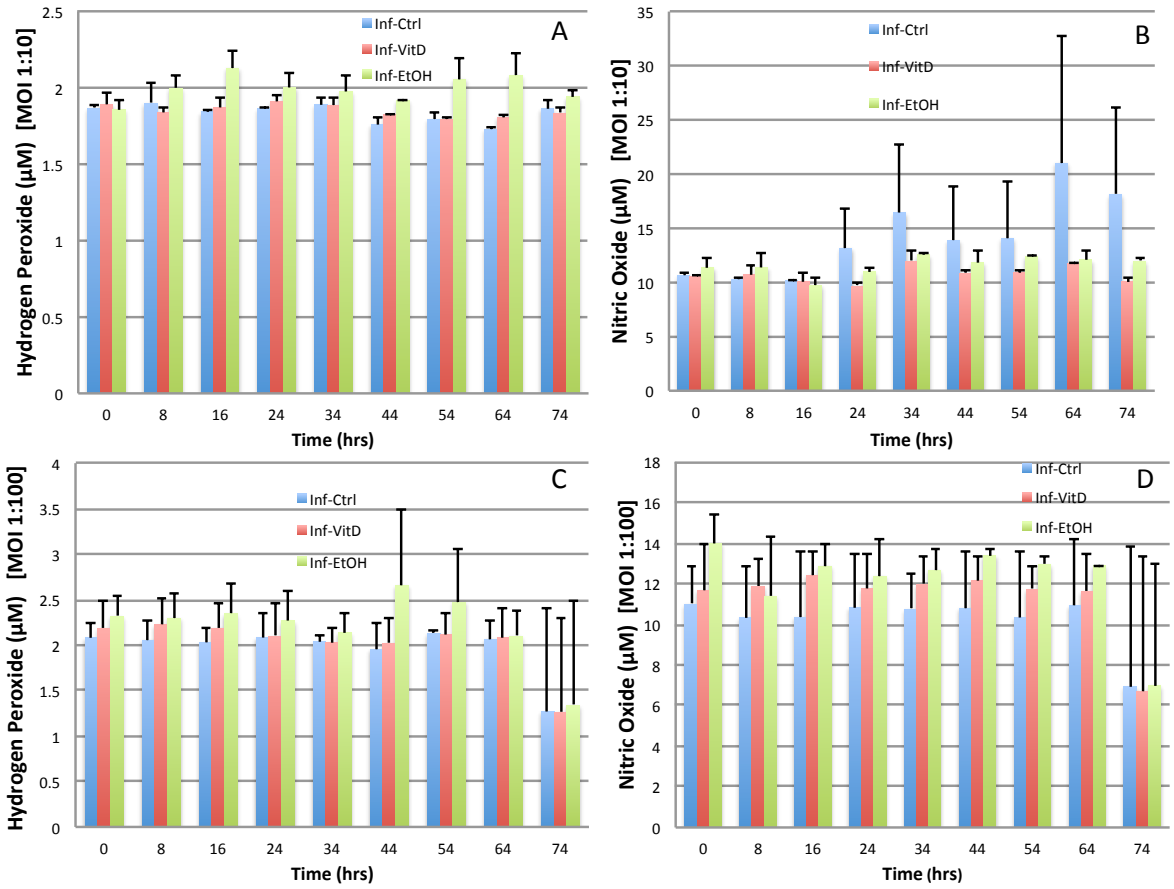

Figure 4. Hydrogen Peroxide and Nitric Oxide production.

Vitamin D_3 modulates pro- and anti-inflammatory cytokines depending on infection level

Prior studies have demonstrated that vitamin D_3 has been able to modulate the production of several cytokines important in host cell defense against intracellular infectious agents. We explored IL-10, IL-12 and TNF- α (Figure 5) due to previously reported observations of vitamin D3's modulatory control over their production [32], [36], [43], [100], [101].

We found that during low-level of infection, compared to control cells, vitamin D_3 conditioned cells maintained 33% to 81% of the concentration of IL-10, with vitamin D_3 increasing consistently over time (Figure 5). Non-conditioned control cells peaked quickly and then maintained relatively the same or minimally increasing IL-10 concentrations. Vitamin D_3 cells and control cells were significantly different at most time intervals, 8-24, 16-34, 24-44, 34-54 (Table 3). Vitamin D_3 conditioned cells produced consistently higher concentrations of IL-10 than ethanol conditioned cells, with vitamin D3 cells ranging

from 119% to 132% that of ethanol and significantly differing at every interval, except the first. The rate of change of IL-10 production was positive in both control and vitamin D_3 cells for time intervals 0-16, 8-24, and 16-34 hours, but in later time intervals the direction of the rate of change for the control cells was negative, differing from vitamin D_3 cells, which continued to maintain positive change, indicating increasing levels of IL-10 (Table 6). Vitamin D_3 cells produced the least amount of IL-12 throughout, in comparison to control (69%-74% that of control) and ethanol (71%-88% that of ethanol; Figure). Vitamin D_3 and control cells were significantly different at intervals 0-24 to 34-54 (Table 3) while vitamin D_3 and ethanol cells were significantly different at intervals 24-44 and 34-54. Vitamin D_3 cells maintained a positive rate of change for IL-12 production throughout, dissimilar from control, which contained two time intervals with a negative rate of change ranging from 0.15x to 1.46x (24-44, 54-74; Figure 5; Table 6). TNF-α concentrations for vitamin D_3 conditioned cells and control were the same (100%) at all intervals except 0-16 in which vitamin D3 was only 93% that of control, during low infection level. A similar pattern with TNF-α production was seen when comparing vitamin D_3 and ethanol cells, with the concentration of vitamin D_3 ranging between 98% and 102% that of ethanol. We observed a slight increased concentration of TNF-α (102%) when comparing vitamin D_3 and ethanol cells during the last two time intervals (Figure 5).

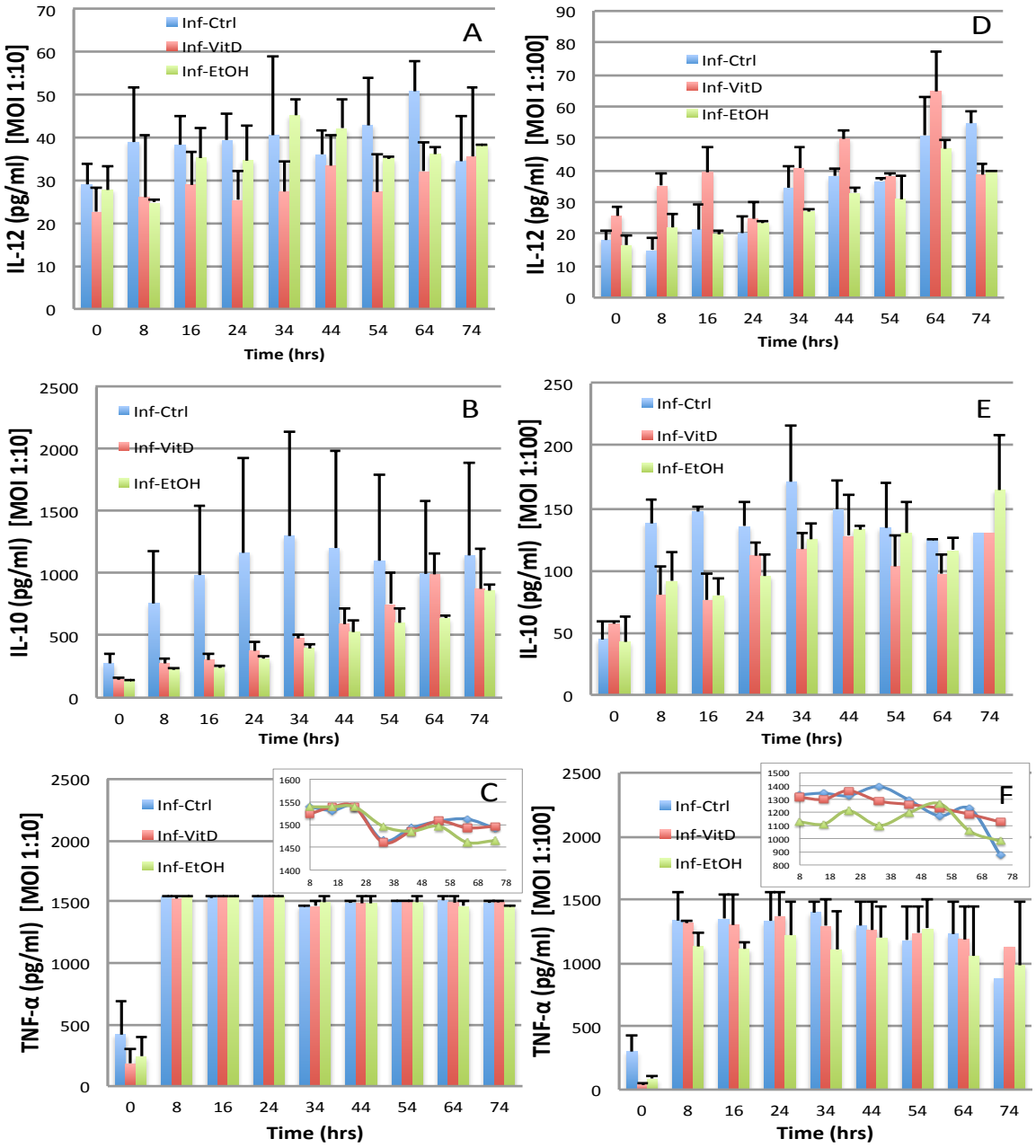

Figure 5. Cytokine ELISA Assays. At low-level of infection vitamin D_3 cells concentration of IL-12

During high-levels of infection vitamin D_3 cells produced higher concentrations of IL-10, though still comparatively lower than the control cells, with vitamin D_3 cells maintaining 64% to 84% IL-10 concentration than that of control cells and significantly different from control cells at two intervals 8-24, 16-34 (Figure 5). In comparison to ethanol cells, vitamin D_3 cells produced comparable levels of IL-10 for the intervals 0-16, 8-24, 16-34, 24-44 (Figure 5). However following the 24-44 hour interval IL-10 levels

were consistently reduced over time in vitamin D_3 conditioned cells down to 80% the level in ethanol conditioned cells. Vitamin D_3 cells maintained a positive rate of change during a majority of time intervals, differing from control cells, which was positive only during the first two intervals (Table 6). The magnitude of the rate of change in IL-10 concentration for vitamin D_3 ranged from 0.13x up to 36x the rate of change of control (Table 6). Converse of what was observed during low infection levels, vitamin D_3 produced the highest concentration of IL-12 throughout all time intervals and across all conditions (Figure 4). Vitamin D_3 cells had an initial value 185% that of control cells, with its minimum value equivalent to control cells during the last time interval, 54-74 hrs. Vitamin D_3 conditioned cells showed a consistently decreasing IL-12 concentration over time while concurrently increasing IL-10, a known inhibitor of IL-12 (Figure 5). Vitamin D_3 conditioned cells IL-12 concentration was significantly different from control cells at 0-16 hour interval (Table 3) during high-level infection. The response of vitamin D_3 cells compared to ethanol indicates the cells produced 172% to 121% the level of IL-12 observed in ethanol conditioned cells. Ethanol conditioning resulted initially in higher concentrations of IL-12 than in control and this immunologic behavior reversed at later intervals, but always producing less than vitamin D_3 conditioned cells. During high-level infection TNF-α production in vitamin D_3 conditioned cells ranged from 89% to 108% compared to control cells, with vitamin D_3 exceeding that of control during the final interval, 54-74 hrs (Figure 5). Compared to ethanol cells, vitamin D_3 cells produced higher concentrations of TNF-α ranging from 104% to 115% that of ethanol cells. Vitamin D_3 cells reduced their TNF-α concentration over time except at time intervals 8-24 and 54-74 hrs. Vitamin D3 TNF-α concentrations were significantly different from ethanol at intervals 8-24, 16-34, and 24-44 hrs (Table 3).

Vitamin D_3 availability as well as the level of infection greatly affected cytokine production. Comparing low and high-levels of infection we observed that IL-10 production in vitamin D_3 conditioned cells was at a concentration level more comparable to control cells during high-levels of infection. In low-levels of infection vitamin D_3 conditioning resulted in concentrations of IL-10 that are consistently higher than that of ethanol conditioned cells (Figure 5). However for high-level infection the cells produced IL-10 at equivalent concentrations as that of ethanol conditioned cells during the early post infection time frames, lowering IL-10 production to below that of ethanol conditioned cells at later time intervals (Figure 5). The

modulation of IL-10 during low-level infection and the temporal variation during high-level infection, indicates a vitamin D3 and infection level dependent IL-10 response that was not observed for either control or ethanol conditioned cells. This variation in IL-10 production results in significantly different rates of change between high and low-level infected cells conditioned with vitamin D_3 between 24-64 hours (Table 7) . IL-12 concentration was lowest in vitamin D_3 conditioned cells during low-level infection, but was highest in vitamin D_3 conditioned cells during high-level infection (Figure 5A,D). In low and high-level infection vitamin D_3 cells were consistently increasing their concentration of IL-12 over time. In comparison to the immunologic responses of control and ethanol conditioned cells, it appears that vitamin D_3 at low-level infection maintains an oscillatory range from the median ratio of 10-20% in ethanol and 0-5% in control; while comparably coming closer to the concentration of control and ethanol as time progresses in the high-level infection. Vitamin D_3 cells production of TNF-α in low-level infection is very similar to that of control and ethanol cells but in high-level infection we observed a marked difference (Figure. 5B,F). At all intervals during high-level infection, with the exception of the last two time periods, vitamin D_3 conditioned cells produced less TNF-α than control cells; vitamin D_3 conditioned cells produced 4-15% more TNF-α than ethanol conditioned cells during all time intervals. From these results we concluded that vitamin D_3 is able to variably modulate the cytokines IL-10, IL-12, and TNF-α in an infection dependent manner increasing IL-10 and reducing IL-12 during low-level infection, and during high-level infection greatly increasing IL-12 and decreasing IL-10 levels while maintaining an intermediate TNF-α level distinct from control and ethanol conditions.

Correlations between host responses differ based on conditioning and level of infection

Using correlational analysis we evaluated to what degree bacterial load, effector molecules, and cytokines correlated with level of infection and cell conditioning. We found that TNF-α and IL-10 positively correlated for control, vitamin D_3, and ethanol cells, irrelevant of level of infection with a correlation coefficient of 1 ($p<0.05$; Table 3). For low-level infection in control conditions, extracellular bacterial load was positively correlated with LDH and NO (corr coeff: 0.708, 0.839; $p<0.05$; Table 3). We also found in low-level infection of vitamin D_3 (corr coeff: -0.714, -0.714) and ethanol conditioned cells

(corr coeff: -0.750, -0.750) intracellular load and IL-10 negatively correlated, as well as intracellular load and TNF-α ($p<0.05$; Table 5).

At high-level of infection across all conditions H2O2 and NO positively correlated (corr coeff: 0.882 to 0.959). Vitamin D_3 conditioned cells at high (corr coeff: 0.705) and low (corr coeff: 0.761) level infection had a positive correlation between LDH and IL-12 production, this was also true of high-level infected ethanol (corr coeff: 0.716) cells but not for low-level infected ethanol cells. Ethanol conditioned cells at high (corr coeff: -0.722) and low-level (corr coeff: -0.834) of infection had a negative correlation between intracellular load and IL-12 production, however this correlation was not observed in vitamin D_3 conditioned cells during low nor high-levels of infection. We examined the correlations between gene expression and molecule concentration. We found that in in low level infection across all conditions IL-10 positively correlated to NOS2, but if high infection only ethanol conditioned cells maintained the positive correlation. In this case vitamin D3 regulated the correlation disrupting the connection between IL-10 and NOS2. In high level infection vitamin D3 conditioned cells only, positively correlated VDR to NCF1 but in low level infection ethanol conditioned cells have a negative correlation while all others have no significant correlation. Vitamin D3 conditioned cells NOS2 gene expression positively correlated with LDH for high level infection but for control at high level infection the correlation was negative, and at low level infction ethanol conditioned cells had a positive correlation. This further supports ethanol's ability to dysregulate the immune response and the relationship between cytotoxicity and NO. In vitamin D3 conditioned cells cyp27b1 positively correlates with NOS2 in high level infection, indicative of increasing activity of NO and vitamin D3 at a higher infection burden (Table 8).

To determine how vitamin D_3 may impact the relative dynamics of host response to *Mycobacterium* infection, we evaluated the correlation between the rate of change of bacterial load, effectors, and cytokines given conditioning and infection level (Table 6 contains rate of change ratios and Table 8 displays statistically significant correlations). We found more correlations between the rates of change during high-level of infection when compared to low, this may be due to the cells enacting a more synergistic response during more severe infections. Vitamin D_3 (corr coeff: -0.786; Table 4)and ethanol (corr coeff: -0.783; Table 4) conditioned cells had a shared rate of change negative correlation in common

between the extracellular bacterial load and IL-10 during low-level infection, which may be indicative of an ethanol and infection level dependent correlation. The rate of change for H_2O_2 and LDH (corr coeff: 0.92; Table 4) and IL12 and NO (corr coeff: 0.712; Table 8), were positively correlated and occurred only for vitamin D_3 conditioned cells under high-level infection. The vitamin D_3 cells and control cells under high-level infection both exhibited positively correlated rate of change values for H_2O_2/NO (corr coeff: 0.946, 0.892; Table 4) and NO/LDH (corr coeff: 0.816, 0.785; Table 4), but not ethanol conditioned cells.

Table 5. Pearson Correlation.

		Control		Vitamin D3		Ethanol	
		Low	High	Low	High	Low	High
H2O2	NO		+		+		+
INTRA	IL-10			-		-	
TNF-a	IL-10	+	+	+	+	+	+
IL-12	LDH			+	+		+
EXTRA	LDH	+					
EXTRA	NO	+					
LDH	NO	+					
INTRA	IL-12					-	-
INTRA	TNF-a			-		-	

We used a heatmap for time-point based comparison of condition-specific system wide response during low and high-level infection (Figure. 6A,B). Results of the system-wide heatmap analysis indicate that TNF-α was comparatively high across all conditions and levels of infection, with vitamin D_3 conditioned cells consistently having the lowest amount of TNF-α at time 0 and control cells having the highest (Figure. 6A,B). When comparing high infection versus low infection IL-10 concentrations using the heatmap we observed that low-level infection produced much higher concentrations of IL-10 than high-level infection across all conditions. During low-level infections control cells produced the highest amounts of IL-10 and ethanol cells produced the lowest. IL-12 concentrations in low-level infection are decreased when compared to high-level infection. Additionally vitamin D_3 cells during high-level infection produced large amounts of IL-12 in comparison to the production of other cytokines or effectors in general. H_2O_2 and NO production during both high and low infection levels achieved their relative maximum at

time 0 for all conditions and steadily decreased over time. This pattern held for all conditions and in general for both levels of infection, although comparatively the high-level of infection resulted in relatively higher amounts of H_2O_2 and NO. LDH production during high-level infection is lower than in low-level infection, however this may be due to initial host cell death.

Table 6. Rate of Change Pearson Correlations Table.

		Control		Vitamin D3		Ethanol	
		Low	High	Low	High	Low	High
EXTRA	IL-10			-		-	-
H2O2	NO		+		+		
H2O2	LDH				+		
TNF-a	IL-10	+	+				
NO	IL-10						-
IL-12	LDH						+
IL-12	NO				+		
NO	LDH		+		+		

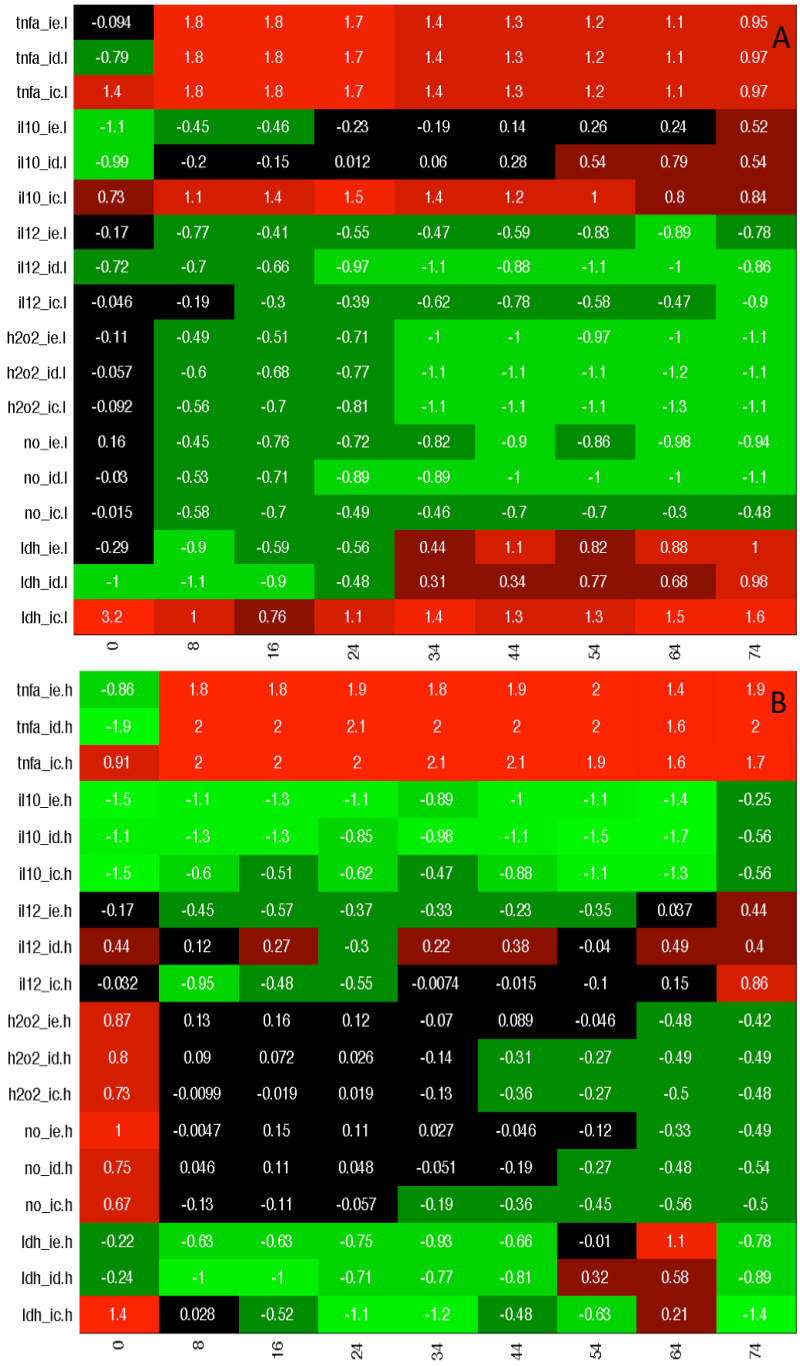

Figure 6. System wide heatmap analysis.

<u>Vitamin D3 conditioning differentially modulates gene transcription</u>

Previous studies have theorized that vitamin D3's primary modulatory mechanism is its ability to act as a transcription factor. Here we have explored the regulation of four genes of interest. We chose two vitamin D3 relevant genes (VDR, CYP27B1) and two effector molecule (NOS2, NCF1) relevant genes, all

of which have been shown to be regulated by the vitamin D response element in their promoter region. We observed a difference in gene regulation based on infection level and host cell conditioning.

VDR (vitamin D receptor) gene expression in low infection was upregulated in vitamin D3 conditioned cells at early and later time points (0, 8, 74h) as opposed to control and ethanol (except at 0h). Ethanol conditioned cells down regulated gene expression of VDR at all time points except 0h. Control cells upregulated VDR gene expression at middle time points (44, 64h) in low level infection (Figure 7, Table 7-8). In a high level infection ethanol conditioned cells had the largest increase in gene expression of VDR across all conditions and time points, followed by a down regulation of VDR expression at all other time points. Control conditioned cells upregulated (0, 24, 34h) and downregulated expression of VDR gene but vitamin D3 conditioned cells upregulated VDR gene expression throughout all time points measured (0, 8, 34, 44h).

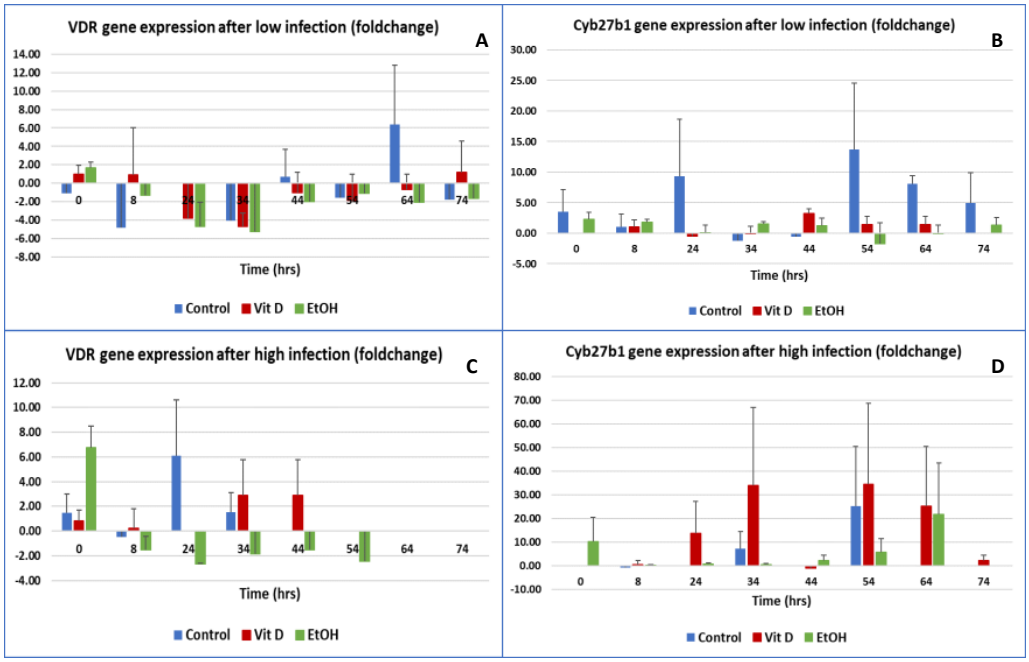

Figure 7. Vitamin D relevant gene foldchange over time.

Cyp27b1, the enzyme which converts inactive vitamin D3 to active, gene expression in low infection was upregulated the highest in control condition cells. Vitamin D3 conditioned cells upregulate gene expression between 1.08-3.22 fold change, whereas control cells upregulated expression to a range of

1.04-13.68 at time points measured. At several time points cyp27b1 expression in low infection, vitamin D3 conditioned cells appeared to increase gene expression above that of ethanol conditioned cells but maintained a level below that of control. In the high level infection vitamin D3 conditioned cells upregulate cyp27b1 gene expression above that of all other conditions ranging from 2.32 to 34.13. At high level infection cyp27b1 is preferentially upregulated by all conditions, with vitamin D3 and control conditioned cells downregulating expression at only a single time point, 8h (-0.61) and 44h (-0.93), respectively. This differs slightly from low level infection expression of cyp27b1 in which vitamin D (24h, 34h, -0.52 to -0.06) , control (34h, 44h, -1.29 to -0.55), and ethanol (54h, 64h, -1.73 to -0.01) conditioned cells downregulate expression at a larger magnitude and for more time points. At low level infection down regulation of cyp27b1 appears to be temporally regulated, with vitamin D3 occurring the earliest(24h) and ethanol occurring the latest(64h) (Figure 8, Table 7-8).

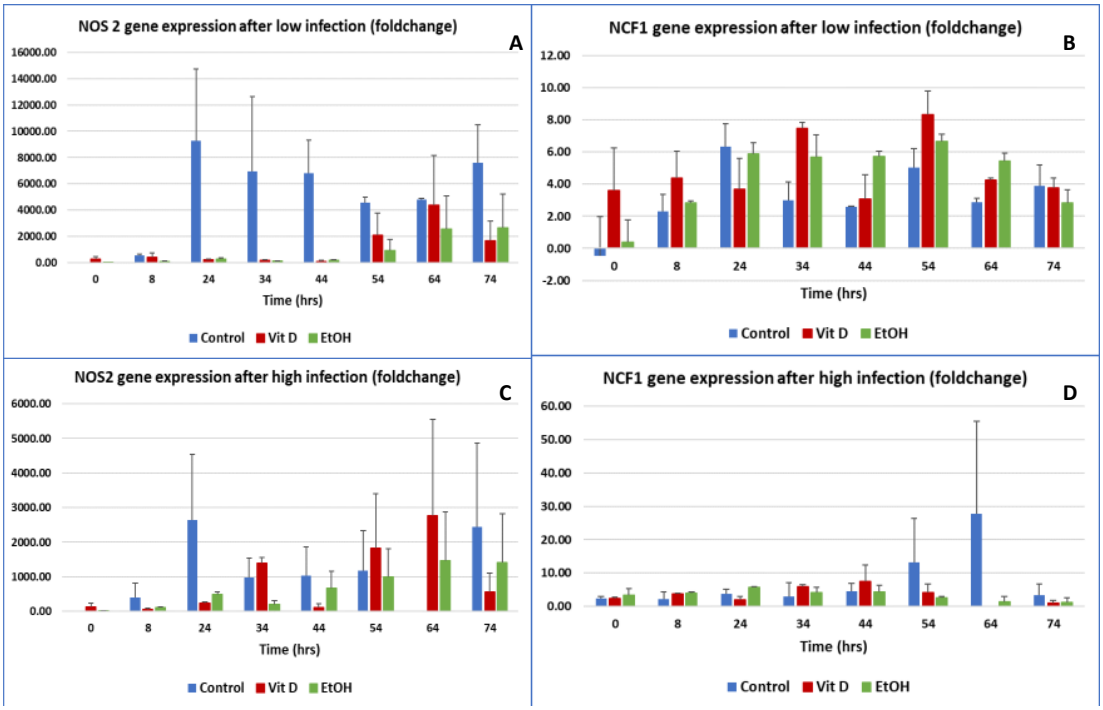

t

Figure 8. Phagosome effector molecule related genes.

NOS2, the gene for inducible nitric oxide synthase enzyme, experiences no negative regulation in either low or high level infection. In low level infection control condition cells upregulate NOS2 the most, ranging from 13.16 to 9291.07, while ethanol express the least (7.36 to 2640.98), vitamin D3 conditioned

cells express a median amount (257.75 to 4386.56). In low infection control cell expression of NOS2 was oscillatory peaking at 24 and 74h, while vitamin D3 and ethanol conditioned cells increased expression over time, except at 74h in which vitamin D3 cells reduce expression levels slightly (from 4386.56 to 1678.48). In high level infection all cells display some manner of oscillatory behavior regarding NOS2 gene expression. The pattern was most heavily evident in control and vitamin D3 conditioned cells. Control cells experienced their maximum gene expression at 24h (2640.04), while vitamin D3 conditioned cells experienced their maximum much later at 64h (2773.52, Figure 7).

NCF1, the gene for p47phox an essential part of the NADPHoxidase complex, experienced no negative gene regulation except in low infection control conditioned cells at 0h (-0.47). At early (0, 8h) and median (34, 54h) time points vitamin D3 conditioned cells have the highest upregulation of NCF1 gene. In low level infection control and vitamin D3 conditioned cells had a shifted oscillatory patter with control peaking first at 24h and vitamin D3 conditioned cells peaking second at 24h. Overall vitamin D3 had the maximum gene expression across all conditions at 54h. In high level infection ethanol conditioned expressed more NCF1 than all other conditions (0-24h), at median time points (34, 44h) vitamin D3 conditioned cells express more. Later in the high level infection control cells overtook other conditions, and expressed the maximum amount of NCF1 (54-74h).

Table 7. Pearson correlation for gene foldchange

		control		vitamin d		ethanol	
		low	high	low	high	low	high
tnfa	vdr						-
il10	nos2	+		+		+	+
cyp27b1	extra						+
cyp27b1	ldh						+
il12	nos2						+
ncf1	vdr				+	-	
cyp27b1	h2o2			-		-	
ldh	nos2		-		+	+	
ncf1	no					+	
cyp27b1	nos2				+		
h2o2	nos2			-			
h2o2	vdr	-					
ncf1	nos2	+					

Table 8. Welch's t Test for gene foldchange

Condition 1	Condition 2	p-value
nos2.ctrl.l	nos2.etoh.l	0.004
nos2.ctrl.l	nos2.vitd.l	0.009
nos2.ctrl.h	nos2.ctrl.l	0.006
vdr.vitd.h	vdr.vitd.l	0.048
cyp27b1.vitd.h	cyp27b1.vitd.l	0.035

Discussion

In this study we have presented, to our knowledge, the first large-scale dynamic profile of J774 macrophage to *Mycobacterium smegmatis* infection during vitamin D_3 exposure. Data from our study demonstrated that level of infection greatly alters host cell response, indicating that the observed effects of vitamin D_3 are likely contextual. Results also illuminated differences in immune responses modulated by the addition of vitamin D_3 versus the vehicle, ethanol. We identified a unique set of vitamin D_3 associated responses to infection that are distinct from vehicle and some that are differentially modulated by level of infection. By evaluating the host innate immunological response across multiple time points we provide a dynamic view of the contribution of vitamin D_3 to the host-*Mycobacterium* interaction [5].

Vitamin D_3 conditioned host cells display reduced bacterial load and decreased cytotoxicity due to vitamin D_3 specific variations in dynamics of immune response

Vitamin D_3 conditioned J774 cells exhibited reduced intracellular and extracellular bacterial load compared to control, a finding corroborated by previous studies, which to varying degrees utilized 1,25-dihydroxyvitamin D_3, 25-OH_2 D_3 and retinoic acid [5], [26], [89], [102]. We found that while ethanol does appear to have a stimulatory effect on host cells, reducing bacterial load below that of vitamin D_3 cells, it presents with a unique and divergent response from vitamin D_3 including higher cytotoxicity for both high and low infection conditions. The significant amount of host cell death experienced early on by control cells during high-level infection resulted in a significantly reduced quantity of replicating cells and lower

cell numbers at later time points in comparison to non-control conditions. Due to the lower cell numbers we saw decreased concentrations of LDH. Previous work with ethanol found it to be a stimulator of host apoptosis, though it was found to have no direct effect on *Mycobacteria* [103], [104]. We found the intracellular bacterial load of vitamin D_3 cells to be greater than ethanol conditioned cells but less than control for both low and high-level infections. The extracellular bacterial load mirrored this pattern during high-levels of infection, however during low-levels of infection this pattern was reversed. Although both ethanol and vitamin D_3 promote bacterial clearance, vitamin D_3 varies the relative magnitude and temporal dynamics of immune response, resulting in the lowest cytotoxicity levels in comparison to ethanol and control, even at the expense of higher intracellular load.

The production of H_2O_2 and NO in the presence of vitamin D3 is dependent on severity of infection

Several inflammatory factors can lead to reduced bacterial load. We explored reactive oxygen and nitrogen species to determine possible vitamin D_3 related mechanisms through which bactericidal activity occurred. H_2O_2 and NO bioavailability, both produced in the phagosome following host cell phagocytosis, are differentially modulated by vitamin D_3. Our results showed that vitamin D_3 production of H_2O_2 differed from ethanol only exposed cells. Vitamin D_3 enabled cells to maintain sufficient levels to facilitate greater bactericidal activity than control, but lower than ethanol during both low and high infection. This presumably resulted in reduced host cell death [105]. Even more pronounced was the effect of vitamin D_3 and level of infection on NO production, with vitamin D_3 cells producing the lowest NO levels during low-level infections and intermediate levels of NO during high-level; again modulating NO levels to less than that of ethanol only cells. At high-level of infection NO and H_2O_2 production had a significantly positive correlation in cells, across all conditions ($p<0.05$; Table 3). Previous studies have found H_2O_2 to be critical in NO production due to H_2O_2 production of metabolic precursor involved in NO metabolism [106], [107]. The correlation between both species may be indicative of a temporal relationship between H_2O_2 and NO, though why it is detectable in high-level infections and not low may be due to the failure of H_2O_2 to clear infection. For low-level infections, H_2O_2 production may be sufficient to clear or control infection, as we observed statistically significant distinctions (Table 2) between control, vitamin D_3, and ethanol cells over several dispersed time intervals. However, during high mycobacterial infection the most significant

differences between vitamin D_3 cells and the non-vitamin D_3 conditioned cells occurred mainly during the first 16 hours of infection. Distinctions in vitamin D_3 NO response occurred later in low infection and throughout for higher level infection, suggesting a greater reliance on vitamin D_3 associated regulation of NO during later stages of uncleared low-level infection and higher levels of infection. Our results indicate that the modulation of both reactive species by vitamin D_3 differs based on level of infection. Furthermore during low and high infection, the vitamin D_3 response significantly differs from the vehicle, with the difference more pronounced for H_2O_2 during low infection and more evident in NO levels after 34 hours post infection. Vitamin D_3 conditioned cells were able to optimize the production of H2O2 and NO, so that the least amount of cytotoxicity occurred due to aggressive host production of oxidative species. This occurred concurrently with vitamin D3 host cells clearance of a higher concentration of bacteria, thus allowing for a healthier host cell and a higher clearance of bacterial load. Vitamin D_3 conditioning prevents the detrimental overproduction of oxidative species in lower-level infections and encourages increased production in high-level infections, resulting in a much more balanced and controlled immune response.

Vitamin D_3 regulates cytotoxicity and reactive nitrogen species in an IL-12 dependent manner

Vitamin D_3 modulation of effectors reduced the inflammatory effects of the vehicle, maintaining LDH levels below that of ethanol only cells during high and low infection load. The NO and LDH variations observed associated directly to vitamin D_3, with correlations to IL-12 bioavailability (LDH, Table 3) or the rate of change of IL-12 (NO, Table 3). While several IL-12 mechanistic studies have observed the effect of IL-12 on lymphocytes and production of NO, some studies have investigated IL-12's effect on macrophages and have shown connections between IL-12 or its components (IL-12p40) and increased NO production [105], [108]–[110]. .At low and high-levels of infection, we found that production of LDH and production of IL-12 had significant ($p<0.05$, Table 3) positive correlations for vitamin D_3 conditioned cells; this correlation was also present and significant during high-level infection in ethanol conditioned cells. While IL-12 and NO concentrations did not emerge as significantly correlated, the rate of change of their concentrations were positively correlated during high-levels of infection (Table S2). Additionally, similar to NO concentrations during low-level infection, IL-12 concentrations for vitamin D_3 cells are the lowest among the three conditions; vitamin D3, ethanol, control. IL-12 modulation

in vitamin D_3 exposed cells is clearly a characteristic of the presence of the nutraceutical and the level of infection, with IL-12 lowest in vitamin D_3 during low-level infection and the highest during high-level infection. The statistically significant negative correlation between IL-12 and intracellular bacterial load observed during high and low-level infection in ethanol cells was not present in vitamin D_3 conditioned cells, although appearing as nearing significance for low-level infections (data not shown). Given the lack of significant IL-12/intracellular bacterial load correlation for vitamin D3 cells, we questioned whether vitamin D_3 differentially modulates IL-12 or components of IL-12, in a manner that downregulates the proinflammatory responses associated with the cytokine[100], [111]. Studies have linked IL-12p40 downregulation to vitamin D_3, proposing that vitamin D_3 downregulates NF-kB activation, which in turn negatively impacts IL-12p40 production. During low-level infection such an inhibitory mechanism may contribute to the low-levels of IL-12 in vitamin D_3 cells. Vitamin D_3 also self-regulates, inactivating itself by upregulating the production of vitamin D-24-hydroxylase (CYP24A1) [112], [113]. Feedback inhibition of active vitamin D3 in combination with increased activation of proinflammatory pathways may contribute to the increased IL-12 concentrations observed during later time intervals of low-level infection and during high-level infection (Figure 5 A, D). Studies have shown that IL-12 modulates NO production in macrophage monocultures in an IFN-γ dependent manner, with IL-12 promoting endogenous production of IFN-γ by macrophages [39], [114]. As we observed for IL-12, the NO concentrations in higher infection conditions are higher than in low infection conditions during the earlier time intervals (Figure. 4 B,D).

Vitamin D_3 conditioning leads to differential modulation of and interaction between cytokines IL-10, IL-12 and TNF- α resulting in novel behavior

A possible explanation for the modulation of the cytokines, IL-10, IL-12 and TNF- α is the presence of vitamin D_3 response elements located in the promoter area of the genes [31], [32], [101], [106]. Through this element vitamin D_3 bound to its receptor can act as a transcription factor up-regulating and down-regulating the transcription of the gene. TNF-α is negatively correlated with intracellular bacteria concentrations during low-level infection for both vitamin D_3 and ethanol conditioned cells; we found there to be a highly positive correlation between TNF- α and IL-10 production in all conditions and at all levels of infection. Previous *in vitro* studies had indicated IL-10 as a down-regulator of TNF-α [41], [115]–[117],

however some clinical studies found that TNF- α and IL-10 concentrations often rose and fell contemporaneously when the immune system was challenged by infection or vaccination [118]–[120]. Our results suggest a much more complex relationship between TNF- α and IL-10 with respect to inflammation and the minimization of cellular damage. Level of infection triggers a specific response in both vitamin D_3 and ethanol. We found that in vitamin D_3 and ethanol conditioned cells during low-level infection the production of TNF-α and IL-10 both have a negative correlation to intracellular bacterial load ($p<0.05$,Table 3). This response is expected in terms of the production of IL-10, which has a suppression effect on the inflammatory aspects of the immune system; ideally the host cell would endeavor to decrease inflammatory response through IL-10, if bacterial load was reducing, in order to circumvent any damage a vigorous response would cause [41], [40]. TNF-α in this case may be the cause of the reduced intracellular load, as previous studies have shown that the presence of TNF-α corresponds with decreased intracellular bacterial load [121]. This negative correlation between intracellular bacterial load and IL-10 is seen only in vitamin D_3 and ethanol exposed cells, with IL-10 levels in control cells higher than in either condition. Vitamin D_3 cells consistently had higher IL-10 levels than ethanol only cells, irrespective of infection level. These interactions, along with the findings that ethanol conditioned cells had a negative correlation between intracellular bacteria and IL-12 at all levels of infection, indicate a possible dysregulation caused by the vehicle, as the expected outcome would be IL-12 concentrations increasing as bacterial load also increases in an effort to clear infection. During low-level infection we observed significant differences in the level of TNF-α produced by vitamin D_3 cells when compared to the vehicle; ethanol cells maintained higher TNF-α levels than vitamin D_3 cells. The converse of this pattern was seen in high-level infection, with control having maintained the highest concentration of TNF-α regardless of infection level. During high-level infection we observed that high amounts of host cell death at hour 64 and 74 resulted in a slight decrease in concentration that we consider to be a death related incident.

1,25-dihydroxyvitamin D_3 is pivotal in the modulation of host immune response to infection. Vitamin D_3 has been identified as a dynamic modulatory co-factor, able to alter macrophage cell behavior in response to level of infection and environmental pressure. This unique modulatory capability led to increased host survivorship, decreased bacterial load, and overall increased capability to fight off infection.

While there is still much to be understood in regards to the mechanism by which vitamin D_3, modulates the innate immune system, our study provides evidence that vitamin D_3 modulation is context dependent and time-variant, as well as highly correlated to level of infection. Our results also provide support towards disambiguating vitamin D_3 immunomodulatory effects from the vehicle, most notably in IL-12/NO modulation. Overall this study furthers our understanding of how vitamin D_3 mechanistically fulfills the dual role of regulator of bactericidal effector molecules and protector against host cell damage and cytotoxicity.

Chapter 3 Expansion of established methodology into BCG infection of primary cell vitamin D3 deficiency

Introduction

Tuberculosis (TB), caused by the bacterium *Mycobacterium tuberculosis (Mtb)*, is a global health crisis affecting over 10 million people worldwide and causing over one million deaths per year[1]. Following infection bacteria are phagocytosed by alveolar macrophages and exposed to effector molecules and harmful enzymes within the phagosome [4], [5]. Depending on the effectiveness of the host immune response, bacterium may be cleared or the host may succumb to infection. Current therapeutic regimens aim to control active disease through the use of antibiotics such as, isoniazid (INH) and rifampin (RIF) [4], [6], [7]. However the immune response to *Mtb infection* and therapeutics can vary depending on health vulnerabilities such as nutrient deficiency, and health risks including alcohol use and smoking (Table 1). While studies have traditionally investigated the impact of individual immune depressive factors, there is increasing evidence that the intersection of vulnerabilities, such as vitamin D_3 deficiency and health risk behaviors like alcohol use disorders (AUD), may result in compounding negative immunological effects.

Classically, vitamin D_3 is associated with the absorption of calcium and phosphorous, however research into its non-classical role in immune regulation has become increasingly important, particularly given the high rates of vitamin D_3 deficiency in the adult population [30]–[33]. Macrophages are known to express vitamin D_3 receptors (VDR) and can produce the enzyme Cyp27B1 (1α-hydroxylase), which converts 25-hydroxyvitamin D_3 to biologically active 1α,25-dihydroxyvitamin D_3 [31], [34]. The modulation of immune response by vitamin D_3, leads to a more effective innate and adaptive response. Studies dating back over a century found positive correlations between vitamin D_3 supplementation and overall health of TB infected patients [4], [23]. Vitamin D_3 has been observed to have a profound effect on the production of several key immune regulating cytokines and effector molecules (Table 1). Vitamin D_3 promotes activation of macrophage cells and the formation of multinucleated giant cells, commonly present in TB granulomas [29]. Our current study, as well as previous studies by others, have observed that exposing host cells to vitamin D_3 results in enhanced immune response to infection and greater host cell preservation (Table 1, Figure 10) [4], [5], [24], [26], [29].

While previous studies have provided key insights regarding vitamin D_3 modulation of host response, many of these studies failed to investigate common comorbidities associated with malnutrition [5], [16], [24]–[26], [44], [45], [88], [89]. Malnutrition and alcoholism have long correlated with suboptimal immune function and efficacy, with alcohol commonly associated with a detrimentally upregulated inflammatory response [46]. Acute binge drinking, as well as moderate drinking can have a large effect on the immune system [47]. Chronic alcohol exposure has been shown to interfere with the functions of essential vitamins and nutrients, including folic acid and vitamins D, C, and E, but these studies are few and fail to investigate the compounding effect of alcohol exposure, impaired vitamin function, and infection [90]–[93]. Proper controls in our previous study necessitated the use of ethanol as a vehicle control and while other results suggested that the effect of alcohol was negligible, we found a bacterial load-dependent dysregulation associated with alcohol exposure. Alcohol, even in small concentrations had a noticeable effect on macrophage behavior and cytokine production, resulting in increased H_2O_2, NO, and cytotoxicity, as well as negative correlations between bacterial load and IL-12 production [27]. While recognized that alcohol exposure decreases the efficacy of vitamin D_3, most studies fail to extend beyond alcohol use's effects on classical vitamin D_3 functions [90], [91], [93], [96]. Our current study addresses several of the limitations of previous vitamin D_3 studies and investigates the impact of in vivo deficiency on immune response during infection given exogenous vitamin D_3 supplementation or alcohol exposure. We coupled an *in vivo* vitamin D_3 deficiency model and an *ex vivo Mycobacterium bovis* BCG murine infection model to quantify the impact of vitamin D_3 supplementation and alcohol exposure on immune response during infection. In our study we utilized *M. bovis* Bacillus of Calmette and Guerin (BCG) infection of murine bone marrow derived macrophages (BMDM) as a surrogate for Mtb infection. *M. bovis* BCG is commonly used as a model organism for the study of *Mtb* [15], and while it does not capture all aspects of TB disease, it has been used to capture multiple features of TB disease, such as macrophage function and bacterial response during stress [16], [17]. BCG is typically not harmful to humans when compared to *M. tuberculosis*, but acts pathogenically in mice in a similar manner as *Mtb.* We chose to utilize the inbred laboratory strain C57BL/6 mice as our animal model to enable the development of an *in vivo* vitamin D_3 deficiency model, and to minimize effects due to genetic variations in host [18], [21], [22]. BMDMs, which are more abundant and readily generated from mice, were used in

lieu of alveolar macrophages. Given that the immunomodulatory role of vitamin D3 represents a non-classical, atypical response to potentially unregulated infection, the recruitment of circulating immune cells, such as bone marrow originating monocytes, to control infection is highly plausible.

Compared to prior observations in murine cell lines, in our current study the effect of alcohol exposure was found to more profoundly dysregulate primary murine macrophages, with ethanol exposed cells generally characterized as hyper- or hyporesponsive. *In vivo* diet was the greatest determinant of immune response, and while exogenous vitamin D_3 supplementation had a normative effect on diet deficient host, supplementation was not sufficient to compensate for the effects of diet deficiency.

Methods

In vivo vitamin D_3 deficiency model

Three-week old C57BL/6J female mice (Jackson Labs) were fed TD89123 vitamin D3 deficient diet (Envigo) or TD89124 vitamin D3 sufficient control diet for 13 weeks. TD.89124 diet is considered to be a normal diet and provides all the necessary nutrients for healthy rodent growth. Mice were weighted once a week and weight was recorded (Figure 9). At 16 weeks of age mice were sacrificed and bone marrow derived macrophages (BMDM) were collected.

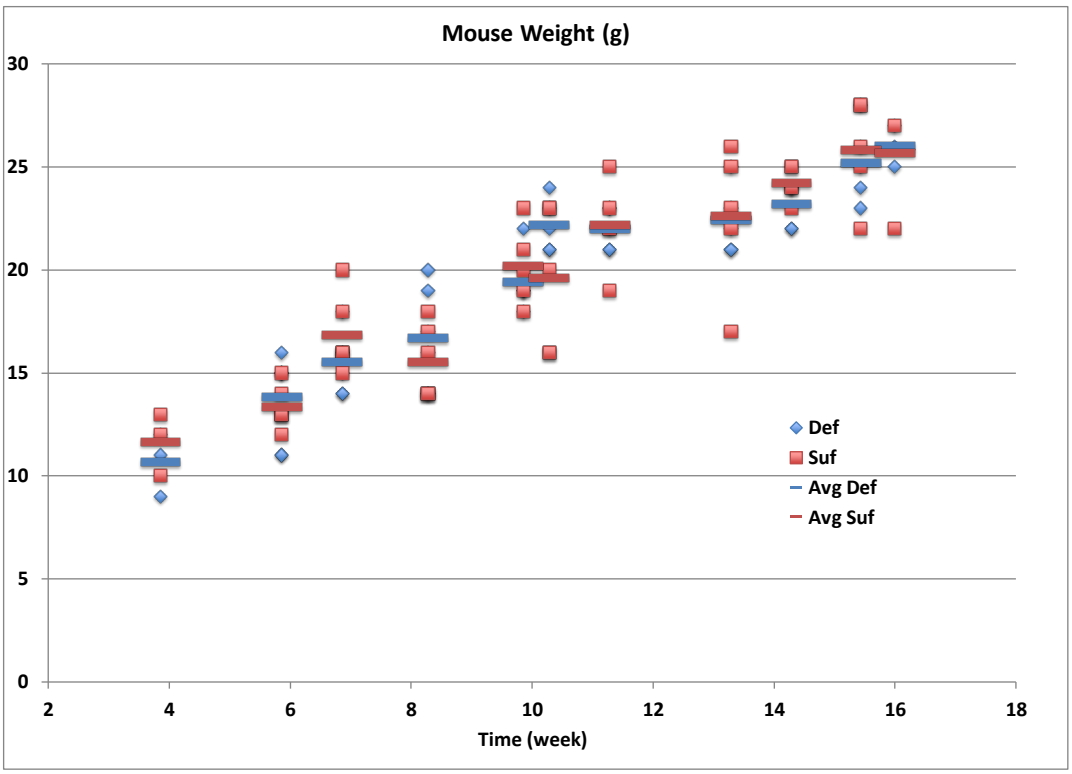

Figure 9. Mouse Weight over time while on vitamin D3 sufficient and deficient diet

BMDMs were matured for 6-7 days at 37˚C and 5% CO2 in DMEM (Dulbecco's Modified Eagle Medium) containing 10% fetal bovine serum, 1% multi-clonal stimulation factor, 1% penicillin-streptomycin (pen/strep), and 1% L-glutamine. BMDM cells were dislodged from plate by gentle pipetting and centrifuged at 1500 rpm for 10 minutes and then resuspended to a concentration of $5x10^5$ cells/ml in DMEM complete without pen/strep. Cells were distributed to 24-well plates and incubated for 2 hours to allow adherence.

Bacterial culture

M. bovis (BCG; gifted from Graviss Lab, Houston Methodist Research Institute, TX) was grown from frozen stock in Middlebrook 7H9 media using Hardy Diagnostics 7H9 dehydrated culture media (C6301), containing 0.2% glycerol, 10% OADC and 0.05% Tween-80. After undergoing one subculture bacteria was grown to late log phase and used to infect host cells.

Ex vivo infection, vitamin D_3 supplementation, and alcohol exposure models

DMEM complete without pen/strep was prepared containing either (1) 4ng/ml of 1,25-dihydroxyvitamin D_3, (2) an equivalent amount of 1,25-dihydroxyvitamin D3 solvent, 0.8% ethanol, or (3) control media (Figure 1A). Molecular biological grade ethanol was used as a secondary control for the vitamin D_3 solvent, to model alcohol exposure and investigate the effects of ethanol on the system. Vitamin D_3 deficient and sufficient diet BMDM cells in their appropriate exposure media (vitD_3, ethanol, or control) were infected at an MOI of 1:1 host cells to bacteria (BCG). Study was performed in triplicate. BCG was centrifuged at 1500rpm for 10 minutes and then resuspended to a desired concentration in the DMEM complete with or without vitamin D_3/ethanol. The supernatant was removed from 24-well plates and replaced with control, vitamin D_3 or ethanol containing media. Cells were then incubated at 37˚C and 5% CO2 for 4 hours. After infection was complete supernatant was removed and host cells were washed twice with phosphate buffer saline solution (PBS), then control, vitamin D_3 or ethanol media containing 50µg/ml of gentamicin was added to wells followed by 14 hours of incubation. After incubation with gentamicin, plates were washed with PBS twice and fresh control, vitamin D_3 or ethanol containing media was added to appropriate cells. Cells were then incubated for 120 hours.

Sample collection and immune response quantification

Samples were collected at hour 0, 24, 48, 72, 96 and 120 hours post infection. Imaging occurred using an Olympus CKX41 microscope immediately prior to every sample collection time point (Figure 10). This experiment was replicated three times, resulting in three trial groups per condition.

Quantification of bacterial load

At hours 0, 24, 48, 72, 96 and 120 post infection, supernatant from the 24-well plate was collected and serially diluted 10-fold. Dilutions were then plated on 7H11 agar plates (C6292, Hardy Diagnostics) to quantify the extracellular bacterial load. Wells were washed once with PBS then incubated with 1% Triton X-100 for 10 minutes, to allow cells to lyse. The lysate was then collected, serially diluted 10-fold, and plated on 7H11 agar plates to quantify intracellular bacterial load. After 16 days incubation, countable colony forming units (CFU) were enumerated to determine extracellular and intracellular bacterial load. It should be noted that at hour 0 extracellular counts were present; this may be caused by inefficiency of

gentamicin to fully eradicate BCG infection, though it does lower bacterial counts significantly (Figure 11). Supernatant not utilized for CFU counts was stored in -80˚C and later used for cytokine and reactive species quantification.

Cytokine and effector assays

Using supernatant collected from 24-well plates (Figure 11 shows immune response variables measured), 25(OH) Vitamin D ELISA (ENZO, ADI-900-215-0001) was performed in accordance with manufacturer's instructions with a sensitivity range 0.5-1010 ng/ml. Griess reagent (Promega, G2930) was utilized to quantify NO2– concentrations. LDH cytotoxicity assay (Pierce, 88954), performed in accordance with manufacturer's instructions, was used to quantify cell death. Known concentrations of host cells were lysed and their corresponding LDH concentrations used to generate a linear regression subsequently applied to LDH assay readings from experimental samples to determine amount of cell death. Hydrogen Peroxide Assay Kit (Abcam, ab102500) was utilized to quantify H2O2 concentrations. To quantify IFN-γ, IL-1β, IL-12p70, IL-10, IL-2, IL-4, IL-5, IL-6, KC/GRO, and TNF-α concentrations over time, a V-PLEX proinflammatory panel (MSD, K15048D) was utilized.

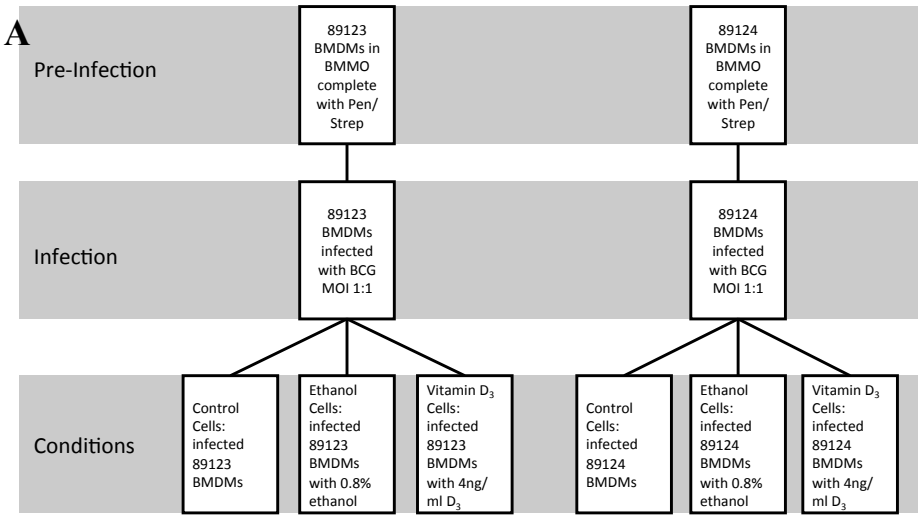

89123 - D_3 deficient diet
89124 - D_3 sufficient diet

B

In vivo Condition	*In vitro* Exposure	Assays/Immune Response Variables	Quantifiable Immunological Outcome
89123 (vitD deficient) **89124 (sufficient)**	Control (no exposure) VitD (supplementation) Etoh (alcohol)	vitD3, NO *Cytokines/Chemokines* - IFN-g, IL-10, IL-12p70, IL-1B, IL-2, IL-4, IL-5, IL-6, KC/GRO, TNFa	*M. bovis* BCG (extracellular, intracellular) LDH (cell death)

Figure 10. Experimental setup and LMM categories.

Statistical analysis

Statistical analysis was performed using MATLAB [98]. Using data from the three trials we performed outlier analysis and normalized the data to vitamin D_3 sufficient diet control cells (Suf) at each time point within each assay (Table 11). After normalization values were averaged together and the standard error of the mean was calculated. Welch's t test was performed for each time window (0-120, 24 hour time window intervals) and for all time points combined (0-120, without windowed intervals) to identify statistically significant variations in immune response between experimental conditions. Rate of change over time was calculated using non-normalized data and the results normalized to results from Suf control cells. Pearson correlation analysis was applied to non-normalized data to calculate correlations between cytokines and effector molecules.

Linear mixed model analysis

The immune response data included multiple repeated measures that are correlated within each experimental sample (18 experimental samples corresponding to 6 conditions times three trials). Therefore we analyzed the data using a two-level Linear Mixed Model (LMM) using the method of residual restricted maximum likelihood with a first-order autoregressive covariance (AR(1)) structure to model autocorrelated errors. For Level 1 analysis, the within-condition level, the repeated immune response measurements (Figure 10B) were expressed as a regression function based on collection time (i.e., hours from the first collection). Differences in the Level-1 immune response profiles were then used to account for the random variation across experiments in the Level 2 model.

The LMM, which models both random effects and fixed effects, enables the level-2 equations to model the slope coefficients from the level-1 predictors as the outcomes for the level-2 predictors. Due to the small sample size of 18 experimental samples and the large number of possible predictors (12 assays including cytokines, chemokines, NO, and vitamin D), the LMM models could not converge when all 12 assays were included in the model. In Step 1 of the analysis, a LMM that included all 12 assays was generated for each of the four outcome variables of interest (intracellular, extracellular, sum of intra and

extracellular bacterial load, LDH/cytotoxicity) to identify assays that had a significant effect ($p<0.05$) on the prediction of each of the four outcomes; these were termed significant predictors. The LMM analysis used a natural log transformation of the outcome variables. During Step 2 of the analysis, generation of the complete model, the significant predictors identified in Step 1 along with the two effects of diet (termed cond1) and treatment (termed cond2; control/no treatment, vitamin D_3 supplementation, or alcohol exposure) were used as inputs to the Level 2 model. For all statistical tests, significance levels were set at $p<0.05$. All analyses were performed using SAS version 9.4 (SAS Institute, Inc. 2014 Cary, NC).

Results

Building on previous findings regarding the impact of *in vitro* vitamin D_3 supplementation on the bioavailability and rate of production of key cytokines and effector molecules, we found *in vivo* vitamin D_3 deficiency to have the greatest effect on cytokine and effector production. Exogenous supplementation had a secondary, more moderate effect on the relative concentration and rate of change of immune response molecules.

<u>Vitamin D_3 sufficient diet promotes reduced host cell death while maintaining bacterial loads comparable to vitamin D_3 deficient diet cells.</u>

M. bovis BCG CFUs determined from 7H11 plating of diluted samples collected over time showed that Vitamin D_3 deficient diet greatly impacted initial intracellular BCG loads. The intracellular loads of vitamin D_3 sufficient (Suf) and deficient (Def) control were statistically significantly different. Cells originating from vitamin D_3 sufficient mice were found to have almost 3-fold less relative bacterial CFUs than Def conditioned cells at 0h (Figure 11). When comparing Suf and Def conditioned cells it was evident at 0, 24, 48 and 96h post infection that *in vivo* diet played a large roll in intracellular load with Def having between 1.5-3 fold greater bacterial load. Extracellular bacterial load was also impacted by vitamin D_3 diet deficiency (Figure 11, Table 11). At all time points except 24 and 96h, extracellular load of Suf conditioned cells had less bacterial load than Def and was found to be statistically significantly different ($p<0.05$, Table 9-10).

Table 9. Time interval Welch's t Test

		0-24	24-48	48-72	72-96	96-120
Intracellular Bacteria						
Def+VitD	Suf			0.023		
Def	Def+VitD			0.032		
Extracellular Bacteria						
Def+VitD	Suf				0.011	0.022
Def+VitD	Suf+VitD				0.045	
Def	Suf					0.001
Def+EtOH	Suf					0.039
Cytotoxicity						
Suf	Suf+VitD	0.013		0.045	0.018	
Suf	Suf+EtOH	0.020		0.021	0.009	0.017
Def	Suf+VitD	0.048				
Def	Suf+EtOH	0.048				
Def+EtOH	Suf		0.011	0.006		
Def+VitD	Suf		0.040			
Def	Suf			0.042		
Vitamin D						
Def+VitD	Suf				0.019	
Def+VitD	Suf+EtOH				0.020	
Def+VitD	Suf+VitD				0.040	
Nitric Oxide						
Suf	Suf+VitD			0.000	0.000	
Def	Suf+VitD			0.007	0.001	0.019
Def+EtOH	Suf+VitD			0.022	0.027	
Def+VitD	Suf+VitD			0.023		
Def	Suf				0.010	0.012
Suf+VitD	Suf+EtOH				0.025	
KC/GRO						
Def+EtOH	Suf+VitD	0.037	0.005			
Suf	Suf+VitD	0.043				
Def+EtOH	Suf+EtOH		0.004	0.022		
Def+EtOH	Suf		0.012			
Def	Def+EtOH					0.047
TNF-α						
Def+VitD	Suf+VitD	0.023				
Def+VitD	Suf	0.031				

		0-24	24-48	48-72	72-96	96-120
IL-12						
Def+EtOH	Suf+VitD	0.042	0.042	0.000	0.002	
Def	Suf		0.001	0.001	0.046	
Def	Suf+VitD		0.001	0.000	0.013	
Def+VitD	Suf		0.005			
Def+VitD	Suf+VitD		0.007			
Suf	Suf+EtOH		0.030			
Suf+VitD	Suf+EtOH		0.032	0.043		
Def+EtOH	Suf		0.046	0.000	0.008	
Suf	Suf+VitD			0.008	0.000	
IL-1β						
Def	Suf+VitD	0.001	0.001	0.010		
Def	Suf+EtOH	0.004	0.006			
Suf	Suf+VitD	0.005				
Def	Suf	0.006	0.000	0.004		
Def+VitD	Suf+VitD	0.016	0.026			
Def+EtOH	Suf+VitD	0.025	0.016	0.016		
Def+EtOH	Suf		0.015	0.009		
Def+VitD	Suf		0.021			
Def+EtOH	Suf+EtOH		0.039			
IFN-γ						
Def	Suf+VitD	0.002	0.000	0.001	0.049	
Def	Suf	0.010	0.000	0.005		
Def+VitD	Suf+VitD	0.011	0.009			
Suf	Suf+VitD	0.029		0.001	0.006	
Def	Suf+EtOH	0.042				
Def+EtOH	Suf+VitD		0.010	0.002		
Def+VitD	Suf		0.024			
Def+EtOH	Suf		0.027	0.035		
IL-2						
Def	Suf+VitD	0.013	0.000			
Def	Suf	0.026	0.000	0.001	0.013	0.022
Def	Suf+EtOH	0.028	0.043			
Def+VitD	Suf+VitD	0.045	0.016			
Def+EtOH	Suf+VitD		0.013			
Def+EtOH	Suf		0.014	0.045		
Def+VitD	Suf		0.017			

		0-24	24-48	48-72	72-96	96-120
IL-4						
Def	Suf	0.001	0.002	0.000	0.046	
Def	Suf+VitD	0.004	0.002	0.000	0.003	
Def	Suf+EtOH	0.023				
Def+VitD	Suf+VitD	0.041	0.039			
Def+EtOH	Suf+VitD		0.017	0.000	0.003	
Suf	Suf+VitD			0.002	0.001	
Def+EtOH	Suf			0.009		
Suf+VitD	Suf+EtOH			0.032		0.019
Suf	Suf+EtOH					0.016
IL-10						
Suf	Suf+VitD	0.000	0.002	0.001	0.000	0.001
Suf	Suf+EtOH	0.000				
Def	Suf+VitD	0.000	0.000	0.000	0.001	0.031
Def	Suf+EtOH	0.000	0.000	0.000		
Def	Suf	0.002	0.000	0.000	0.012	
Def+EtOH	Suf+VitD	0.011	0.003	0.001		
Def	Def+VitD	0.012	0.001	0.000	0.045	
Def+VitD	Suf+VitD	0.013	0.012			
Suf+VitD	Suf+EtOH	0.036		0.014		
Def+EtOH	Suf+EtOH	0.038	0.021			
Def	Def+EtOH	0.040	0.006	0.003		
Def+EtOH	Suf		0.030	0.011		
Def+VitD	Def+EtOH			0.041		
IL-5						
Def	Suf+VitD	0.002	0.001	0.001	0.004	0.014
Def+VitD	Suf+VitD	0.003	0.006			
Def	Suf	0.006	0.002	0.001	0.005	0.016
Suf	Suf+VitD	0.009			0.043	
Def	Suf+EtOH	0.021	0.012	0.015		
Def+VitD	Suf	0.021	0.011			
Def+EtOH	Suf+VitD		0.006	0.008	0.034	
Def+EtOH	Suf		0.009	0.011	0.044	
IL-6						
Def+VitD	Suf+VitD	0.003				
Suf	Suf+VitD	0.004	0.030			
Def+EtOH	Suf+VitD	0.007	0.017			
Def+VitD	Suf+EtOH	0.014				
Def+EtOH	Suf+EtOH	0.022	0.036			
Def	Suf+VitD	0.039	0.023			
Def+VitD	Suf	0.046				
Def	Suf+EtOH		0.033			
Def	Suf		0.047			
Suf	Suf+EtOH			0.010		

Extracellular and intracellular BCG load clearance appeared to be negatively impacted by the exogenous addition of vitamin D_3 and ethanol, resulting in less controlled infection. The vitamin D_3 sufficient diet's reduced bacterial load is negated by the exogenous addition of vitamin D_3 and ethanol. At several time points (intracellular:0, 24, 48, 72, 96h, extracellular: 0, 48, 72, 96h) we observed that Suf+EtOH conditioned cells' bacterial CFU values exceeded Suf cells, further supporting our initial supposition that exogenous addition of alcohol negatively impacts bacterial clearance. The intracellular load for Suf+EtOH cells was found to be statistically significantly different from Suf ($p<0.05$, Table 12). We found similar trends with vitamin D_3 deficient diet but with less frequency. The bacterial load of Def+EtOH exceeded that of Def (intracellular: 72, 96h , extracellular: 0, 72h). These results suggest that while diet-associated vitamin D_3 sufficiency has a positive effect on bacterial load clearance, the exogenous addition of vitamin D_3 dissolved in ethanol interferes with and potentially hinders bacterial clearance.

Table 10. Welch's t test table

	Def	**Def+VitD**	**Def+EtOH**	**Suf**	**Suf+VitD**	**Suf+EtOH**
Def		IL-10, VitD		IFN-γ, IL-10, IL-12, IL-1β, IL-2, IL-4, IL-5, IL-6, Intra, KC/GRO, NO	IFN-γ, IL-10, IL-12, IL-1β, IL-4, IL-5, IL-6, KC/GRO, NO, TNF-α	IL-10, IL-6, KC/GRO
Def+VitD	*IL-10, IL-5, VitD*		VitD	IL-12, IL-1β, IL-2, IL-5, IL-6, VitD	IFN-γ, IL-10, IL-12, IL-1β, IL-4, IL-5, IL-6	IL-6, VitD
Def+EtOH	*IL-10*	*VitD*		IL-10, IL-12, IL-1β, IL-2, IL-4, IL-5, Intra	IFN-γ, IL-10, IL-12, IL-1β, IL-4, IL-5, IL-6, NO	IL-6
Suf	*Extra, IFN-γ, IL-10, IL-12, IL-1β, IL-2, IL-4, IL-5*	*Extra, IFN-γ, IL-12, IL-2, IL-5, Cytotox, TNF-α, VitD*	*Extra, IL-10, IL-12, IL-1β, IL-5, Intra, Cytotox, TNF-α, VitD*		Extra, IFN-γ, IL-10, IL-4, IL-5, IL-6, Cytotox	IL-12, Intra, Cytotox
Suf+VitD	*IFN-γ, IL-10, IL-12, IL-1β, IL-2, IL-4, IL-5, Cytotox, NO*	*IFN-γ, IL-2, IL-5, IL-6, TNF-α*	*IFN-γ, IL-10, IL-12, IL-4, IL-5, IL-6, KC/GRO, TNF-α*	*IFN-γ, IL-10, IL-12, IL-1β, IL-4, IL-5, IL-6, KC/GRO, Cytotox, NO*		IFN-γ, IL-10, IL-12, IL-4, IL-5
Suf+EtOH	*IFN-γ, IL-10, IL-1β, IL-2, IL-4, IL-5, Cytotox*	*Intra, VitD*		*IL-10, IL-6, Intra, Cytotox*	*NO*	

Differences in diet and exogenous vitamin D_3 supplementation/alcohol exposure were also evident in cellular cytotoxicity, which showed a clear difference in LDH levels (used to quantify host cell cytotoxicity) between *in vivo* diets (Figure 13). Diet-dependent cytotoxic response differed from 24h post infection onward, with Suf cells having the least amount of cell death when compared to Def. Within each respective diet we see a distinct pattern in which Suf/Def cells exhibit the least cytotoxicity and Suf+EtOH/Def+EtOH exhibit the greatest level of cytotoxicity. Vitamin D_3 sufficient diets (Suf, Suf+VitD, Suf+EtOH) had lower amounts of cell death than their counterparts (Def, Def+VitD, Def+EtOH), ranging from 1.15 to 2.46 fold increase over Suf cells. The resulting cytotoxicity experienced

by Suf+VitD/Def+VitD and Suf+EtOH/Def+EtOH conditions further support our supposition regarding the harmful effect of alcohol on cell immune response.

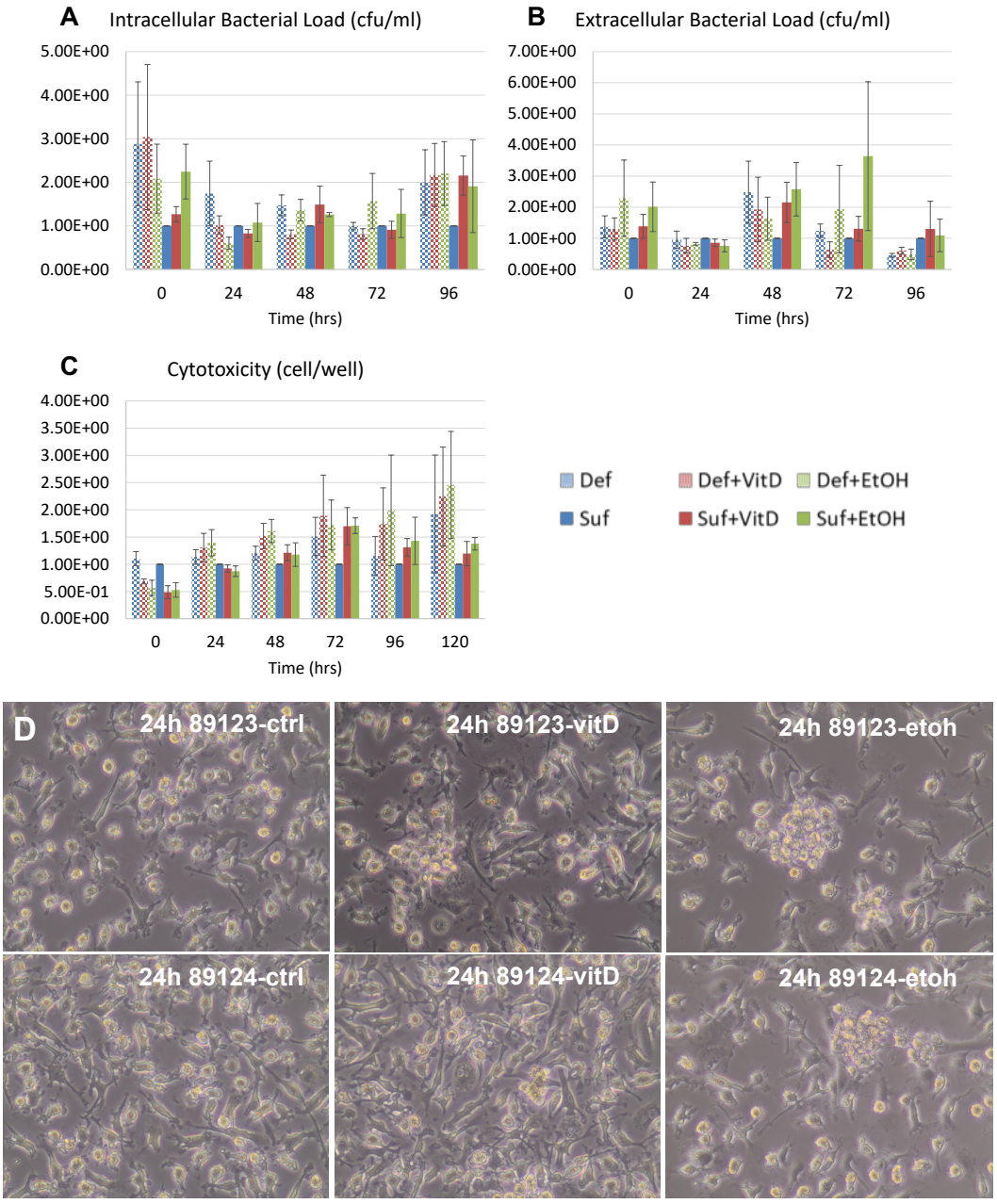

Figure 11. Bacterial Load and Host Cell Cytotoxicity

<u>Effector molecules are differentially modulated by vitamin D_3 diet and supplementation.</u>

Utilizing a colorimetric assay we determined vitamin D_3 and NO concentration dynamics during cellular response to infection. As expected host cells treated with vitamin D_3 exogenously exhibited the

highest concentration of vitamin D_3 (Def+VItD, Suf+VitD). An unexpected result was the excessive concentrations of vitamin D_3 observed throughout for Def+VitD cells (1.5-2.25 fold greater than Suf, Figure 11). This observation may be due to the difficulty of detecting the receptor bound form of vitamin D_3 using the ELISA assay, or may hint at improved utilization of the vitamin by sufficient cells, though further testing would be required to substantiate this hypothesis. We found that the Def+VitD cells' vitamin D_3 concentrations were statistically significantly different from all other conditions (Figure12, Table 12).

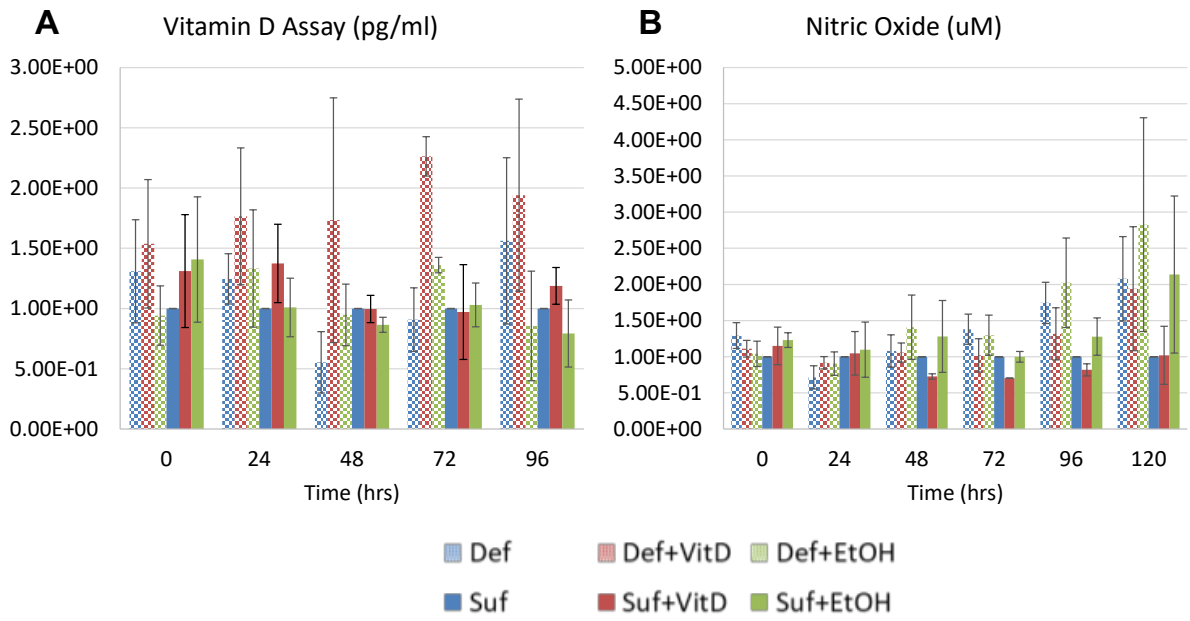

Figure 12. Effector Molecules Vitamin D3 and Nitric Oxide

Similar to the findings in our previous study the divergent production of nitric oxide (NO) between conditions is temporally associated [27]. We observed larger differences between conditions at later time points and more similarities in NO production at earlier time points (Figure 12). From 48h onward diet-associated differences in NO production became apparent, with vitamin D_3 sufficient diet conditions producing less NO than their vitamin D_3 deficient counterparts. Further separation between the conditions occurred within each diet, with vitamin D_3 supplemented cells (Def+VitD, Suf+VitD) producing the least amount of NO from 48-120h and ethanol exposed cells (Def+EtOH, Suf+EtOH) producing the highest concentrations from 48-120h. Similar patterns were observed in our previous study using *in vitro* conditioned cell lines and *M. smegmatis*. In the current study we found NO production by Suf+VitD cells

to be significantly different from Suf+EtOH, Def+EtOH, Suf, and Def cells (Figure 12, Table 9-10). Our findings reaffirm our previous conclusion that vitamin D_3 supplementation as well as alcohol exposure can directly modulate the production of reactive nitrogen species, with upregulation by alcohol potentially resulting in detrimental outcomes for the host cell given NO's toxicity and ability to easily diffuse across the phagocytic membrane.

Proinflammatory cytokines present with two very distinctive responses to vitamin D_3 deficiency

IL-12, IL-1β, IFN-γ, and IL-2

We used a multiplex ELISA assay to quantify IL-12, IL-1β, IFN-γ, and IL-2 production over time. Our previous studies found IL-12 to be highly regulated by vitamin D_3 in murine cell lines with production changing in response to infection level when vitamin D_3 was present. Other studies have found IL-1β to be highly regulated by vitamin D_3 in humans but studies in mice were inconclusive (Table 1) [27]. Similar to NO production and cytotoxicity, proinflammatory cytokines IL-12, IL-1β, and IFN-γ production was differentiated heavily by diet and moderately by exogenous supplementation. IL-12, IL-1β, and IFN-γ followed a similar trend as that observed in NO in which vitamin D_3 sufficient diet (Suf, Suf+VitD), with the exclusion of Suf+EtOH, produced lower levels of the cytokine compared to vitamin D_3 deficient conditions (Def, Def+VitD, Def+EtOH). For IL-12 and IFN-γ production at 96 and 120h, Suf+EtOH exceeds that of all other conditions. Exogenous supplementation of cells in addition to diet resulted in further stratification of IL-12 and IL-1β with Suf+EtOH/Def+EtOH cells producing the highest levels and Suf+VitD/Def+VitD cells producing the lowest levels within their respective diets (Figure). Supporting these observations we found that IL-12 production by Suf cells was significantly different from Def, Suf+EtOH, and IL-12 production by Suf+VitD was significantly different from Def+VitD, Suf+EtOH (Figure 16). For IL-1β production, Suf and Suf+VitD were significantly different from Def, Def+EtOH, Def+VitD . Vitamin D_3 supplemented cells produced the least IFN-γ (Def+VitD at 24, 48, 72, 120h and Suf+VitD at 0, 24, 48, 72, 96, 120h), Def produced the most (at 0, 24, 48, 72), and Suf+VitD was significantly different from all other vitamin D_3 deficient conditions ($p<0.05$). The effect of diet on IL-2 production followed a similar trend as IFN-γ from 0 to 48h but diverges after 48h with Suf+VitD producing the greatest amount of IL-2 at 72h, 120h and Suf+EtOH producing the highest concentration at 96h. IL-2

production in Suf conditioned cells was significantly different from Def, Def+VitD, and Def+EtOH conditions ($p<0.05$). In all cases with IL-12, IL-1β, IFN-γ, and IL-2 Suf conditioned cells were found to be statistically significantly different from Def cells ($p<0.05$,). The clear Suf versus Def skew in cytokine production is indicative of the overarching effect of diet on the establishment of a baseline or normative pro-inflammatory response. Although diet was the main differentiator, alcohol related dysregulation was apparent even for sufficient diets, with Suf+EtOH exhibiting a large increase in rate of production at 96h and continuing to produce the highest IL-12,

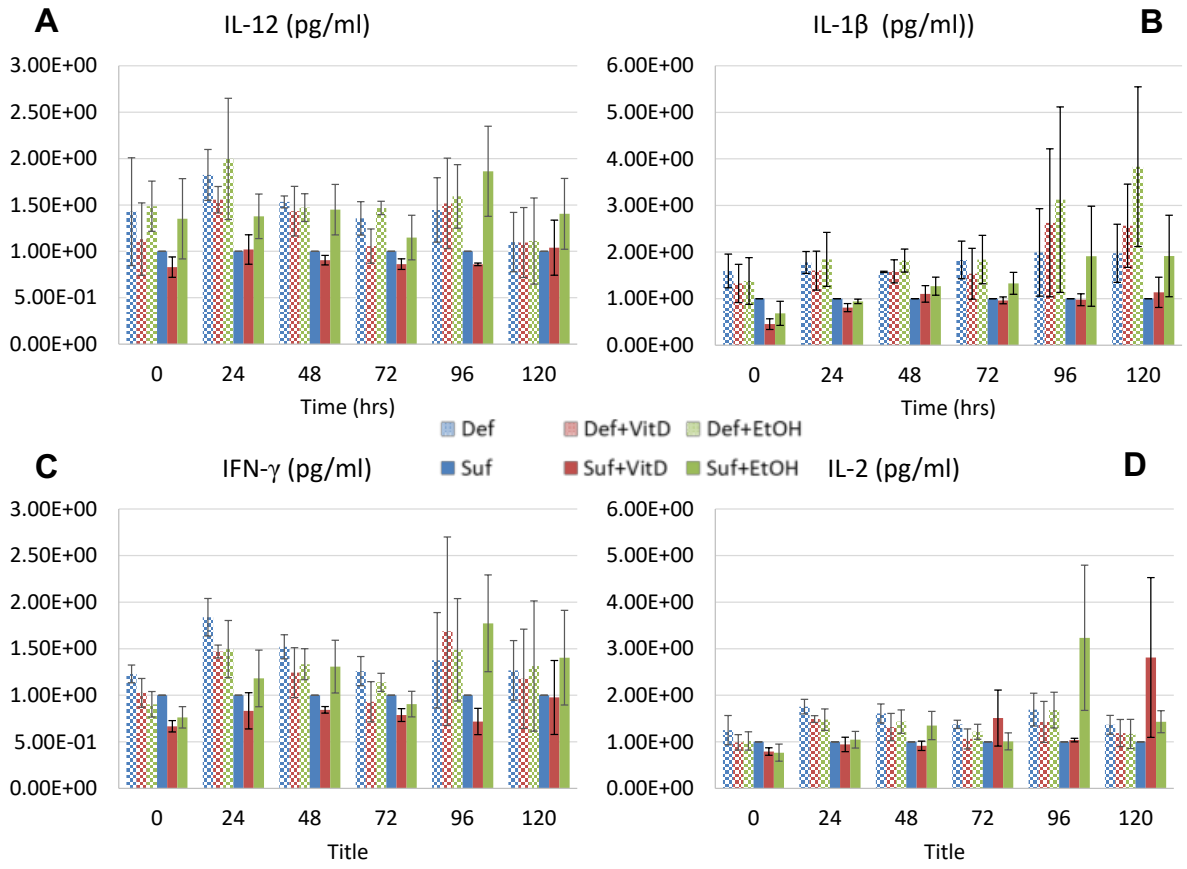

Figure 13. Pro-inflammatory cytokines differentially regulated by in vivo diet and in vitro conditioning

KC/GRO, TNF-α, and IL-6

KC/GRO, TNF-α, and IL-6 exhibited a very different response to vitamin D_3 deficient and sufficient diet during infection in comparison to other proinflammatory cytokines. Their concentration and

rate of production were positively correlated to one another across all conditions Consistent with our previous study, a distinction between vitamin D_3 sufficient and deficient diet cytokine production was only observed for the 0h time point (Figure 17). The diet-dependent skew observed for other proinflammatory cytokines was only apparent at 0h for this group of cytokines, with vitamin D_3 deficient diets producing higher levels than vitamin D_3 sufficient diets. Sufficient diet cells supplemented with vitamin D_3 (Suf+VitD) produced the lowest initial concentrations of KC/GRO, TNF-α, and IL-6 at 0h. At 24hr production by Def and Def+VitD cells was similar and greater than all other conditions by 1.25 fold. However, by 48h Def+VitD decreased and Def maintained a 1.25 fold increase through 96h (TNF-α) and 120h (KC/GRO, IL-6). For IL-6 all deficient diet conditions (Def, Def+VitD, Def+EtOH) were significantly different from sufficient diet counterparts (Suf, Suf+VitD, Suf+EtOH), with Suf+VitD also differing significantly from Suf (Figure 16 Table 14). For KC/GRO Def was significantly different from all Suf conditions (Figure 16, Table 14).

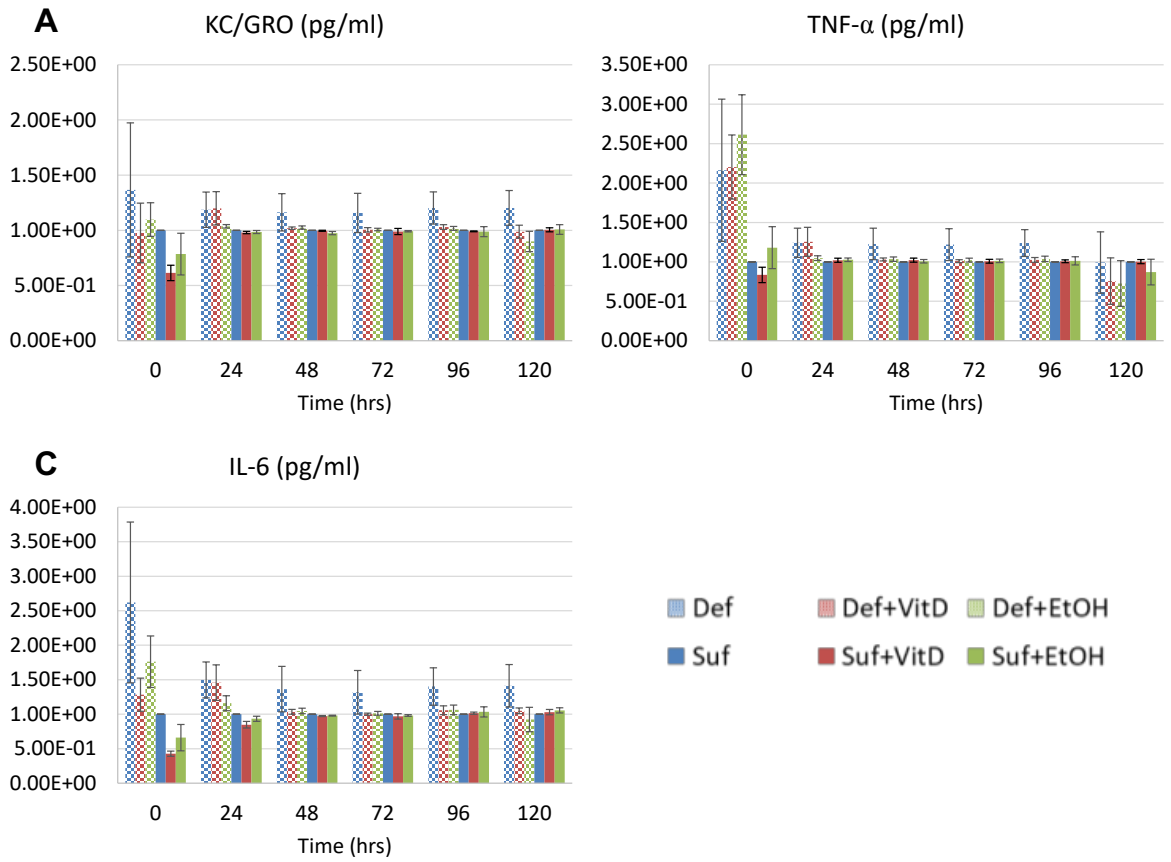

Figure 14. Pro-inflammatory cytokines regulated primarily by presence of infection

Anti-inflammatory cytokine production is affected by in vivo vitamin D_3 deficient diet but supplementation has notable effects

Utilizing the multiplex ELISA assay we quantified IL-4, IL-5, and IL-10 production over time. Consistent with our observations for the proinflammatory cytokines and NO, anti-inflammatory production was influenced heavily by diet (Figure 15). Vitamin D_3 sufficient diet (Suf, Suf+VitD, Suf+EtOH) produced the least of all three cytokines (IL-4, IL-5, IL-10) overall when compared to deficient diet cells, with Suf+VitD producing the minimum at all time intervals. Def cells' production of IL-4, IL-10, IL-5 was vastly different from that of Suf cells, with Def cells producing 1.25-1.75 fold, 1.25-2.4 fold, 1.5-3.5 fold, respectively, more than Suf cells. At 96 and 120h for Suf+EtOH cells anti-inflammatory cytokine production observably increased from 0.8-1.5 fold increase to a fold increase of 1.4-3.0 (Figure 15,). For IL-4, IL-5, and IL-10 Suf+VitD is significantly different from all other conditions (Figure 15). Suf cells differed significantly for all three cytokines when compared to Def, Def+EtOH and Suf+VitD. Suggesting that vitamin D_3 supplementation irrespective of the modulatory effects of its vehicle ethanol, in general supplemented cells were able to act independent of and in conjunction with diet to produce the lowest concentration of anti-inflammatory cytokines within each diet condition.

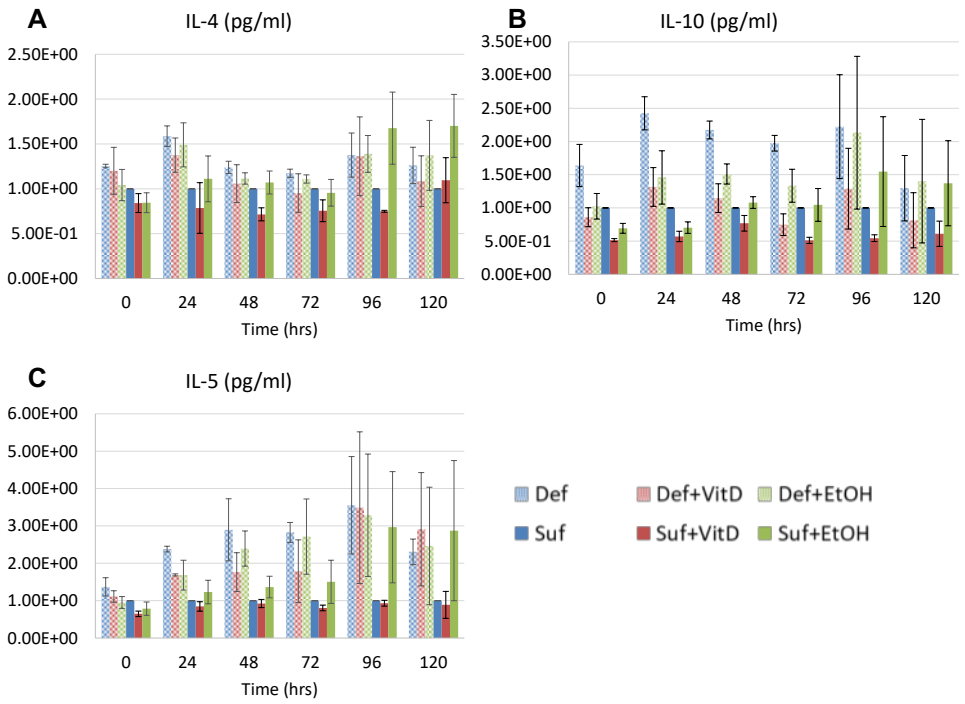

Figure 15. Anti-inflammatory cytokines

Vitamin D_3 diet does not appear to preferentially skew the host cells toward an M1 or M2 response, as cytokine production seems to be categorically down regulated at the majority of time points for Suf diet cells. Even with this apparent downregulation of both anti- and pro-inflammatory cytokine production Suf cells still maintain the lowest amount of cytotoxicity from 48-120h.

<u>Role of cytokines as predictors of immune response outcomes is diet dependent</u>

Significant predictors vary by diet

We used a two-level LMM to determine which immune response variables were predictive of host response driven outcome of *M. bovis* BCG infection given diet, supplementation, or alcohol exposure. Separate LMMs were generated including: (1) an LMM for each immune response outcome of interest: bacterial load (extracellular, intracellular, and combined intra- plus extracellular bacterial load) and LDH (host cell cytotoxicity); and (2) LMMs using data from combined/all diets, data from mice on vitamin D_3 deficient diet (89123), and data from mice on vitamin D_3 sufficient diet (89124). The combinations of (1) and (2) resulted in the generation of 12 different LMMs (Supplementary Tables 4-6). Table 4 lists the

identified significant predictors (Level 1 LMM) for each of the quantified immune response outcomes (intra, extra, sum of intra and extra, and LDH) by diet (coefficients for Suf and Def graphically depicted in Supplementary Figure 6). Diverse sets of assays emerged as significant predictors in an outcome and diet-associated manner, with: Def diet predictors (NO, IL-10, IL-1β,TNF-α) overlapping with combined (Def and Suf) diet predictors (NO, IL-10, IL-1β, KC/GRO TNF-α), but differing from the relatively few Suf diet predictors (IL-5, TNF-α).

Table 11. Significant predictors by diet and immune response outcome used in Level 2 LMM.

All	
Outcome	**Significant cytokine**
log_intra	no, il10, il1b, tnfa
log_extra	il1b
log_intra+extra	no, il10, il1b, tnfa
log_ldh	il1b, kcgro, tnfa

89123	
Outcome	**Significant cytokine**
log_intra	il10, il1b, tnfa
log_extra	il1b
log_intra+extra	no, il10, il1b, tnfa
log_ldh	tnfa

89124	
Outcome	**Significant cytokine**
log_intra	none
log_extra	il5
log_intra+extra	none
log_ldh	tnfa

Immune response outcome predictors were similar between the combined diet and deficient diet models, with KC/GRO emerging as a significant predictor when the diets were combined. Very few significant predictors were identified for the sufficient diet, with only IL-5 and TNF-α emerging as significant predictors of infection outcome for the sufficient diet, and IL-5 being the only differentiating predictor for deficiency. Of the eleven assays that have a significant correlation to outcomes of interest (Table 3, Supplementary Table 4-5), all six of the significant predictors in the LMM level 1 model appear as having significant correlations with outcomes of interest. While four significant predictors (NO, IL-10, IL-1β, TNF-α) emerged for intracellular load for the combined or deficient data set, only TNF-α under sufficient diet had significant correlations to intracellular load. NO is correlated with extracellular load for both diets under alcohol exposure, however it only emerges as a significant predictor for the deficient diet for total bacterial load. Although IL-1β, KC/GRO, and TNF-α are the only predictors identified for the LDH outcome in the LMM analysis, all predictors in the LMMs had significant correlations to LDH outcome regardless of diet, except NO and KC/GRO which correlated to LDH under Def conditions. In

sum, mainly for deficient and combined diets four predictors (NO, KC/GRO, IL-1β, TNF-α) had some consistency between the LMM-based immune response outcomes they associate with and statistically significant correlations with the same outcomes. The relatively lower number of significant predictors for the sufficient diet mirrors the reduced number of correlations between immune response assays and outcomes for the sufficient diet.

Combined diet and treatment LMM reveal IL-1β, TNF-α as key effectors of immune outcome under deficiency.

Table 17 and 18 show the parameter estimates of fixed effects when experimental data from all diets and all conditions were included in the LMM. For intracellular bacterial load, IL-1β accounted for a statistically significant negative reduction ($\beta_{IL\text{-}1\beta}$= -0.0008, p<0.001) and the effect of TNF-α on intracellular load differed significantly by diet ($\beta_{diet*TNF\text{-}\alpha}$= -0.0002, p=0.0358). For extracellular load, time (β_{time}= 0.0148, p<0.0001) and IL-1βB ($\beta_{IL\text{-}1\beta}$= -0.0004, p=0.0309) were positively and negatively related to extracellular bacteria levels. For the total bacterial load (Table 5), results mirrored that of the LMM model for intracellular load. IL-1β contributed negatively to combined load ($\beta_{IL\text{-}1\beta}$= -0.0008, p=0.0093) and the effect of TNF-α differed significantly by diet ($\beta_{diet*TNF\text{-}\alpha}$= -0.0002, p=0.0185). For the LDH LMM, as expected the positive slope associated with time (β_t= 0.0101, p<0.001), concurred that the LDH levels increased over the course of infection. Compared with the control treatment group, alcohol exposure and vitamin D_3 exposure had negative or a reductive effect on LDH levels (β_{etoh}= -0.739, p=0.0082; β_{vitd}= -0.5872, p=0.0314), which is most consistent with observations at early time points post infection.

Table 12. LMM for total bacterial load for the combined diet data set.

Solution for Fixed Effects (ln(intra+extra))					
Effect	**cond1**	**cond2**	**Estimate**	**Standard Error**	**Pr > |t|**
Intercept			11.8184	0.3159	<.0001
Time			-0.00205	0.002977	0.4959
cond1	89123		0.4696	0.3028	0.1304
cond2		+EtOH	0.2896	0.3381	0.3987
cond2		+VitD	-0.2434	0.3488	0.4914
no			0.01424	0.05166	0.7839
il10			0.002493	0.001823	0.1792
il1b			-0.00078	0.000277	**0.0093**
tnfa			0.000161	0.000094	0.0943
no*cond1	89123		0.02803	0.04623	0.5478
no*cond2		+EtOH	-0.00648	0.03668	0.8612
no*cond2		+VitD	0.07212	0.04865	0.1475
il10*cond1	89123		0.000656	0.001686	0.6997
il10*cond2		+EtOH	0.002533	0.002225	0.2599
il10*cond2		+VitD	0.00087	0.00223	0.6978
il1b*cond1	89123		-0.00011	0.000254	0.6799
il1b*cond2		+EtOH	0.000063	0.000356	0.8614
il1b*cond2		+VitD	0.000162	0.000322	0.6209
tnfa*cond1	**89123**		-0.00022	0.00009	**0.0185**
tnfa*cond2		+EtOH	-0.00021	0.000114	0.0691
tnfa*cond2		+VitD	-0.00002	0.000107	0.842

Vitamin D_3 deficient LMM. None of the previously identified predictors, time, or treatment effect, had significant effects on intracellular load (Table 17 and 18). Other than the temporally associated positive increase of extracellular load (β_{time}= 0.008, p=0.026) and LDH (β_{time}= 0.019, p<0.001), IL-10 and IL-1β were the only other notable predictors of infection outcome for Def cells. IL-10 and IL-1β positively and

negatively, respective, affected total bacterial load (β_{IL-10}= 0.0033, p=0.025; $\beta_{IL-1\beta}$= -0.0009, p=0.025).

Vitamin D_3 sufficient LMM. For intracellular and total bacterial load, no significant predictors were identified for the vitamin D_3 sufficient diet's immune outcome variables (Supplementary Table 6). Similar to the Def LMM, the temporal increase of extracellular bacterial load was statistically significant (β_{time}= 0.0147, p=0.012). The LMM analysis for Suf showed that in addition to temporally increasing, TNF-α had a significant positive effect on LDH levels (β_{time}= 0.0131, p<0.0001; $\beta_{TNF-\alpha}$= 0.0001, p=0.04). TNF-α in conjunction with vitamin D_3 supplementation or alcohol exposure was found to have an increasing effect relative to control on LDH ($\beta_{TNF-\alpha*etoh}$= 0.0002, p=0.008; $\beta_{TNF-\alpha*vitd}$= 0.0002, p=0.002).

Correlations in immune response have a diet dependent skew

We examined correlations between assays within each condition using non-normalized concentration and rate of change data; correlations with a p-value of p<0.05 are reported (Table 15, 16). Results showed condition-associated trends in correlation. Deficient diet cells had the most significant correlations overall (56) while Suf+EtOH had the least (37) (Table 15, 16). The reduced correlation in Suf+EtOH may further support our hypothesis regarding the dysregulating effect of alcohol, which we expand on in the discussion. Cytotoxicity was found to be positively correlated for all conditions to IFN-γ, IL-10, IL-12, IL-1β, IL-2, IL-4, IL-5. Cytotoxicity was positively correlated to KC/GRO for Def and Def+EtOH, and to IL-6, TNF-α for Def cells. These correlations suggest a close tie between cytotoxicity and cytokines stratified by in vivo diet conditioning (Figure 4, 6). IL-6, TNF-α, and KC/GRO varied most significantly at 0h but do show some differences in concentration in Def diet cells, which is reflected in the correlation to cytotoxicity. NO correlations appeared most prevalent in vitamin D_3 sufficient diet conditions (Suf, Suf+VitD, Suf+EtOH) with NO production positively correlating to IFN-γ, IL-12, IL-2, IL-4, IL-5 production. IFN-γ positively correlated to cytotoxicity, IL-10, IL-12, IL-1β, IL-2, IL-4, IL-5 for all conditions. Similarly, IL-12 positively correlated to cytotoxicity, IL-1β, IL-2, IL-4, IL-5 for all conditions. TNF-α positively correlated to IFN-γ, IL-10, IL-2, IL-4, IL-5, IL-6 for all vitamin D3 deficient diet conditions (Def, Def+VitD, Def+EtOH). Interestingly IL-6 production correlated positively to intracellular (Suf, Suf+VitD) and extracellular (Suf) BCG bacterial load, tying the correlation between IL-6

and bacterial load to in vivo vitamin D_3 bioavailability. We found no statistically significant negative correlations for concentration of immune response variables.

Table 13. Time interval rate of change Welch's t Test

		0-48	24-72	48-96	72-120
Intracellular Bacteria					
Suf	Suf+VitD				0.015
Extracellular Bacteria					
Def	Suf			0.032	0.009
Cytotoxicity					
Def+EtOH	Suf	0.019			
Suf	Suf+EtOH		0.002		
Suf	Suf+VitD		0.033		
Nitric Oxide					
Def	Suf		0.016	0.041	
Def	Suf+VitD		0.022		
IL-1β					
Suf	Suf+VitD	0.006			
IFN-γ					
Def	Suf		0.001		
Def	Suf+VitD		0.039		
Def+EtOH	Suf		0.046		
IL-2					
Suf	Suf+EtOH	0.050			
KC/GRO					
Suf	Suf+VitD	0.044			
Def+EtOH	Suf		0.022		
IL-6					
Suf	Suf+VitD	0.004			
Def+EtOH	Suf+VitD	0.013	0.042		
Def+EtOH	Suf+EtOH	0.038	0.044		
Def	Suf+VitD		0.035		
Def	Suf+EtOH		0.038		
IL-4					
Def	Suf		0.014		
IL-5					
Def+EtOH	Suf	0.028			

Our non-normalized concentration correlations were mainly positive and often spanned across all conditions. However, the rate of change correlations were found primarily in vitamin D_3 deficient diet

cells, with Def cells having the most rate of change correlations (37) and Suf+EtOH cells having the least (16). Non-normalized rate of change data presented with numerous diet dependent correlations. IL-5 had positive rate of change correlations in sufficient diet cells only with IFN-γ, IL-12, IL-4(Suf, Suf+VitD, Suf+EtOH), IL-1β (Suf+VitD), IL-2 (Suf), IL-10 (Suf, Suf+VitD). Notably, there were no IL-5 associated correlations for deficient conditions. Intracellular and extracellular BCG bacterial load rates of change were positively correlated for Suf+EtOH and Suf+VitD conditioned cells. Cytotoxicity and NO rates of change positively correlated for Def+EtOH Rates of change for KC/GRO, TNF-α, and IL-6 were positively correlated to each other, for every condition. We observed some negative correlations for rate of change, whereas there were none for the non-normalized concentration dataset. The majority of negative correlations were associated with the vitamin D assay results. Negative correlations occurred between vitamin D_3 assay and IL-5 rates of change for Def and Suf cells but not their supplemented or alcohol exposed counterparts (Suf+VitD, Suf+EtOH, Def+VitD, Def+EtOH), indicating a possible disruption of vitamin D_3 associated interactions by the addition of ethanol, the vitamin D_3 solvent. Vitamin D rate of change assay results were found to negatively correlate with IL-12 for Suf diet cells, a result which is supported heavily in literature and consistent with our prior observations for in vitro studies using low levels of mycobacterial infection (MOI 1:1) [100]. Negative rate of change correlations were observed between vitamin D levels and IFN-γ for Suf and Suf+VitD; this relationship is corroborated by previous studies conducted predominately with T cells.

Discussion

In the current extension of our study we examined the effects of in vivo vitamin D_3 deficiency on ex vivo *M. bovis* BCG infection and supplementation/alcohol exposure. We found that while exogenous conditioning of the cells did result in altered macrophage behavior, in vivo diet was the greatest determinant of cytokine and effector molecule production in response to bacterial challenge. The ramifications of extended in vivo vitamin D_3 deficiency had a lasting effect on host immune responsiveness, which persisted nearly two-weeks post cell isolation (12 days, including 7 days of ex vivo maturation plus 5 days infection study). For all anti-inflammatory cytokines diet was the greatest determinant for differences in concentration and rate of change of immune response variables; this diet-based distinction occurred for the majority of pro-inflammatory cytokines (IL-12, IL-1β, IFN-γ, and IL-2).

However, exogenous supplementation of vitamin D_3 or ethanol exposure further stratified cytokine/effector production.

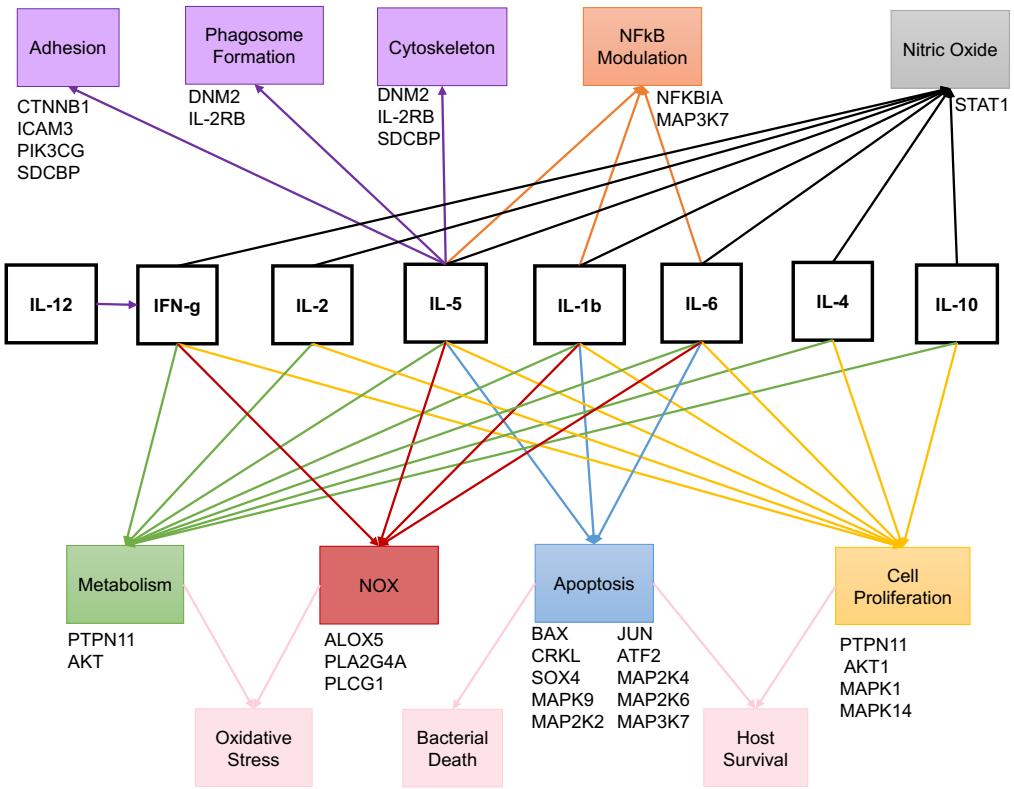

Figure 16. Correlation-based component analysis

Analysis of vitamin D_3 associated cytokine signaling and crosstalk

Using correlations from both non-normalized concentration and rate of change data we identified several instances in which diet and supplementation influenced the relationship between cytokines. In some cases correlations were more prevalent in vitamin D_3 sufficient diet cells (IL-5 rate of change), in deficient diet cells (IL-1β, IL-6 rates of change), or held across all conditions (concentrations of IL-1β, IL-4, IL-10, IL-5, IFN-γ, IL-2). By examining differences and commonalities among diet or supplementation associated correlations we were able to characterize the mechanistic action of vitamin D_3 and the immunological impact of deficiency/sufficiency. Using the presence or absence of diet associated correlations as a guide, we identified commonalities and differences in cytokine related signaling pathways and their components using the NetPath database [122]. Among cytokine correlations that held across all diet conditions (concentrations of IL-1β, IL-4, IL-10, IL-5, IFN-γ, IL-2) we identified which components

were present among the majority of cytokine pathways. The same analysis was applied to correlations that stratified by diet (IL-5, IL-1β, IL-6 rates of change). Using this comparative approach we eliminated non-correlation and non-diet associated components, and organized resulting components into functional groups (Figure 7, Supplementary Figure 7) related to cytokines differentially modulated by vitamin D_3. While there are additional known links between cytokines analyzed and functional groups, connections shown are relevant to diet-associated correlations and suggest possible mechanisms through which vitamin D_3 is able to modulate immune response to mycobacterium infection.

Vitamin D_3 modulates connections between signaling pathways

IL-1β, TNF-α, IL-6, and IL-12 signaling pathways disrupted in vitamin D_3 sufficient cells

IL-1β receptor is known to stimulate the production of IL-6 and TNF-α. We found that IL-1β correlates to IL-6 and TNF-α in Def diet cells only, but correlates to all Def conditions for KC/GRO (Def, Def+VItD, Def+EtOH). From these results we presume that vitamin D_3, introduced both through diet and supplementation, as well as, alcohol exposure, disrupts or interferes with the pathway connecting IL-1β with TNF-α and IL-6. Vitamin D_3 is a known inhibitor of NF-κB, a modulator down stream of the IL-1β receptor that leads to the transcription of TNF-α and IL-6 [123]. While vitamin D_3 is widely accepted as an NF-κB inhibitor the role of alcohol in relation to NF-κB is not yet clear. Some studies report that alcohol is able to downregulate the production of NF-κB, this downregulation might explain the decreased production of TNF-α, IL-6, and KC/GRO in Def+EtOH cells, which was below that of Def cells [124]. NF-κB is also thought to be downregulated by vitamin D_3 during infection [125]. We have identified two components (NFKBIA, MAPK3K7) contained in the signaling pathway of some of the pro-inflammatory cytokines we found to be modulated by vitamin D_3. NFKBIA, an inhibitor of NF-κB, is associated with the signal pathways for IL-5, IL-1β, and IL-6. MAPK3K7, a positive regulator of NF-κB, is found in the signaling pathway of IL-6 and IL-1β. These components and their regulation may help explain the mechanism through which vitamin D_3 downregulates NF-κB within the system.

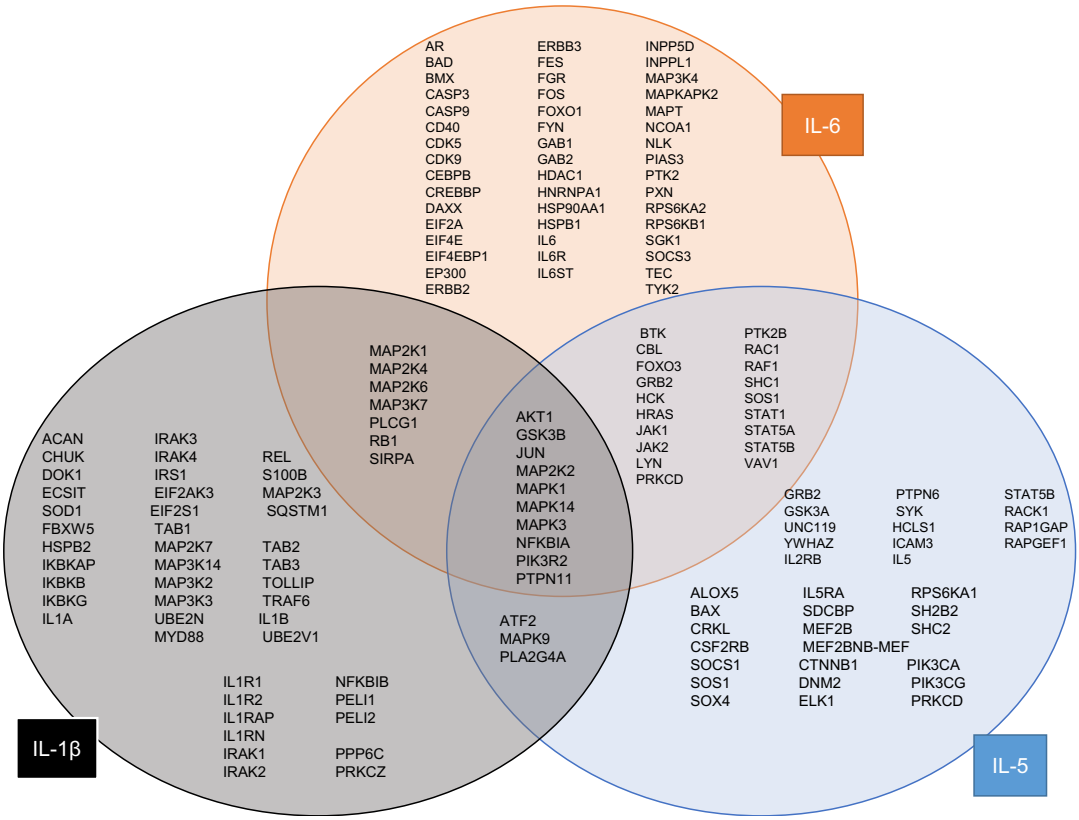

Figure 17.Venn Diagram of IL-6, IL-1β, and IL-5 Components

We also found that IL-6 is positively correlated to IL-12 in Def diet cells only (Def, Def+VitD, Def+EtOH). IL-6 has been shown to inhibit SOCS3 and SOCS3 has been shown to inhibit the production of IL-12 [110], [126] . The lack of IL-6/IL-12 correlation for Suf diet cells suggests that vitamin D_3 sufficiency in vivo may disrupt IL-6 mediated inhibition of SOCS3, therefore disrupting IL-6 downstream effect on IL-12. Across all conditions IL-12 positively correlates to IFN-γ, IL-4 to IFN-γ, and IL-12 to IL-4. Previous studies have found the IL-12 may auto-stimulate the endogenous production of IFN-γ in macrophage cells [110], [127], but it is not yet known if IL-12 is able to influence the production of IL-4.

IL-5, IL-12, and IFN-γ **correlations present in vitamin D_3 sufficient diet cells**

Our results found that vitamin D_3 supplementation in conjunction with vitamin D_3 sufficient diet, resulted in a decrease in anti-inflammatory and pro-inflammatory cytokines below that of ethanol exposed (Suf+EtOH) and often below unconditioned cells as well (Suf). The rate of change of IL-5 positively correlated with the rate of change of IFN-γ, IL-10, IL-12, IL-1β, IL-2, IL-4 in Suf diet cells, indicating IL-5

is able to affect both the JAK/STAT and MAPK pathways. Additionally we found that vitamin D_3's rate of change was negatively correlated to IL-5, IL-12, and IFN-γ for Suf diet cells. Previous studies have found IL-5 stimulates the upregulation of the IL-2Rβ chain[128]. IFN-γ, IL-4, IL-5 may be produced through the same pathway in macrophages [129]. Though IFN-γ is primarily produced by T-cells, several studies have reported that infected macrophages are able to produce small quantities of IFN-γ for the purpose of auto-stimulation. IFN-γ was found to be positively correlated to cytotoxicity, IL-10, IL-12, IL-1β, IL-2, IL-4, IL-5 for all conditions [110]. IFN-γ production in T-cells is commonly associated with the presence of TNF-α, IL-6, and IL-12, however we only observed IL-12 as positively correlated with IFN-γ over all conditions. Previous works have proposed that macrophages express an IL-12 receptor and are potentially able to upregulate their own IL-12 production and produce small amounts of IFN-γ through this receptor [110], [130]. This potential mechanism may explain the positive correlation between IL-12 and IFN-γ, however additional studies exploring the endogenous production of IFN-γ by macrophages are needed to further clarify these interactions.

Table 14. Rate of Change t Test table

	Def	**Def+VitD**	**Def+EtOH**	**Suf**	**Suf+VitD**	**Suf+EtOH**
Def						
Def+VitD					TNF-α	
Def+EtOH					IL-6, KC/GRO, TNF-α	IL-6
Suf	*Extra, IFN-γ, IL-10, IL-4, IL-5, VitD*	*Extra, IFN-γ, IL-1β, IL-5, KC/GRO*	*IL-12, IL-2, IL-5, TNF-α*		IL-6	
Suf+VitD	*IL-10, KC/GRO*		*IL-6, KC/GRO, TNF-α*	*IL-1β, IL-5, IL-6, intra, KC/GRO*		
Suf+EtOH	*IFN-γ, IL-10, IL-2*			*IFN-γ, IL-5, Cytotox*		

Table 15. Non-normalized Date Pearson Correlation Heatmap

		Def coeffcient	Def+VitD coeffcient	Def+EtOH coeffcient	Suf coeffcient	Suf+VitD coeffcient	Suf+EtOH coeffcient
Cytotox	IFN-γ	0.796	0.677	0.901	0.777	0.857	0.791
Cytotox	IL-10	0.826	0.659	0.865	0.819	0.771	0.826
Cytotox	IL-12	0.699	0.667	0.771	0.696	0.776	0.788
Cytotox	IL-1β	0.874	0.884	0.919	0.913	0.868	0.862
Cytotox	IL-2	0.750	0.586	0.784	0.622	0.743	0.771
Cytotox	IL-4	0.796	0.666	0.841	0.692	0.843	0.866
Cytotox	IL-5	0.867	0.697	0.714	0.722	0.914	0.793
Cytotox	IL-6	0.679					
Cytotox	KC/GRO	0.690		0.594			
Cytotox	TNF-α	0.669					
IFN-γ	TNF-α	0.922	0.898	0.750			
IL-10	IFN-γ	0.959	0.812	0.976	0.962	0.876	0.888
IL-10	TNF-α	0.876	0.809	0.774		0.603	
IL-12	IFN-γ	0.975	0.930	0.933	0.962	0.968	0.994
IL-12	IL-10	0.950	0.884	0.934	0.973	0.893	0.848
IL-1β	IFN-γ	0.895	0.748	0.920	0.844	0.856	0.892
IL-1β	IL-10	0.922	0.806	0.931	0.920	0.902	0.899
IL-1β	IL-12	0.843	0.847	0.891	0.856	0.868	0.877
IL-2	IFN-γ	0.980	0.967	0.953	0.951	0.933	0.726
IL-2	IL-10	0.934	0.840	0.948	0.926	0.856	
IL-2	IL-12	0.974	0.951	0.877	0.947	0.917	0.759
IL-2	IL-1β	0.839	0.688	0.816	0.730	0.726	
IL-2	TNF-α	0.964	0.943	0.899	0.746	0.751	
IL-4	IFN-γ	0.992	0.991	0.959	0.976	0.972	0.944
IL-4	IL-10	0.944	0.809	0.935	0.958	0.868	0.824
IL-4	IL-12	0.951	0.934	0.981	0.982	0.968	0.951
IL-4	IL-1β	0.874	0.754	0.921	0.811	0.910	0.810
IL-4	IL-2	0.957	0.955	0.870	0.957	0.843	0.902
IL-4	TNF-α	0.899	0.904	0.644	0.620		
IL-5	IFN-γ	0.892	0.843	0.755	0.994	0.962	0.882
IL-5	IL-10	0.894		0.726	0.948	0.929	0.859
IL-5	IL-12	0.845	0.674	0.587	0.961	0.912	0.862
IL-5	IL-1β	0.904		0.651	0.799	0.906	0.723
IL-5	IL-2	0.826	0.778	0.754	0.970	0.914	0.733
IL-5	IL-4	0.890	0.795	0.599	0.980	0.923	0.888
IL-5	TNF-α	0.686	0.625	0.617	0.601		
Extra	IL-6				0.632		
IL-6	IFN-γ	0.932	0.905	0.727		0.596	
IL-6	IL-10	0.889	0.790	0.751		0.604	
IL-6	IL-12	0.942	0.868	0.661			0.576
IL-6	IL-1β	0.743					
IL-6	IL-2	0.974	0.953	0.887	0.744	0.808	
IL-6	IL-4	0.911	0.899	0.603	0.597		
IL-6	IL-5	0.709	0.661	0.639	0.605	0.578	
IL-6	TNF-α	0.993	0.986	0.985	0.978	0.953	0.971
Intra	Extra					0.802	0.776
Intra	IL-6				0.620	0.681	
Intra	TNF-α					0.621	
KC/GRO	IFN-γ	0.938	0.922	0.820	0.619		0.614
KC/GRO	IL-10	0.889	0.854	0.841	0.607	0.680	0.596
KC/GRO	IL-12	0.942	0.930	0.785	0.641		0.644
KC/GRO	IL-1β	0.752	0.653	0.642			
KC/GRO	IL-2	0.975	0.968	0.944	0.786	0.818	
KC/GRO	IL-4	0.918	0.922	0.733	0.669		
KC/GRO	IL-5	0.713	0.654	0.641	0.650	0.602	
KC/GRO	IL-6	0.999	0.985	0.975	0.974	0.956	0.967
KC/GRO	TNF-α	0.996	0.989	0.987	0.997	0.993	0.994
NO	Cytotox	0.670	0.629				
NO	Extra			0.611			0.598
NO	IFN-γ				0.708		
NO	IL-10						0.590
NO	IL-12				0.588		
NO	IL-2				0.659		
NO	IL-4				0.600		
NO	IL-5		0.890	0.913	0.711		0.720
TNF-α	IL-12	0.933	0.883	0.708	0.589		
TNF-α	IL-1β	0.732					

Legend
1.000
0.900
0.800
0.700
0.600
0.500

Table 16. Non-normalized Rate of Change Correlation Heatmap.

		Def	Def+VitD	Def+EtOH	Suf	Suf+VitD	Suf+EtOH		
		coeffcient	coeffcient	coeffcient	coeffcient	coeffcient	coeffcient		Legend
Cytotox	Extra					-0.694			1.000
Cytotox	intra			-0.843					0.900
Cytotox	NO						0.767		0.700
IL-10	IFN-γ	0.918		0.923	0.806				0.500
IL-12	IFN-γ	0.970	0.920	0.944	0.910	0.930	0.988		0.000
IL-12	IL-10	0.892	0.763	0.839	0.888				-0.500
IL-1β	IFN-γ	0.834	0.684	0.879					-0.700
IL-1β	IL-10	0.855	0.871	0.942	0.757	0.878	0.856		-0.900
IL-1β	IL-12	0.734	0.821	0.805					
IL-2	IFN-γ	0.960	0.952	0.925	0.892		0.757		
IL-2	IL-10	0.870	0.736	0.881	0.888				
IL-2	IL-12	0.936	0.965	0.825	0.918	0.922			
IL-2	IL-1β	0.802	0.707	0.836					
IL-4	IFN-γ	0.986	0.992	0.955	0.912	0.989	0.887		
IL-4	IL-10	0.925		0.832	0.782				
IL-4	IL-12	0.940	0.893	0.988	0.943	0.897	0.928		
IL-4	IL-1β	0.817		0.820					
IL-4	IL-2	0.913	0.948	0.822	0.897	0.683	0.862		
IL-5	IFN-γ				0.966	0.706	0.730		
IL-5	IL-10				0.746	0.833			
IL-5	IL-12				0.911	0.689	0.771		
IL-5	IL-1β					0.888			
IL-5	IL-2				0.906				
IL-5	IL-4				0.961	0.757	0.731		
IL-6	IFN-γ	0.947	0.935	0.915					
IL-6	IL-10	0.862	0.720	0.841	0.788				
IL-6	IL-12	0.890	0.924	0.809	0.694				
IL-6	IL-1β	0.795	0.706	0.761					
IL-6	IL-2	0.969	0.970	0.983	0.784	0.823			
IL-6	IL-4	0.931	0.930	0.812					
Intra	Extra					0.794	0.808		
KC/GRO	IFN-γ	0.944	0.908	0.915					
KC/GRO	IL-10	0.852	0.764	0.835	0.800				
KC/GRO	IL-12	0.880	0.936	0.823	0.675				
KC/GRO	IL-1β	0.783	0.752	0.775					
KC/GRO	IL-2	0.958	0.966	0.982	0.768	0.772			
KC/GRO	IL-4	0.935	0.897	0.831					
KC/GRO	IL-6	0.998	0.993	0.996	0.976	0.901	0.951		
TNF-α	IFN-γ	0.939	0.902	0.916					
TNF-α	IL-10	0.857	0.753	0.842	0.782				
TNF-α	IL-12	0.882	0.915	0.808					
TNF-α	IL-1β	0.749	0.715	0.738					
TNF-α	IL-2	0.949	0.959	0.972	0.753	0.736			
TNF-α	IL-4	0.936	0.890	0.808					
TNF-α	IL-6	0.992	0.988	0.996	0.976	0.901	0.946		
TNF-α	KC/GRO	0.996	0.994	0.986	0.999	0.997	0.996		
VitD	IFN-γ				-0.756	-0.770			
VitD	IL-12				-0.751				
VitD	IL-4					-0.814			
VitD	IL-5	-0.827			-0.671				
VitD	KC/GRO						-0.739		
VitD	TNF-α						-0.723		

Modulation of bacterial clearance mechanisms

Vitamin D_3 impacts adhesion and cytoskeletal proteins

IL-5 showed rate of change correlations primarily in vitamin D_3 sufficient diet, therefore we focused on pathway components unique to IL-5 and examined possible mechanisms related to our findings and findings from other studies. We recurrently discovered adhesion and cytoskeleton proteins, most notably CTNNB1, ICAM3, IL-2RB (Figure 7, Supplementary Figure 7). Previous studies have found that vitamin D_3 plays a large role in the bioavailability of CTNNB1, which is heavily involved in the Wnt pathway [131], ICAM3, a ligand for lymphocyte function associated antigen 1 [132], and IL-2RB, an IL-2 receptor [81]. These components may contribute to phagocytosis-associated bacterial clearance, which is a mechanism potentially modulated by vitamin D_3 and could contribute to the differences in bacterial load between the conditions. We noted that ethanol suppresses adhesion molecules necessary for phagosome formation, which is consistent with the high extracellular load present in ethanol exposed cells [133]

Vitamin D_3 deficiency has long-term effect on effector molecule usage and production

Results from the vitamin D assay suggest a dysfunction of the enzymatic conversion between active and inactive vitamin D_3. At all time points levels of vitamin D_3 are highest for Def+VitD cells, with the most noticeable variations at 48, 72h. Based on these results we postulate that the age of onset of vitamin D_3 deficiency has long-term consequences on the function of vitamin D_3 enzymes, with the relatively early onset of deficiency in our study resulting in an underutilization of exogenously supplemented vitamin D_3.

We found that the majority of our cytokines measured contained STAT1 component in their pathway (IFN-γ, IL-6, IL-5, IL-1β, IL-10, IL-2, IL-4). STAT1 is a known upregulator of iNOS (inducible nitric oxide synthase), which produces nitric oxide. For 0, 24h we observed vitamin D_3 supplemented cells (Def+VItD, Suf+VitD) producing similar levels of NO to their diet counterparts (Def+EtOH, Def+VItD). From 48-120h we observed a very different response, vitamin D_3 supplementation (Def+VItD) reduces NO production below that of alcohol exposed cells (Def+EtOH, Def+VItD). At several time points supplementation reduces NO production below that of Def/Suf diet cells. Results indicate that vitamin D_3

supplementation impacts the production of NO in a temporal manner, reducing the production of NO over time. Alcohol exposure has a dysregulatory effect most notably increasing NO levels for Suf cells in comparison to Def cells, and is able to affect the production of NO earlier in Def cells.

Correlations of IL-5's rate of change and IL-1β's rate of change with that of other cytokines' were impacted by vitamin D_3 sufficiency or deficiency, respectively. We found arachidonate 5-lipoxygenase (ALOX5) and type ll phospholipase A2 (PLA2G4A), components of IL-5 and IL-1β pathways, are key in NADPH oxidase complex formation (NOX) (Figure 7). ALOX5 is an enzyme that converts arachidonic acid into leukotrienes, which mediate an inflammatory response and leads to the formation of NOX [134], [135]. PLA2G4A is an enzyme that catalyzes the release of arachidonic acid from membrane phospholipids. Arachidonic acid release and PLA2G4A are heavily dependent on calcium bioavailability and may relate to vitamin D_3's classical function as an inducer of calcium absorption into the cell [136].

Coordination of cell proliferation, energy metabolism, and apoptosis

Previous studies have linked vitamin D_3 and PTPN11, AKT1, MAPK, and MAPK14 [137]–[140], which are components involved in the signaling mechanism of several of the cytokines vitamin D_3 differentially modulates (IL-1β, IL-4, IL-10, IL-5, IFN-γ, IL-2) (Figure 7, Supplementary Figure 7). MAPK1 and MAPK14 are linked closely with cell proliferation, while PTPN11 and AKT1 have been shown to modulate cell proliferation and mitochondrial metabolism, leading to oxidative stress [140]–[143]. This may indicate a possible mechanism for vitamin D_3's modulation of oxidative stress and increased host cell survival.

Inhibition of apoptosis

IL-5 exhibited notable rate of change correlations primarily in vitamin D_3 sufficient diet. Differing from IL-5, both IL-1β and IL-6 primarily had rate of change correlations in deficient diet cells. However only IL-5 and IL-1β concentrations also correlated with cytotoxicity levels across both diets. We compared these cytokines due to their stratified rate of change correlations and found a number of components along the IL-5 and IL-1β signaling pathway that are heavily involved in the modulation of apoptosis, including BAX [144], CRKL [145], and various others (Figure 7) [146]–[149]. The functional

commonalities of these components suggest that modulation of apoptotic pathways in Suf diet cells is IL-5 dependent, while deficiency engenders a more IL-1β dependent modulation of apoptotic processes. Extracellular load was decreased by vitamin D_3 supplementation in the case of both vitamin D_3 deficient and sufficient diets, with loads below that of alcohol exposed cells at a majority of time intervals. Given that dysregulation of apoptosis can lead to higher extracellular bacteria, IL-5 associated modulation of apoptotic and cell proliferation pathways indicates a possible mechanism through which vitamin D_3 sufficient diet cells are able to maintain significantly lower cell toxicity levels and, in comparison to deficient diet cells, comparable or slightly lower extracellular bacteria loads.

Activation of cell proliferation, energy metabolism

Previous studies have linked vitamin D_3 with PTPN11, AKT1, MAPK, and MAPK14 [137]–[140], all of which are components involved in the signaling mechanism of several of the cytokines vitamin D_3 differentially modulates (IL-1β, IL-4, IL-10, IL-5, IFN-γ, IL-2, IL-6) (Figure 7). MAPK1 and MAPK14 are linked closely with cell proliferation. PTPN11 and AKT1 have been shown to modulate cell proliferation and mitochondrial metabolism, leading to oxidative stress [140]–[143]. Differential modulation of cytokine signals transduced through these components hints at a possible mechanism by which vitamin D_3 can temper oxidative stress and increase host cell survival.

Diet and condition-associated differentiating effects of cytokines impact the outcome of immune response to infection

While statistical analysis helped identify immune responses that were different or correlated as a result of the treatment (vitamin D_3 diet, exogenous supplementation, or alcohol exposure), LMM analyses enabled us to investigate whether diet impacted the cytokines that emerged as significant in determining outcome of infection. Time had a significant positive effect on extracellular bacterial load and LDH across all three LMMs, implying that, controlling for all other predictors or factors, extracellular bacterial load and LDH levels increased over time, which is expected for this BCG infection level. Diet alone did not have a significant predictive effect in the combined LMM, but treatment had a significant effect on LDH (lower

LDH relative to control treatment for ethanol and vitamin D_3). However, diet had a significant effect on the relationship between TNF-α and intracellular or total bacterial load. Mirroring the diet associated skew observed for rate of change correlations, IL-1β had a negative effect on total bacterial load in the combined LMM and the vitamin D_3 deficient LMM. Additionally, IL-1β had a negative effect on intra and extracellular load in the combined LMM. This suggests that IL-1β is a critical immune response variable in determining mycobacterium load particularly in vitamin D_3 deficient individuals, which is consistent with IL-1β's signaling pathway components that affect apoptosis, NOX and NO formation. The LMM analysis provided a flexible analytic approach for understanding the impact of cell condition and cytokines on infection outcomes. However, due to the relatively small sample size given the number of immune response variables that are potential predictors, the LMM had an increased risk of insufficient power and occurrence of type II errors. Additional replicates are needed to produce a more predictive model.

Conclusion

Our study has examined the ramifications of vitamin D_3 deficiency, in combination with supplementation and alcohol exposure during mycobacterium infection. By quantifying the effects of both in vivo diet and ex vivo vitamin D_3 supplementation, we were able to investigate immunological connections that were minimally explored in other studies. Overall results demonstrate the benefit of in vivo sufficiency, and suggest that vitamin D_3 is beneficial as a 'rescue' supplement in deficient host but not sufficient host, which in part is due to the vehicle utilized for ex vivo supplementation. As in our previous study, the efficacy of immune response during ex vivo infection was greatly diminished by deficiency and severely impaired by the addition of ethanol during infection. Cytokines significantly differed between conditions. More notably, production was primarily stratified by diet, with sufficient diet (Suf) and sufficient diet plus supplementation (Suf+VitD) differing from deficient diets (Def, Def+VitD, Def+EtOH). Alcohol exposure (Suf+EtOH) continued to have a dysregulating effect and vary from other Suf conditions, with vitamin D_3 deficient diet (Def, Def+VitD, Def+EtOH) and sufficient/alcohol exposed cells (Suf+EtOH) resulting in similar infection responses characterized by high amounts of host cell death and similar cytokine levels.

Diet-associated correlation of cytokines and the relation to functional components within their signaling pathways provided a novel insight into the mechanistic impact of vitamin D_3 deficiency and alcohol exposure on immune response to infection. The stratification of Suf associated IL-5 and Def associated IL-1β response indicates a clear difference in the immunological profile of the sufficient versus deficient host, with variations related to phagocytosis, NOX/NO effector production, apoptosis, and cell proliferation pathways. The lower number of Suf-associated significant correlations and LMM predictors, particularly pro-inflammatory predictors, is potentially indicative of the robustness of the vitamin D_3 sufficient diet's immune response system, which appears resilient to infection-associated perturbations. Conversely, the increased correlations and predictors for the Def condition potentially reflect the concerted effort of the Def immune system to respond simultaneously to infection and diet or alcohol-related stress. These results provide a basis for further investigation of potential mechanisms driving the compounding effect of nutrition and alcoholism on infection related immune response.

Chapter 4 In silico model of the regulatory effects of vitamin D3 on immune-relevant cytokines and effector molecules during mycobacterium infection

Introduction

In silico model of the uptake and metabolic use of vitamin D3 to modulate gene regulation.

Using a quantitative systems biology approach in the study of host pathogen interactions allows for the description of large networks of interacting components and for the extension of traditional interaction diagrams to dynamic predictive mathematical models [150]. Our transdisciplinary approach combines empirical data generation and computer based simulations to capture the mechanistic effects of vitamin D_3 deficiency on mycobacterium-infected murine cells. This allows us to build a platform for predicting the dynamic *in vitro* response of the murine host macrophage cell when infected in a vitamin D_3 insufficient or sufficient environment. Our simulation of the mechanistic pathway through which vitamin D_3 is able to modulate the production of immune-relevant cytokines will provide insight into the downstream effects of vitamin D_3; an effect only superficially and correlatively defined previously.

Alveolar macrophages are an important line of defense in *Mycobacterium* infection. Macrophages are known to express vitamin D receptors (VDR) and are able to produce the enzyme Cyp27B1 (1α–hydroxylase). Cyp27B1 is able to convert 25-hydroxyvitamin D_3 to biologically active 1α,25-dihydroxyvitamin D_3 [24]. The inactive form, 25-hydroxyvitamin D_3, accounts for the majority of vitamin D3 circulating throughout the host body, though the active form incites a much more acute response.

Classically, vitamin D_3 is commonly associated with the absorption of calcium and phosphorous, however interest in its non-classical role in immune regulation has become increasingly important, particularly given the high rates of vitamin D_3 deficiency in the adult population [33]. The active form of vitamin D_3 (1α,25-dihydroxyvitamin D_3) has been found to have a profound effect on the production of tumor necrosis factor alpha (TNF-α), interleukin-6 [24], interleukin-10 [26], as well as interleukin-1β [5]. D_3 encourages activation of murine macrophage cells and the formation of multinucleated giant cells [29]. The adaptation of the behavior of the immune cell leads to a modulated response better equipped to deal with infection and preservation of host cells. There is currently not a well-established model of macrophage immune response during modulation by vitamin D_3 and there is very little information regarding the kinetics

of this process. Of the models that exist several lack volumetric conversion, do not account for enzymatic reactions (using purely first order rate reactions), are qualitative in their mechanistic descriptive equations, and lack supporting information regarding the generation of their parametric data [10], [55], [151], [152]. Modeling the mechanistic pathway through which vitamin D_3 is able to dynamically impact the behavior of host cells will provide insight into the ramifications of host vitamin deficiency and infection; as well as potential ways to manipulate host immune response through these pathways.

The key output of of our model is vitamin D3 dependent production of Interleukin-10 (IL-10). IL-10 is a key immunosuppressive cytokine produced by macrophages and other immune cells. The primary function of IL-10 is to limit inflammatory response, skewing the host cell to a Th-2 anti-inflammatory response and thus aiding in the perseverance of host cells. In addition IL-10 is able to regulate growth and differentiation of immune cells, along with many other functions [40], [41].

LAM (lipoarabinomannan) is a component of the mycobacterial cell wall, and a primary virulence factor for mycobacterium, enabling the bacteria to infect macrophage cells. It also plays a role in mycobacterium's ability to evade host immune response by preventing apoptosis of host cell, and the fusion of the phago-lysosme [44]. LAM activates the NF-κB signaling cascade by binding to membrane bound toll-like receptor TLR-4, which phosphorylates MyD88 inside the host cell. This cascade leads to the destruction of the IκB binding protein, resulting in the release of NF-κB into the cytoplasm. NF-κB then enters the nucleus and acts as a transcription factor for the enzyme Cyp27B1. Cyp27B1 is known to be upregulated by the binding of TLR-4, TLR-2, and TLR-1 but the exact mechanism by which transcription is regulated is yet unknown [31], [34],[153],[154].

Albumin and vitamin D_3 binding protein (VDBP) transport 25-hydroxyvitamin D_3 and very small quantities of 1α,25-dihydroxyvitamin D_3 to site of infection. 10-20% of D3 is bound to albumin, 80-90% bound to DBP and 0.02-0.05% is free [155]. This is the case for both inactive and active forms of vitamin D_3. Bound D_3 then enters the cytoplasmic compartment, where the binding proteins are degraded and the inactive form of vitamin D_3 (IVD) is enzymatically transformed by Cyp27B1 to its biologically active form (AVD). The active form of vitamin D_3 is then bound to the vitamin D receptor protein (VDR). It is transported into the nucleus and binds to the retinoic acid-retinoic acid receptor complex (RXR:RA), which

forms a heterodimer that is able to act as a transcription factor [31]. The heterodimer binds to corresponding vitamin D response elements (VDRE) found in the promoter region of the target gene, which is consequently up- or down-regulated, resulting in an increase or decrease of production of that protein. The VDRE is found on numerous genes for both humans and mouse including IkB, IL-10, HAMP [156], which are found in both, CAMP [157] and DEFB4[34] found only in humans, as well as numerous others. In this model we focus on the upregulation of IL-10 in the presence of vitamin D_3 and infection.

Our model captures the mechanistic effects vitamin D_3 has on a LAM activated macrophage cell. This allows us to predict the behavioral response of the host cell when exposed to varying quantities of bound and unbound vitamin D_3 in the presence of mycobacterial infection.

<u>In silico model of vitamin D3 modulated effector molecule production</u>

In our model we expand our model to capture the effect of vitamin D3 on the production of effector response molecule H2O2. The active form of vitamin D_3 (1α,25-dihydroxyvitamin D_3) has been found to have a profound effect on the production of several chemokines and effector molecules, such as, Hydrogen peroxide (H_2O_2)[36], interleukin-6 [26], and several others. The behavioral adaptation of the macrophage cell from D_3 sufficient hosts leads to a superior response, with the macrophage better equipped to cope with Mtb infection, and resulting in conservation of host cells. Utilizing portions of our previous *in silico* model of the effects of vitamin D_3 supplementation and mycobacterium infection on the production of IL-10, we further expanded our mechanistic model of infection to capture the phagocytic compartment of the host cell[28].

H_2O_2 is a key oxidizing microbial agent produced by macrophages and other immune cells, such as neutrophils. The primary function of H_2O_2 is to damage biomolecules important to the function of the invading bacterium[158]. Oxidative stress is known to cause metabolic defects and yield hydroxyl radicals which cause damage to biological molecules, such as DNA [158]. H_2O_2 is known to diffuse across membranes and into the bacterial cytoplasm causing severe damage to the bacterium[159].

Our previous *in silico* model's, primary activator was LAM (lipoarabinomannan), a component of the mycobacterial cell wall. We maintain these pathways in the 2nd iteration of our model as well as the vitamin D3 enzymatic cascade.

In our model VDRE is upregulating the transcription of vital components of the NADPH oxidase complex, $p47^{phox}$ and $p67^{phox}$. These proteins remain in the host cell cytoplasm until induced by an upstream chemoattractant pathway. After activation they combine with several other protein complexes (FAD, $gp91^{phox}$, p22, Rac, GTP) to form the NADPH oxidase complex, a phagocyte-associated transmembrane structure, capable of producing superoxide anions[160]. In this model we focus on the dynamic upregulation of $p47^{phox}/p67^{phox}$ and subsequent increased production of H_2O_2 in the presence of infection in vitamin D_3 sufficient and insufficient hosts.

Previous *in silico* models of the NADPH oxidase complex greatly simplified substrate interactions down to a single equation or failed to fully expound upon the intricate mechanistic processes [161], [162]. This model builds upon our previous *in silico* model to create a biologically consistent NADPH oxidase model resulting in the production of H_2O_2. We have validated this model by utilizing data from macrophage cells infected with mycobacterium but many other cells throughout the body utilize this oxidative process for many purposes, such as ischemic tolerance, cell death and inflammatory response modulation [159].

Pathway and system stoichiometry were derived from literature [24], [32], [34], [44], [163]–[165].

Fully integrated mechanistic model of vitamin D3 immunomodulation

Macrophages are key players in host innate response, as the primary host cell of the intracellular pathogen, *Mtb*. Macrophages are known to express vitamin D receptors (VDR) and are able to produce the enzyme Cyp27B1 (1α–hydroxylase) and Cyp24A1. Cyp27B1 is able to convert 25-hydroxyvitamin D_3 to biologically active 1α,25-dihydroxyvitamin D_3, while Cyp24A1 acts as feedback inhibitory enzyme, converting active to inactive vitamin D3.[24]. The inactive form, 25-hydroxyvitamin D_3, accounts for the majority of vitamin D_3 circulating throughout the host body, though the active form incites a much more acute response.

Vitamin D_3 is a secosteroid produced in the skin via UVB-induced photolysis of prehormone, 7-dehydrocholesterol, or consumed through diet. Classically, D_3 functions as an inducer of calcium and

phosphorous absorption in the intestine, however there has been increasing interest in the non-classical immunological regulatory functions of vitamin D3 as correlations between vitamin D_3 and disease outcome amass [33]. The immunologic response of the macrophage cells from D_3 sufficient hosts leads to a superior response when compared to vitamin D3 deficient cells, with the with +D3 macrophage better equipped to cope with Mtb infection, resulting in decreased of host cell death. Utilizing portions of our previous *in silico* model of the effects of vitamin D_3 supplementation and mycobacterium infection on the production of IL-10 and H2O2, as well as portions of the Salim et.al, Yamada et.al., and Sharp et.al. models we further expanded our mechanistic model of infection to capture the phagocytic compartment of the host cell[28], [97], [163], [164], [166].

Our simulation of the mechanistic pathway through which vitamin D_3 is able to modulate host assembly of complex structures will provide insight into the downstream effects of vitamin D_3; an effect only superficially and correlatively defined previously. There is currently not a well-established model of macrophage behavior modulation by vitamin D_3 and there is very little information regarding the kinetics of this process. Modeling the mechanistic pathway through which vitamin D_3 is able to dynamically impact the behavior of host cells will provide insight into the ramifications of host vitamin deficiency and infection; as well as potential ways to manipulate host immune response through these pathways.

Methods

<u>In silico model of the uptake and metabolic use of vitamin D3 to modulate gene regulation.</u>

To mathematically model the mechanistic effects of vitamin D_3 on an infected cell we used a system of ordinary differential equations composed of kinetic rate equations, which were solved numerically using the MatLab ODE15s solver. Michaelis-Menten and mass action kinetics were used to generate reaction rate equations and parameters for our model were obtained from kinetic databases (e.g. BioNumbers[167], BRENDA[168]) and literature. The parameters of our model were optimized to experimental results using MATLAB and Dakota [169],[98].

Our model was divided into three compartments: the immediate extracellular area, the cytoplasmic compartment, and the nuclear compartment. Each compartment required its own volume exchange and transport rate. Our model captures two primary immune response functions, the LAM-induced production of Cyp27B1 enzyme and the vitamin D mediated production of IL-10. Sharp et al. previously modeled the mechanistic interactions of the LPS/LAM - MyD88 pathway leading to the activation of NF-κB, therefore we developed our model using the same parameter values and equations as the Sharp et.al. model; the behavior of our MyD88 pathway was consistent with the Sharp model [164]. Yamada et al. previously modeled the JAK/STAT signal cascade leading to the creation of the STAT homodimer [163]. The STAT homodimer has similar function and form to the vitamin D_3/retinoic acid heterodimer, therefore the kinetic rates of the formation of the STAT homodimer and the rates of its activities were used to approximate the rates of the vitamin D/retinoic acid heterodimer.

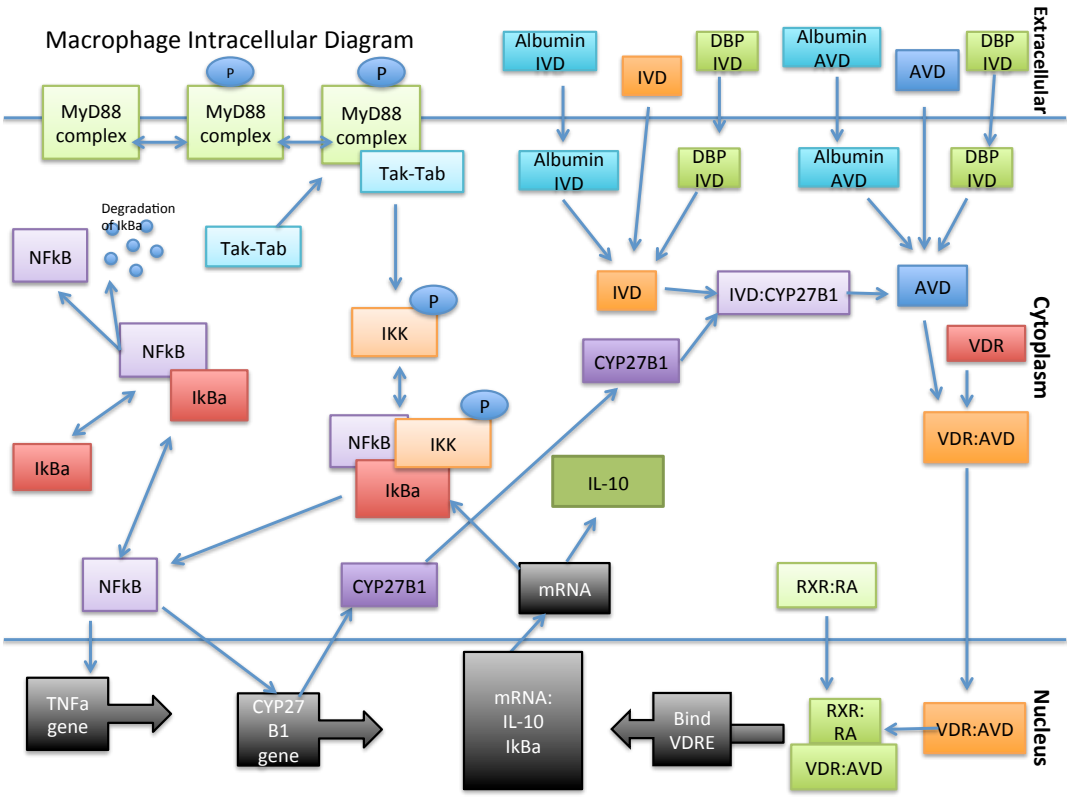

Figure 18. Intracellular Model Diagram.

We assume LPS/LAM bound TLR is the activating species for the system. We draw the assumption that the cell has already encountered the bacterial protein and vitamin D_3 is already available in

the local extracellular area. After the cell uptakes bound vitamin D_3, degradation of the transport proteins DBP and albumin begins. This reaction was modeled using mass action kinetics resulting in the following equation,

$$v = k_1[ivd{:}dbp][ivd{:}albumin] + k_2[ivd{:}albumin] * ex2cyt + k_3[ivd{:}dbp] + k_4[ivd{:}albumin] \quad (1)$$

ivd:dbp = inactive vitamin D3 bound to vitamin D3 binding protein

ivd:albumin = inactive vitamin D3 bound to albumin

c = volume exchange ratio for compartmental transport

k_1 = kinetic rate of transportation from extracellular to cytoplasm (DBP)

k_2 = kinetic rate of transportation from extracellular to cytoplasm (Albumin)

k_3 = kinetic rate of protein degradation (DBP)

k_4 = kinetic rate of protein degradation (Albumin)

to determine in active vitamin D3 availability,

Enzymatic transformation was modeled using Michaelis-Menten kinetics with rapid equilibrium assumption due to the excess availability of enzymatic species Cyp27B1 (Equation 2). The enzymatic reaction is the main producer of the systems primary stimulator, biologically active vitamin D_3. Transcription of IL-10 mRNA, our protein of interest, was modeled similarly to Cyp27B1 enzymatic production (Equation 3). This reaction is reliant on the availability of the retinoic acid complex and its capability to bind to the vitamin D_3 receptor complex. The limitations of the retinoic acid complex are incorporated into the equation,

$$v = \frac{vmax_{ivd}[ivd]}{K_5 + [ivd]} \quad (2)$$

and

$$v = k_6[vdr{:}avd][rxr{:}ra] + \frac{vmax_{vdr\,avd_{rxr_{ra}}}[vdr{:}avd{:}rxr{:}ra]}{K_7 + [vdr{:}avd{:}rxr{:}ra]} \quad (3)$$

$vmax_{ivd}$ = max velocity of enzymatic conversion ivd

K_5 = michaelis menten constant for ivd

k_6 = kinetic rate of retinoic acid complex to VDR complex binding

K_7 = michaelis menten constant for the transcription of gene

to account for the bioavailability of substrate.

Using Dakota, model optimization was performed for all parameters using our experimentally generated data, and was used to find a set of model parameters that reproduce results that most closely fit our empirical data. The empirical IL-10 data used for model optimization and comparison was generated from our *in vitro* intracellular infection study using the J774 murine cell line in a *Mycobacterium smegmatis* infection model. *M.smegmatis*, a less virulent analog for *Mycobacterium tuberculosis*, was grown to late growth stage and used to infect J774 murine cells. The infection was performed at a ratio of host to bacterial cell 1:10. Cells were conditioned from time of infection onward. Uninfected cells of all conditions were maintained to ascertain overall health of cells, as well as infected unconditioned cells, and infected vitamin D_3 treated. Supernatant was collected at hourly increments and an ELISA (enzyme-linked immunosorbent assay) was performed to ascertain the concentration of IL-10 at each time point (Figure 21). Linear regression was applied to experimental sufficient (r-squared 0.97) and insufficient (r-squared 1) vitamin D_3 data to generate comparable time steps to outputs from the mathematical model. Experimental data used only captures time points 0, 8, and 16 hours, therefore linear regression is necessary to extrapolate the full 57600 seconds.

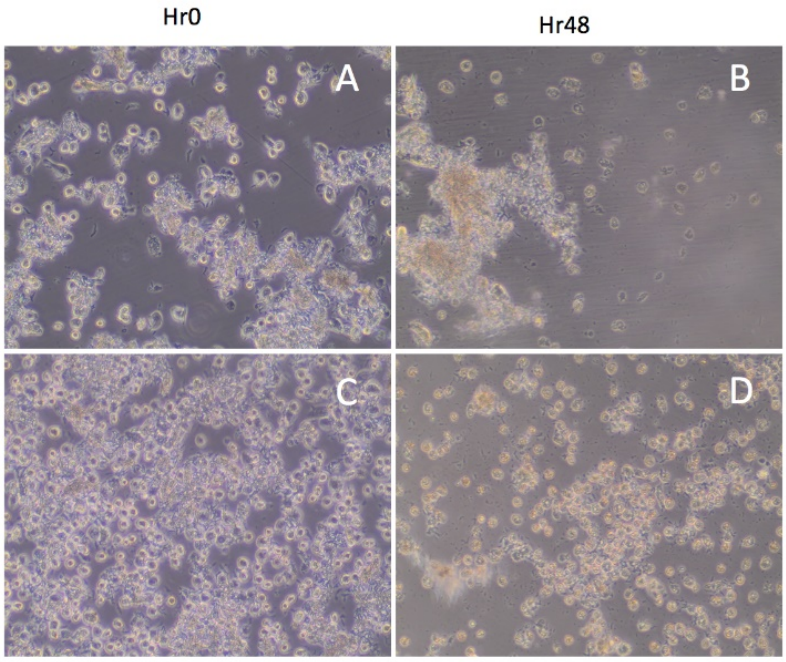

Figure 19. In vitro model of infection.

Table 17. Parameters

Reaction Description	Reaction Equation	Rate Constant		Ref_
Transport Cytoplasm	ivd_alb_ex→ivd_alb_cyt	k1	1 e4/s	[165]
Transport Cytoplasm	ivd_ex→ivd_cyt	k2	1.6e-3/s	[160]
Transport Cytoplasm	ivd_dbp_ex→ivd_dbp_cyt	k3	1 e4/s	[160]
Degradation of Alb	ivd_alb_cyt→ ivd_cyt	k4	5.277e-6/s	[160]
Degradation of DBP	ivd_dbp_cyt→ ivd_cyt	k5	5.277e-6/s	[160]
Enzyme Binding	ivd_cyt + cyp→cyp_ivd_cyt	k6	1 /µM*S	[160]
Enzymatic Synthesis	cyp_ivd_cyt→ avd_cyt + cyp	vmax7 , k7	3.9e-6µm, 2.7µm	[160]
Transport Cytoplasm	avd_alb_ex→avd_alb_cyt	k8	1 e4/s	[160]
Transport Cytoplasm	avd_ex→ avd_cyt	k9	1.6e-3/s	[160]
Transport Cytoplasm	avd_dbp_ex→avd_dbp_cyt	k10	1 e4/s	[160]
Degradation of Alb	avd_alb_cyt→ avd_cyt	k11	5.277e-6/s	[160]
Degradation of DBP	avd_dbp_cyt→ avd_cyt	k12	5.277e-6/s	[160]
Bind to VDR	avd_cyt + vdr →vdr_avd_cyt	k13	1e-4/µM*S	[160]
Transport Nucleus	vdr_avd_cyt→ vdr_avd_nu	k14	0.005/s	[160]
Form Heterodimer	vdr_avd_nu + rxr_ra → vdr_avd_nu_rxr_ra	k15	1e-5/µM*S	[160]
Transcription of CAMP	vdr_avd_nu_rxr_ra→ mrna_il10_nu	k16	5/µM*S	[164]
Transport of mRNA to Cytoplasm	mrna_il10_nu→ mrna_il10_cyt	k17	0.001/s	[159]
IL-10 Protein Production	mrna_il10_cyt→ il10	k18	0.01/s	[159]
Formation of MyD88	piecemyd88→ myd88	k19	0.0001ml^6/(µM^2*S)[164]	
Deconstruction of MyD88	myd88→piecemyd88	k20	0.0001/s	[164]
Phosphorylation of MyD88 complex	myd88→ myd88_p	k21	0.001ml^2/(µM^2*2) [164]	
Dephosphorylation of MyD88 complex	myd88_p→ myd88	k22	0.001/s	[164]
Phosphorylated MyD88 complex bound to TAK and TAB	myd88_p + tak_tab→myd88_p_tak_tab	k23	0.003ml/(µ M*S)	[164]
Phosphorylated MyD88:TAK:TAB unbinds	myd88_p_tak_tab→ myd88_p + tak_tab	k24	0.01/s	[164]
Phosphorylated MyD88:TAK:TABphosphorylates IKK	myd88_p_tak_tab + ikk→ ikk_p	k25, km25	0.1/s, 0.1 µM/ml	[164]
IkBa binds to NFkB	Ikba + nfkb→ikba_nfkb	k26	0.5ml/(µM* s)	[164]
IkBa unbinds from NFkB	ikba_nfkb→ Ikba + nfkb	k27	0.0005/s	[164]
Degredation of IkBa	ikba_nfkb→ nfkb	k28	2.25e-5/s	[164]
Binding of phosphorylated IKK to IkBa:NFkB	ikk_p + ikba_nfkb→ikk_p_ikba_nfk b	k29	0.185 ml/(µM*s)	[164]
Unbinding of phosphorylated IKK from IkBa:NFkB	ikk_p_ikba_nfkb→ ikk_p + ikba_nfkb	k30	0.0005/s	[164]
Destruction of IkBa by IKK_p	ikk_p_ikba_nfkb→ ikk_p + nfkb	k31	0.0204/s	[164]
NFkB induces CYP27B1 gene transcription	nfkb → mrna_cyp	k32	0.0165 ml/(µM*s)	[164]
CYP27B1 mRNA translation	mrna_cyp→cyp	k33	0.00408/s	[160]

Table 18. Initial Concentrations

Initial Conc. uM	Condition
650	ivd_alb_ex
0.0005	ivd_ex
0.0005	ivd_dbp_ex
0	ivd_alb_cyt
0	ivd_dbp_cyt
0	ivd_cyt
0.1625	avd_alb_ex
0	avd_alb_cyt
0.0001	avd_ex
0	avd_cyt
0.00125	avd_dbp_ex
0	avd_dbp_cyt
0	cyp27b1
0	cyp27b1_ivd_cyt
2.00E-04	vdr
0	vdr_avd_cyt
0	vdr_avd_nu
0	vdr_avd_nu_rxr_ra
0	mrna_il10_nu
0	mrna_il10_cyt
0	il10
0	myd88
0	myd88_p
1	tak_tab
0	myd88_p_tak_tab
0	ikk_p
1	ikba
1	nfkb
200	ikba_nfkb
0	ikba_nfkb_ikk_p
0	mrna_cyp27b1
1	rxr_ra
1	piecemyd88

In silico model of vitamin D3 modulated effector molecule production

Michaelis-Menten and mass action kinetics were used to generate reaction rate equations. The parameters for our model were obtained from kinetic databases (e.g. BioNumbers[167], BRENDA[168]) and literature; parameters with uncertain/variable rates, upstream of H_2O_2 production were optimized to our experimental results using MatLab [98]. Production and depletion of H_2O_2 is associated with bacterial growth and killing and is a product of our intracellular signal cascade.

Our computational model was divided into four host cell compartments: the immediate extracellular area, the cytoplasmic compartment, the nuclear compartment and the phagocytic compartment. Each compartment required its own volume exchange and transport rate. The model captures two primary immune response functions, the mycobacterium small protein-induced production of Cyp27B1 enzyme and the vitamin D_3 mediated production of H_2O_2. Utilizing our previous vitamin D_3 intracellular model as a base, we derived the most probable mechanistic pathway from empirical data with well documented experimental protocols and literature reviews [160], [170].

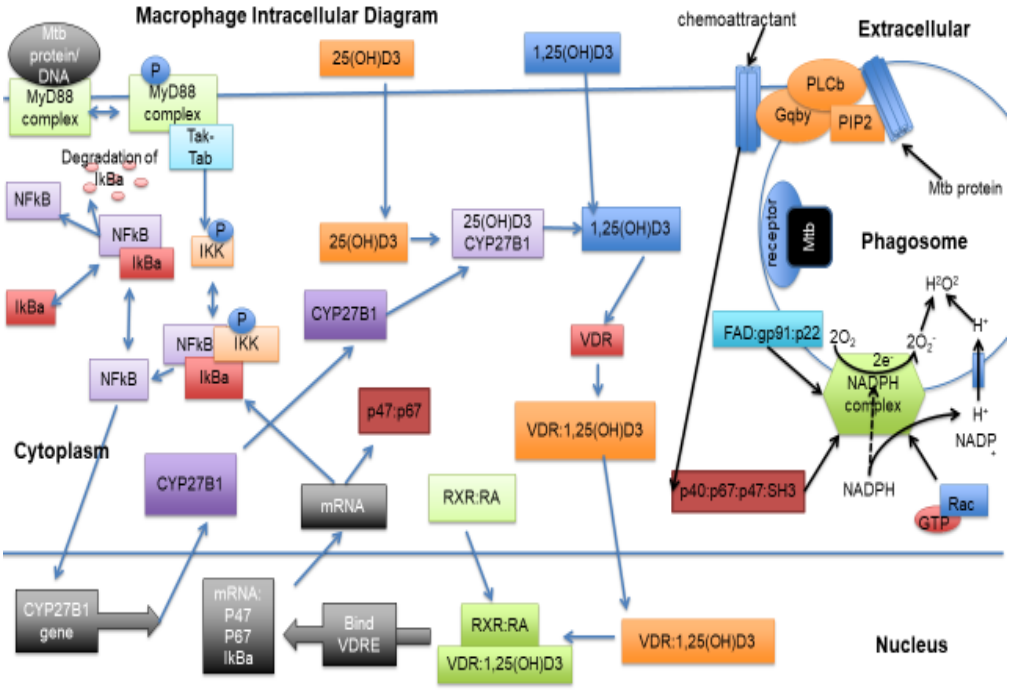

Figure 20. Intracellular Compartment Model Diagram

We made the assumption that the Mtb small protein bound TLR is the activating species for the system and vitamin D_3 is already available in the local extracellular area for sufficient vitamin D_3 models. Further assumptions are as follows, chemoattractant is already present in the local environment and Mtb has already been captured by simulated macrophage. The latter assumptions are based on our own experimental data in which measurement of the molecule of interest, H_2O_2, happens after host cell infection and treatment with antibiotic to remove excess extracellular bacteria (Figure 2). Initial concentrations of H_2O_2 in the simulation were determined by our empirical data. After the chemoattractant binds the Gq –coupled receptor, the protein is activated. This activation causes phospholipaseC β (PLC β) to hydrolyze membrane-associated phosphatidylinositol bisphosphate(PIP2). This brings about the production of inositol triphosphate(IP3) and diacylglycerol(DAG), allowing for the availability of cytosolic calcium(Ca2). Calcium then couples with other protein forming compounds necessary to the downstream activation of the p40 complex which is essential to the formation of the NADPH oxidase complex and the production of H_2O_2. This reaction, as well as several others, was modeled using mass action kinetics. We were able to model calcium availability through the equation,

$$\frac{d[ca2]}{dt} = k1[ip3] - k2[ca2][dag][pkc] - k3[ca2][cpla2] \tag{5}$$

k_1 = kinetic rate of ip3 facilitated calcium transport

k_2 = kinetic rate of calcium-dag-pkc complex formation

k_3 = kinetic rate of calcium-cpla2 complex formation

to determine its dynamic concentration over time. Enzymatic transformation was modeled using Michaelis-Menten kinetics (Equation 2,3). Enzymatic reactions are the main producer of the systems primary stimulators, biologically active vitamin D_3 and Rac-GTP bound protein. Free active vitamin D3 and rac bound GTP was modeled through equations,

$$\frac{d[1,25(OH)2D3]}{dt} = \frac{vmax_{107}[25(OH)D3]}{K_{m107}+[25(OH)D3]} \tag{6}$$

and

$$\frac{d[rac_{gtp}]}{dt} = \frac{vmax_{110}[rac_{gdp_{gef}}]}{K_{m110}+[rac_{gdp_{gef}}]} - k_{112}[rac_{gdp_{gef}}] - k_{113}\left[rac_{gtp_{gap}}\right] \quad (7)$$

km_{107} = michaelis menten constant of enzymatic transformation to active vitamin D

km_{110} = michaelis menten constant of enzymatic transformation to rac bound gtp

to determine their dynamic concentration over time.

Our previous model was optimized utilizing Dakota, model optimization was performed for all parameters using our experimentally generated data, and was used to find a set of model parameters that reproduce results that most closely fit our empirical data. The empirical IL-10 data used for previous model optimization and comparison was generated from our *in vitro* intracellular infection study. For our current model heuristic curation was performed for key NADPH oxidase complex associated parametric rates. We utilized our own experimentally generated data, as well as results found in literature to find model parameters that most greatly impacted H_2O_2 production. To curate our computational model, all kinetic rates involved in the NADPH complex formation and activation were examined and adjusted using empirically generated H_2O_2 concentrations as a biometric. Rates resulting in dissimilar outputs to empirical data were discarded and replaced. The empirical H_2O_2 data used for model curation and validation was generated from our *in vitro* intracellular infection study using the J774 murine cell line and a *Mycobacterium smegmatis* infection model.

M. smegmatis, an avirulent analog for *Mycobacterium tuberculosis*, was grown to late log stage and used to infect J774 murine cells. The infection was performed at a ratio of 1:100, host to bacterial cell. Sufficient cells were continuously conditioned with vitamin D_3 from time of infection onward. Control cells were infected but not provided with exogenous vitamin D_3, creating a vitamin D_3 insufficient environment. Supernatant was collected at 0, 8, 16, 24, 34, 44, 54, 64, 74 hours and a hydrogen peroxide detection assay (Abcam, cat#ab102500) was performed to ascertain the concentration of H_2O_2 at each time point (Figure 2). Polynomial regression analysis was applied to experimental bacterial growth counts taken during infection in both vitamin D_3 sufficient and insufficient environments; the subsequent equation,

$$\frac{d(bac-load-insuffD)}{dt} = 2E - 12[bac]^2 - 0.0002[bac] + 751.96 \quad (8)$$

and

$$\frac{d(bac-suffD)}{dt} = -1.05E - 11[bac]^2 + 0.00006[bac] - 48.23 \quad (9)$$

was utilized to represent total bacterial load during infection in our *in silico* model of both conditions.

Table 19. Model Reactions and Parameters

Reaction Name	Reaction Equation	Rate Constant		Ref
Transport Cytoplasm	ivd_alb_ex→ivd_alb_cyt	k1	1 e4/s	[160]
Transport Cytoplasm	ivd_ex→ivd_cyt	k2	1.6e-3/s	[160]
Transport Cytoplasm	ivd_dbp_ex→ivd_dbp_cyt	k3	1 e4/s	[160]
Degradation of Alb	ivd_alb_cyt→ ivd_cyt	k4	5.277e-6/s	[160]
Degradation of DBP	ivd_dbp_cyt→ ivd_cyt	k5	5.277e-6/s	[160]
Enzyme Binding	ivd_cyt + cyp27b1→cyp27b1_ivd_cyt	k6	1 /µM*S	[160]
Enzymatic Synthesis	cyp27b1_ivd_cyt→ avd_cyt + cyp27b1	vmax7, km7		
Transport Cytoplasm	avd_alb_ex→avd_alb_cyt	k8	1 e4/s	[160]
Transport Cytoplasm	avd_ex→ avd_cyt	k9	1.6e-3/s	[160]
Transport Cytoplasm	avd_dbp_ex→avd_dbp_cyt	k10	1 e4/s	[160]
Degradation of Alb	avd_alb_cyt→ avd_cyt	k11	5.277e-6/s	[160]
Degradation of DBP	avd_dbp_cyt→ avd_cyt	k12	5.277e-6/s	[160]
Bind to VDR	avd_cyt + vdr →vdr_avd_cyt	k13	1e-4/µM*S	[160]
Transport Nucleus	vdr_avd_cyt→ vdr_avd_nu	k14	0.005/s	[160]
Form Heterodimer	vdr_avd_nu + rxr_ra → vdr_avd_nu_rxr_ra	k15	1e-5/µM*S	[160]
Transcription of VDRE mrna	vdr_avd_nu_rxr_ra→ mrna_vdre_nu	vmax16, km16	0.00001uM/l/s, 0.4µM/l	[160]
Transport of mRNA to Cytoplasm (final output)	mrna_vdre_nu→ mrna_vdre_cyt	k17	0.001/s	[160]
VDRE Protein Production (translation)	mrna_vdre_cyt→ vdre_protein	k18	0.01/s	[160]
Formation of MyD88	piecemyd88_bound→ myd88	k19	0.0001	[159]

Table 19. continued

from infection activated TLR			ml^2/(µM^2*S)	
Deconstruction of MyD88	myd88→piecemyd88_bound	k20		
Phosphorylation of MyD88 complex	myd88→ myd88_p	k21	0.001/s	[159]
Dephosphorylation of MyD88 complex	myd88_p→ myd88	k22	0.003ml/(µM*S)	[159]
Phosphorylated MyD88 complex bound to TAK1 and TAB1/2/3	myd88_p + tak_tab → myd88_p_tak_tab	k23	0.01/s	[159]
Phosphorylated MyD88:TAK1:TAB1 unbinds	myd88_p_tak_tab→ myd88_p + tak_tab	k24, km24	[159]	
Phosphorylated MyD88:TAK1:TAB1/2/3 phosphorylates IKK	myd88_p_tak_tab + ikk→ ikk_p	k25	[159]	
IkBa binds to NFkB	Ikba + nfkb→ ikba_nfkb	k26	0.0005/s	[159]
IkBa unbinds from NFkB	ikba_nfkb→ Ikba + nfkb_p	k27	2.25e-5/s	[159]
Degredation of IkBa	ikba_nfkb→ nfkb	k28	[159]	
Binding of phosphorylated IKK to IkBa:NFkB	ikk_p + ikba_nfkb→ikk_p_ikba_nfkb	k29	0.0005/s	[159]
Unbinding of phosphorylated IKK from IkBa:NFkB	ikk_p_ikba_nfkb→ ikk_p + ikba_nfkb	k30	0.0204/s	[159]
Destruction of IkBa by IKK_p	ikk_p_ikba_nfkb → ikk_p + nfkb_p	k31	17uM/l/s	[159]
NFkB induces CYP27B1 gene transcription	2 * nfkb→ mrna_cyp27b1	k32	0.00408/s	[159]
CYP27B1 mRNA translation	mrna_cyp27b1→ cyp27b1	k33	1.00E+00	[159]
LAM/LPS equivalent to # bacteria	LAM→piecemyd88_bound	k34	0.001	[159]
IL-4 upreg production of CYP24A1	il4 → cyp24a1	k35	1	[171]
il-4 production dependent on active vitamin D in cytoplasm	→il4	k36	1	
IFN-g dependent Il-15 production	IFNg→IL15	k38	1	
level of infection, bacterial replication (tentative)	bac→2bac	k39	9.259E-05	

Table 19. continued

level of infection, bacterial death (tentative)	death	k40	9.259E-06	
Total Bacteria to LAM	bac → lam	k41	0.5	
il15 production of cyp24a1	il15→cyp27b1	vmax42, km42		
cyp24a1 bind to 1,25D3	cyp24a1 + avd_cyt→ cyp24a1_avd_cyt	k43	5.00E-01	
cyp24a1 create 25D3	cyp24a1_avd_cyt→ ivd_cyt + cyp24a1	k44	0.001	
Activation of Gq-βγ	gqby + lam → gqby_a	k100	1.00E+00	[171]
Activation of PLCβ	gqby_a + plcb → plcb_a	k101	2.52E+00	171]
Hydrolysis to IP3	plcb_a + pip2 → ip3	k102	3.00E-01	[171]
Hydrolysis to DAG	plcb_a + pip2 → dag	k103	3.00E-01	[171]
IP3 open Ca2+ channel	ip3 → ca2	k104	2.50E+00	[171]
DAG and Ca2+ bind cytosolic PKC	ca2 + dag + pkc → ca2_dag_pkc_cyt	k105	3.50E-01	[171]
cytosolic PKC complex moves to membrane	ca2_dag_pkc_cyt → ca2_dag_pkc	k106	1.00E+00	[171]
Ca2+ bind/activate cPLA2	ca2 + cpla2 → ca2_cpla2	k107	1.00E+00	[171]
cPLA2 binds to ER and releases AA	ca2_cpla2 → aa	k108	8.20E-03	[171]
AA binds to RhoGDI complex	aa + rhogdi_rac_gdp → rhogdi_aa + rac_gdp	k109	1.00E+00	[171]
Rac GDP binds to GEF	gef + rac_gdp → rac_gdp_gef	k110	1.00E+00	[171]
enzymatic conversion gdp to gtp	rac_gdp_gef → rac_gtp +gef	km111,vmax11	2, 0.04	[171]
Rac GTP binds to GAP	rac_gtp + gap → rac_gtp_gap	k112	1.00E+00	[171]
enzymatic conversion gtp to gdp	rac_gtp_gap → rac_gdp + gap	km113, vmax113	1, 0.02	[171]
phosphorylation of p40 complex	ca2_dag_pkc + p40_complex → p40_complex_a	k114	1.00E+00	171]
p40 complex and RacGTP and b558 complex bind	rac_gtp + p40_complex_a + b558_complex → nadph_ox_complex	k115	6.50E-03	[171]
NADPH +2 O2 --> NADP+ + H+ +2O2-	nadph_ox_complex + nadph + o2 → nadp + o2_neg + h_cyt	k116	7.20E-04	[171]
H+ transported across phagocyte membrane	h_cyt → h_phag cytoplasmic pH dependent reaction	k117	1.00E+00	[171]
2 O2- + H+ --> H2O2	h_phag + o2_neg → h2o2_phag	k118	1.00E+00	[171]
passive diffusion H2O2 phagosome to	h2o2_phag → h2o2_cyt	k119	5.93E-02	[171]

Table 19. continued

cytoplasm				
passive diffusion NO phagosome to cytoplasm	no_phag → no_cyt	k120	1.00E-03	[171]
passive diffusion H2O2 cytoplasm to extracellular	h2o2_cyt → h2o2_ex	k121	1.00E-05	[171]
passive diffusion NO cytoplasm to extracellular	no_cyt → no_ex	k122	4.00E-01	[171]
Salim NO	source → no_phag	k123	1.00E+00	
h2o2 extracellular degradation/use	h2o2_ex → sink	k124	3.30E-02	
no extracellular degradation/use	no_ex → sink	k125	1.00E-01	

Table 20. Model Initial Concentration

Initial Concentration	Condition
ivd_alb_ex	650
ivd_ex	0.0005
ivd_dbp_ex	0.0005
ivd_alb_cyt	0
ivd_dbp_cyt	0
ivd_cyt	0
cyp27b1	0
cyp27b1_ivd_cyt	0
avd_alb_ex	16.25
avd_ex	0.0001
avd_dbp_ex	0.0125
avd_alb_cyt	0
avd_dbp_cyt	0
avd_cyt	0
vdr	2.00E-04
vdr_avd_cyt	0
vdr_avd_nu	0
rxr_ra	1
vdr_avd_nu_rxr_ra	0
mrna_vdre_nu	0
mrna_vdre_cyt	0
vdre_protein	0

Table 20. continued

piecemyd88	1
myd88	1
myd88_p	0
tak_tab	1
myd88_p_tak_tab	0
ikk	1
ikk_p	0
ikba	1
nfkb	1
ikba_nfkb	0
ikk_p_ikba_nfkb	0
mrna_cyp27b1	0
piecemyd88_bound	0
lam	0
il4	0
ifng	0
il15	0
cyp24a1	0
cyp24a1_avd_cyt	0
bac	5406250
gqby	1
gqby_a	0
plcb	1
plcb_a	0
pip2	1
ip3	0
ca2	0
dag	0.9
pkc	1
ca2_dag_pkc_cyt	0
ca2_dag_pkc	5
cpla2	1
ca2_cpla2	0
aa	0
rhogdi_rac_gdp	1
rhogdi_aa	0
gef	1
gap	1
rac_gdp	0
rac_gtp	0

Table 20. continued

rac_gdp_gef	0
rac_gtp_gap	0
p40_complex	0
p40_complex_a	0
b558_complex	1
nadph_ox_complex	0
nadph	1
o2	1
h_cyt	0
nadp	0
o2_neg	0
h_phag	0
h2o2	0

Fully integrated mechanistic model of vitamin D3 immunomodulation

Previous models, as well as our own were limited by availability of time course data. We endeavored to overcome this limitation through the generation of our own empirical data, with experimental design focused on the characterization and quantification of our system over time [172], [173]. Only pathways conserved in both mouse and human were presented here.

To mathematically model the mechanistic effects of vitamin D_3 on an infected cell we used a system of ordinary differential equations composed of kinetic rate equations, which were solved numerically using the MatLab ODE15s solver. Michaelis-Menten and mass action kinetics were used to generate reaction rate equations. Enzymatic transformation was modeled using Michaelis-Menten kinetics. Enzymatic reactions are the main producer of the systems primary stimulators, biologically active vitamin D3 and Rac-GTP bound protein. The parameters for our model were obtained from kinetic databases (e.g. BioNumbers[167], BRENDA[168]) and literature; parameters with uncertain/variable rates, were optimized to our own empirically generated data using MatLab [98].

Our computational model was divided into four host cellular compartments: the immediate extracellular area, the cytoplasmic compartment, the nuclear compartment and the phagocytic compartment. Each compartment required its own volume exchange and transport rate. The model captures several primary immune response functions, such as the mycobacterium small protein-induced production of

Cyp27B1 enzyme, the vitamin D_3 mediated production of H_2O_2, the use of cytokines IL-12 and IFN-g, as well as several others. Utilizing our previous vitamin D_3 intracellular models as a base, we derived the most probable mechanistic pathway from empirical data generated using well documented experimental protocols and literature reviews [160], [170].

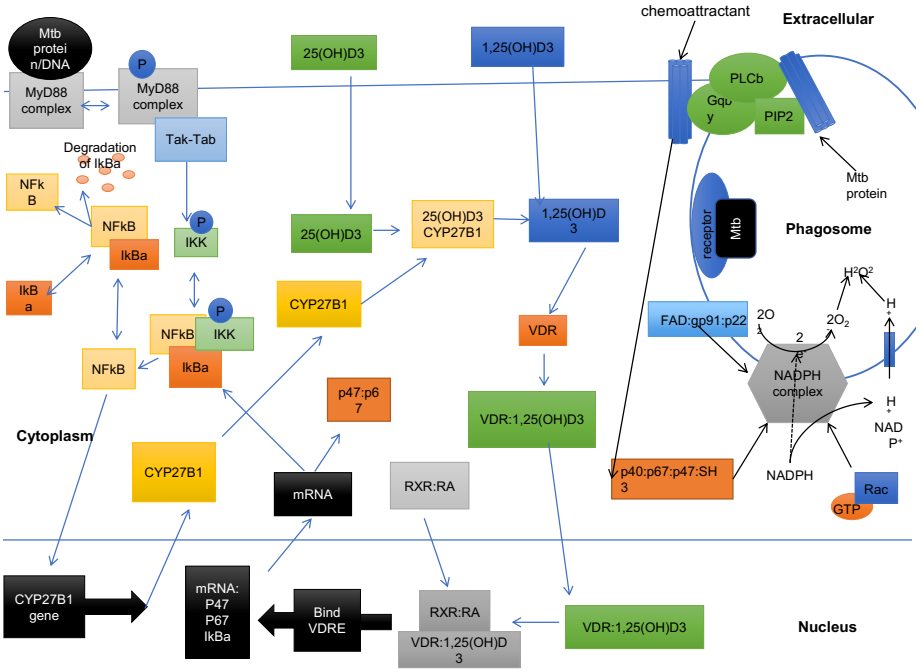

Figure 21. Consolidated and updated intracellular macrophage model

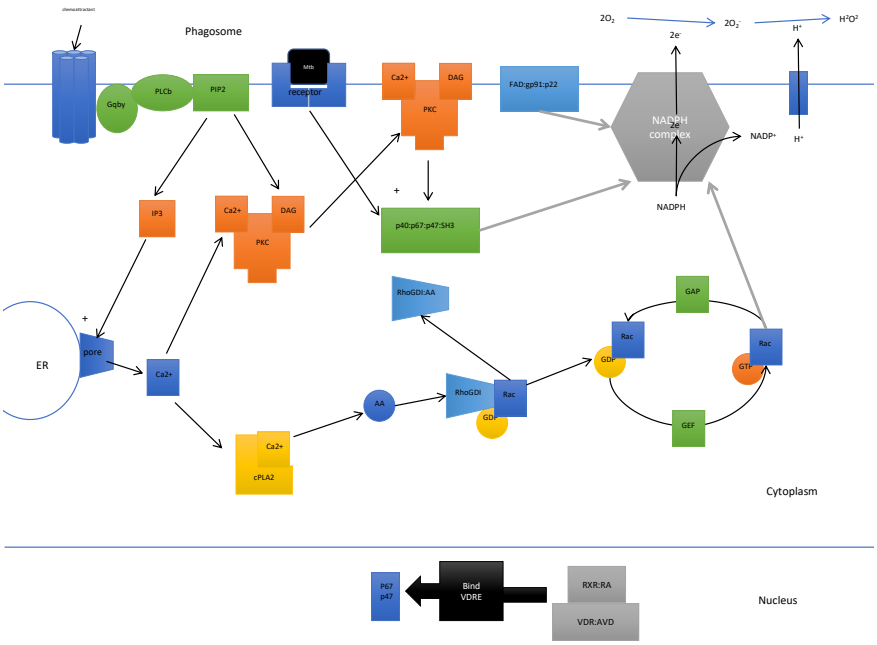

Figure 22. Expanded NADPHoxidase complex formation.

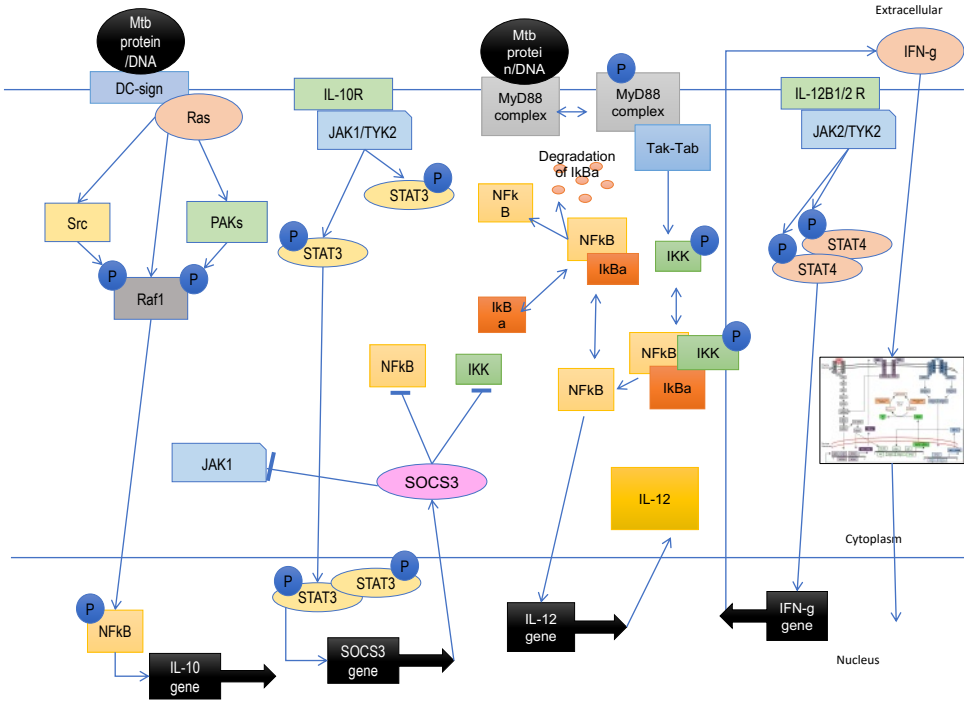

Figure 23. Addition of DC-sign, IL-10, and IL-12 receptor signaling to intracellular model.

Vitamin D3 transport and Enzymatic Transformation

LAM (lipoarabinomannan) is a component of the mycobacterial cell wall, and a primary virulence factor for mycobacterium, enabling the bacteria to encourage its own uptake to facilitate intracellular replication. LAM also plays a role in mycobacterium's ability to evade host immune response by preventing apoptosis of host cell, and the fusion of the phago-lysosme [44]. We assume LPS/LAM bound TLR is the activating species for the system. LAM shares much of the same functionality with LPS with respect to induction of inflammatory responses through recognition by LBP and CD14[174]. We draw the assumption that the cell has already encountered the bacterial protein and vitamin D_3 is already available in the local extracellular area. After the cell uptakes bound vitamin D_3, degradation of the transport proteins DBP and albumin begins. This reaction was modeled using mass action kinetics (appendices, Table 29-30). LAM activates the NF-κB signaling cascade by binding to membrane bound toll-like receptor TLR-4, which phosphorylates MyD88 inside the host cell. The activated MyD88 component is able to activate Tak-Tab which in turn phosphorylates IKK. IKK-p is then able to bind to IkBa inhibited NFkB. This leads to the release of NFkB.

This cascade leads to the degradation of the IκB binding protein, resulting in the release of NF-κB into the cytoplasm. NF-κB formers a homodimer which then enters the nucleus and acts as a transcription factor for the enzyme Cyp27B1. Cyp27B1 is known to be upregulated by the binding of TLR-4,2,1and the presence of IL-15 but the exact mechanism by which transcription is regulated is yet unknown [31], [34],[153],[154] (appendices, Table 29-30). We regulated Cyp27B1 through the equation,

$$\frac{d[cyp27b1]}{dt} = -\frac{vmax_7[ivd_{cytoplasm}][cyp27b1]}{km_7+[ivd_{cytoplasm}]} + k_{33}\left[mrna_{cyp27b1}\right] + k_{40}[il15] \quad (10)$$

$vmax_7$ = max velocity of enzymatic conversion of inactive vitamin D3 to active vitamin d3

km_7 = the substrate concentration at which the reaction rate is half of vmax7

k_{33} = rate of translation of mrna cyp27b1

k_{40} = production term for cyp27b1 based on the presence of il15

to determine its dynamic concentration over time.

Albumin and vitamin D_3 binding protein (VDBP) transport 25-hydroxyvitamin D_3 (IVD) and very small quantities of 1α,25-dihydroxyvitamin D_3 (AVD) to site of infection. 10-20% of D3 is bound to albumin, 80-90% bound to DBP and 0.02-0.05% is free [155]. This is the case for both inactive and active forms of vitamin D_3. Both forms of bound D_3 then enters the cytoplasmic compartment, where the binding proteins are degraded and IVD is enzymatically transformed by Cyp27B1 to its biologically active form, AVD. We regulated cytoplasmic inactive vitamin D3 through the equation,

$$\frac{d[ivd_{cytoplasm}]}{dt} = k_2[ivd_{extra}][ex2cyt] + k_4\left[ivd_{albumin_{cytoplasm}}\right] + k_5\left[ivd_{dbp_{cytoplasm}}\right] - \frac{vmax_7[ivd_{cytoplasm}]}{km_7+[ivd_{cytoplasm}]} + \frac{vmax_{42}[avd_{cytoplasm}]}{km_{42}+[avd_{cytoplasm}]} \quad (11)$$

k_2 = kinetic rate of transportation from extracellular to cytoplasmic compartment for free inactive vitamin D3

ivd_{extra} = inactive vitamin D3 in the extracellular compartment

ex2cyt = volume exchange ratio for compartmental transport

k_4 = kinetic rate of transportation from extracellular to cytoplasm for ivd bound to albumin

k_5 = kinetic rate of transportation from extracellular to cytoplasm for ivd bound to dbp

$vmax_7$ = max velocity of enzymatic conversion of inactive vitamin D3 to active vitamin d3

km_7 = the substrate concentration at which the reaction rate is half of vmax7

$vmax_{42}$ = max velocity of enzymatic conversion of active vitamin D3 to inactive vitamin d3

km_{42} = the substrate concentration at which the reaction rate is half of $vmax_{42}$

to determine its dynamic concentration over time.

The active form of vitamin D_3 is then bound to the vitamin D receptor protein (VDR). It is transported into the nucleus and binds to the retinoic acid-retinoic acid receptor complex (RXR:RA), which forms a heterodimer that is able to act as a transcription factor [31]. We utilized the GC Sharp et.al. model as a baseline for transcription factor interactions[164]. We assume that the vitamin D3 heterodimer transcription factor has similar kinetic rates and activity to that of the NF-kb homodimer with similar functionality (appendices, Table 29-30). The vitamin D-retinoic acid heterodimer binds to corresponding

vitamin D response elements (VDRE) found in the promoter region of the target gene, which is consequently up- or down-regulated, resulting in an increase or decrease in production of target gene. The VDRE has been found on the promoter of numerous genes including IkB, IL-10, HAMP (hepcidin) [156], CAMP(cathelicidin) [157], DEFB4[34] and others.

Following the binding of the vitamin D-retinoic acid heterodimer to the VDRE we have tied the upregulation of three specific genes to the presence of vitamin D3. IkBa, $p47^{phox}$, and $p67^{phox}$, have all been shown to be heavily upregulated by the presence of vitamin D3. As a negative feedback inhibitory factor the presence of AVD also incites the upregulation of transcription of the gene for Cyp24A1 through the production of IL-4. CYP24A1 enzymatically converts AVD to IVD (appendices, Table 29-30). IkBa, an inhibitory molecule of NF-kB prevents the transcription of Cyp27B1 within the scope of this model, but in a more extensive system would prevent NF-kB dependent transcription of several other immune-relevant genes controlling growth, apoptosis, and cytokines[175].

NADPH-oxidase complex formation

Previous *in silico* models of the NADPH oxidase complex greatly simplified substrate interactions down to a single equation or failed to fully expound upon the intricate mechanistic processes [161], [162]. This model builds upon our previous *in silico* model to create a biologically consistent NADPH oxidase model resulting in the production of H_2O_2. We have validated this model by utilizing data from macrophage cells infected with mycobacterium but many other cells throughout the body utilize this oxidative process for many purposes, such as ischemic tolerance, cell death and inflammatory response modulation [159].

We made the assumption that the Mtb small protein bound TLR is the activating species for the system and vitamin D_3 is already available in the local extracellular area for sufficient vitamin D_3 models. Further assumptions are as follows, chemoattractant is already present in the local environment and Mtb has already been captured by simulated macrophage. The latter assumptions are based on our own experimental data in which measurement of the molecule of interest, H_2O_2, happens after host cell infection and treatment with antibiotic to remove excess extracellular bacteria. Initial concentrations of H_2O_2 in the simulation were determined by our empirical data [172] (appendices, Table 29-30).

Production of vital NADPH oxidase complex components, $p47^{phox}$ and $p67^{phox}$ are regulated in a vitamin D3 dependent manor. After transcription and translation these proteins remain in the host cell cytoplasm until induced by an upstream chemoattractant pathway. For the purpose of this model we have identified the chemoattractant as LAM but the system can be stimulated biologically by bacterial proteins, DNA fragments, toxins, foreign antibodies, etc. After the chemoattractant shed/secreted by the bacterium binds the Gq –coupled receptor (Gqby), the protein is activated. This activation causes phospholipaseCβ(PLCβ) to hydrolyze membrane-associated phosphatidylinositol bisphosphate(PIP2). This brings about the production of inositol triphosphate(IP3) and diacylglycerol(DAG), allowing for the availability of cytosolic calcium(Ca2) through its release from the endoplasmic reticulum (ER). Calcium then couples to both PKC and cPLA2. Ca2+, PKC, and DAG form a complex which attaches itself to the cell membrane [162], [176] (appendices, Table 29-30). This is necessary for the downstream activation of the p40 complex which is essential to the formation of the NADPH oxidase complex and the production of H_2O_2. This reaction, as well as several others, was modeled using mass action kinetics. We regulated calcium availability through the equation,

$$\frac{d[ca2]}{dt} = k_{104}[ip3] - k_{105}[ca2][dag][pkc] - k_{107}[ca2][cpla2] \quad (12)$$

k_{104} = kinetic rate of ip3 facilitated calcium transport

k_{105} = kinetic rate of calcium-dag-pkc complex formation

k_{107} = kinetic rate of calcium-cpla2 complex formation

to determine its dynamic concentration over time.

The formation of the Ca2+:DAG:PKC complex activates FAD:gp91:p22 complex to form the NADPH oxidase complex, a phagocyte-associated transmembrane structure, capable of producing superoxide anions[160]. In this model we have chosen to focus on the vitamin D3 dependent upregulation of $p47^{phox}$/$p67^{phox}$ and subsequent increased production of H_2O_2 in the presence of infection in vitamin D_3 sufficient and insufficient hosts. Enzymatic transformation was modeled using Michaelis-Menten kinetics (Equation 2,3). Enzymatic reactions are the main producer of the systems primary stimulators, biologically active vitamin D_3 and Rac-GTP bound protein. We regulated rac:gtp bioavailability through the equation,

$$\frac{d[rac_{gtp}]}{dt} = \frac{vmax_{111}[rac_{gdp_{gef}}]}{km_{111}+[rac_{gdp_{gef}}]} - k_{112}[rac_{gtp}] - k_{115}[rac_{gtp}][p40_{complex}][b558_{complex}] \quad (13)$$

$vmax_{111}$ = max velocity of enzymatic conversion rac:gtp:gef to rac:gtp

km_{111} = the substrate concentration at which the reaction rate is half of vmax111

k_{112} = depletion of rac:gtp

k_{115} = rate of formation of NADPHcomplex utilizing rac:gtp

to determine its dynamic concentration over time.

Production and depletion of H_2O_2 is associated with bacterial growth and killing and is a product of our intracellular signal cascade. H_2O_2 is a key oxidizing microbial agent produced by macrophages and other immune cells, such as neutrophils. The primary function of H_2O_2 is to damage biomolecules important to the function of the invading bacterium[158]. Oxidative stress is known to cause metabolic defects and yield hydroxyl radicals which cause damage to biological molecules, such as DNA [158]. H_2O_2 is known to diffuse across membranes and into the bacterial cytoplasm causing severe damage to the bacterium[159].

Production of IL-10, IL-12, and IFN-g

Through the extracellular binding of Mtb protein or Mtb DNA to cell membrane bound DC-sign we activate intracellular Ras which signals to Src and PAKs to phosphorylate Raf1. Raf1 phosphorylates NFkB resulting in the transcription of IL-10 gene and the subsequent creation of the IL-10 cytokine. IL-10 then signals in the local extracellular environment to the IL-10 receptor present on the macrophage. This causes the phosphorylation of STAT3, which form a homodimer capable of acting as a transcription factor. STAT3 homodimer transcribes the gene for SOCS3. SOCS3 then acts as an inhibitor for JAK1, NFkB, and IKK. The mechanism by which SOCS3 is able to inhibit NFkB are as yet unknown, though it has been speculated that it inhibits the unbinding of NFkB and Ikba (appendices, Table 29-30). Given this proposed mechanism we chose to reversibly convert IKK, the releasing component for NFkB from Ikba, from its free from to an inhibited form based on the availability and concentration of SOCS3. NFkB dependent transcription also results in the production of IL-12 cytokine. IL-12 is transported to the local extracellular space and binds to its membrane bound receptor (IL-12B1/2R). IL-12B1/2R then activates JAK2 and

TYK2 allowing them to phosphorylate STAT4. STAT4 forms a homodimer to transcribe the gene for IFN-g (interferon gamma). IFN-g then feeds into the Salim et.al. model stimulating the downstream production of NO [97]. Nitric oxide then feeds back into our model dispersing throughout the compartments (appendices, Table 29-30). Through the integration of the Salim et.al model we are able to integrate the four compartments and reactions novel to that simulation (1) IFN-g activated JAK/STAT signaling, (2) LAM activated MAPK signaling (3) AP1, IRF-1, TNF-a, and iNOS gene expression, and (4) metabolic production of nitric oxide and arginine [97]. We utilized the equations,

$$\frac{d[ifng]}{dt} = +k_{226}[ifng][RJ] - k_{229}[ifng] - kts_3[ifng][RJ] + kts_4[IFNRJ] \tag{14}$$

and

$$\frac{d[no_{phag}]}{dt} = \left(\frac{kts_{158}[iNOS]*0.13*[arg]}{kts_{159}+[arg]}\right) - k_{120}[no_{phag}] * phag2cyt \tag{15}$$

k_{226} = rate of binding between RJ and ifng

k_{229} = the depletion of ifng

kts_3 = the formation of ifng bound to RJ

kts_4 = the reversal of ifng binding

kts_{158} = max velocity of enzymatic conversion

kts_{159} = the substrate concentration at which half vmax is reached

k_{120} = rate at which no_phag is transported to cytoplasm

phag2cyt = volumetric conversion for transport from phagosome to cytoplasm

ifng = interferon gamma

RJ = receptor bound to JAK

iNOS = inducible nitric oxide

arg = argenine

to determine the dynamic concentration of IFN-g and phagocytic NO over time.

Our first model was optimized utilizing Dakota, model optimization was performed for all parameters using our experimentally generated data, and was used to find a set of model parameters that reproduce results that most closely fit our empirical data [28]. The empirical IL-10 data used for previous

model optimization and comparison was generated from our *in vitro* intracellular infection study. For our current model heuristic curation was performed for key NADPH oxidase complex associated parameters and cytokine signaling molecules. We utilized our own experimentally generated data, as well as results found in literature to find model parameters that most greatly impacted H_2O_2 and NO production. To curate our computational model, all kinetic rates were examined and adjusted using empirically generated data as a biometric. Rates resulting in dissimilar outputs to empirical data were discarded and replaced. The empirical data used for model curation and validation was generated from our *in vitro* intracellular infection study using the J774 murine cell line and a *Mycobacterium smegmatis* infection model.

To mathematically model the mechanistic effects of vitamin D_3 on an infected cell we used a system of ordinary differential equations composed of kinetic rate equations, which were solved numerically using the MatLab ODE15s solver. Michaelis-menten and mass action kinetics were used to generate reaction rate equations and parameters for our model were obtained from kinetic databases (e.g. BioNumbers[167], BRENDA[168]) and literature. The parameters of our model were optimized to experimental results using MatLab and Dakota [169],[98].

Table 21. Model Reactions and Parameters

Reaction Name	Reaction Equation	Rate Constant	
Transport Cytoplasm	ivd_alb_ex→ivd_alb_cyt	k1	1 e4
Transport Cytoplasm	ivd_ex→ivd_cyt	k2	1.60E-03
Transport Cytoplasm	ivd_dbp_ex→ivd_dbp_cyt	k3	1 e4
Degradation of Alb	ivd_alb_cyt→ ivd_cyt	k4	5.28E-06
Degradation of DBP	ivd_dbp_cyt→ ivd_cyt	k5	5.28E-06
Enzyme Binding	ivd_cyt + cyp27b1→cyp27b1_ivd_cyt	k6	1
Enzymatic Synthesis	cyp27b1_ivd_cyt→ avd_cyt + cyp27b1	vmax7, km7	3.9e-6, 2.7
Transport Cytoplasm	avd_alb_ex→avd_alb_cyt	k8	1 e4
Transport Cytoplasm	avd_ex→ avd_cyt	k9	1.60E-03
Transport Cytoplasm	avd_dbp_ex→avd_dbp_cyt	k10	1 e4
Degradation of Alb	avd_alb_cyt→ avd_cyt	k11	5.28E-06
Degradation of DBP	avd_dbp_cyt→ avd_cyt	k12	5.28E-06
Bind to VDR	avd_cyt + vdr →vdr_avd_cyt	k13	1e-4*
Transport Nucleus	vdr_avd_cyt→ vdr_avd_nu	k14	0.005
Form Heterodimer	vdr_avd_nu + rxr_ra → vdr_avd_nu_rxr_ra	k15	1e-5*
Transcription of VDRE mrna	vdr_avd_nu_rxr_ra→ mrna_vdre_nu	vmax16,	0.00001,

Table 21. continued

		km16	0.4l
Transport of mRNA to Cytoplasm (final output)	mrna_vdre_nu→ mrna_vdre_cyt	k17	0.001
VDRE Protein Production (translation)	mrna_vdre_cyt→ vdre_protein	k18	0.01
Formation of MyD88 from infection activated TLR	piecemyd88_bound→ myd88	k19	0.0001l^2^2*
Deconstruction of MyD88	myd88→piecemyd88_bound	k20	0.001l^2^2*2
Phosphorylation of MyD88 complex	myd88→ myd88_p	k21	0.001
Dephosphorylation of MyD88 complex	myd88_p→ myd88	k22	0.003
Phosphorylated MyD88 complex bound to TAK1 and TAB1/2/3	myd88_p + tak_tab → myd88_p_tak_tab	k23	0.01
Phosphorylated MyD88:TAK1:TAB1 unbinds	myd88_p_tak_tab→ myd88_p + tak_tab	k24, km24	0.1, 0.1e-3
Phosphorylated MyD88:TAK1:TAB1/2/3 phosphorylates IKK	myd88_p_tak_tab + ikk→ ikk_p	k25	0.5
IkBa binds to NFkB	Ikba + nfkb→ ikba_nfkb	k26	0.0005
IkBa unbinds from NFkB	ikba_nfkb→ Ikba + nfkb_p	k27	2.25E-05
Degredation of IkBa	ikba_nfkb→ nfkb	k28	0.185
Binding of phosphorylated IKK to IkBa:NFkB	ikk_p + ikba_nfkb→ikk_p_ikba_nfkb	k29	0.0005
Unbinding of phosphorylated IKK from IkBa:NFkB	ikk_p_ikba_nfkb→ ikk_p + ikba_nfkb	k30	0.0204
Destruction of IkBa by IKK_p	ikk_p_ikba_nfkb → ikk_p + nfkb_p	k31	17
NFkB induces CYP27B1 gene transcription	2 * nfkb→ mrna_cyp27b1	k32	0.00408
CYP27B1 mRNA translation	mrna_cyp27b1→ cyp27b1	k33	1.00E+00
LAM/LPS equivalent to # bacteria	LAM→piecemyd88_bound	k34	0.001
IL-4 upreg production of CYP24A1	il4 → cyp24a1	k35	1
il-4 production dependent on active vitamin D in cytoplasm	→il4	k36	1
IFN-g dependent Il-15 production	IFNg→IL15	k38	1
level of infection, bacterial replication (tentative)	bac→2bac	k39	9.259E-05
level of infection, bacterial death (tentative)	death	k40	9.259E-06
Total Bacteria to LAM	bac → lam	k41	0.5
il15 production of cyp24a1	il15→cyp27b1	vmax42, km42	1.90E-06, 1.50E+00
cyp24a1 bind to 1,25D3	cyp24a1 + avd_cyt→ cyp24a1_avd_cyt	k43	5.00E-01
cyp24a1 create 25D3	cyp24a1_avd_cyt→ ivd_cyt + cyp24a1	k44	0.001
Activation of Gq-βγ	gqby + lam → gqby_a	k100	1.00E+00
Activation of PLCβ	gqby_a + plcb → plcb_a	k101	2.52E+00
Hydrolysis to IP3	plcb_a + pip2 → ip3	k102	3.00E-01

Table 21. continued

Hydrolysis to DAG	plcb_a + pip2 → dag	k103	3.00E-01
IP3 open Ca2+ channel	ip3 → ca2	k104	2.50E+00
DAG and Ca2+ bind cytosolic PKC	ca2 + dag + pkc → ca2_dag_pkc_cyt	k105	3.50E-01
cytosolic PKC complex moves to membrane	ca2_dag_pkc_cyt → ca2_dag_pkc	k106	1.00E+00
Ca2+ bind/activate cPLA2	ca2 + cpla2 → ca2_cpla2	k107	1.00E+00
cPLA2 binds to ER and releases AA	ca2_cpla2 → aa	k108	8.20E-03
AA binds to RhoGDI complex	aa + rhogdi_rac_gdp → rhogdi_aa + rac_gdp	k109	1.00E+00
Rac GDP binds to GEF	gef + rac_gdp → rac_gdp_gef	k110	1.00E+00
enzymatic conversion gdp to gtp	rac_gdp_gef → rac_gtp +gef	km111,v max11	2, 0.04
Rac GTP binds to GAP	rac_gtp + gap → rac_gtp_gap	k112	1.00E+00
enzymatic conversion gtp to gdp	rac_gtp_gap → rac_gdp + gap	km113, vmax113	1, 0.02
phosphorylation of p40 complex	ca2_dag_pkc + p40_complex → p40_complex_a	k114	1.00E+00
p40 complex and RacGTP and b558 complex bind	rac_gtp + p40_complex_a + b558_complex → nadph_ox_complex	k115	6.50E-03
NADPH +2 O2 --> NADP+ + H+ +2O2-	nadph_ox_complex + nadph + o2 → nadp + o2_neg + h_cyt	k116	7.20E-04
H+ transported across phagocyte membrane	h_cyt → h_phag cytoplasmic pH dependent reaction	k117	1.00E+00
2 O2- + H+ --> H2O2	h_phag + o2_neg → h2o2_phag	k118	1.00E+00
passive diffusion H2O2 phagosome to cytoplasm	h2o2_phag → h2o2_cyt	k119	5.93E-02
passive diffusion NO phagosome to cytoplasm	no_phag → no_cyt	k120	1.00E-03
passive diffusion H2O2 cytoplasm to extracellular	h2o2_cyt → h2o2_ex	k121	1.00E-05
passive diffusion NO cytoplasm to extracellular	no_cyt → no_ex	k122	4.00E-01
taha NO	source → no_phag	k123	1.00E+00
h2o2 extracellular degradation/use	h2o2_ex → sink	k124	3.30E-02
no extracellular degradation/use	no_ex → sink	k125	1.00E-01
Mtb Protein Binds DC-sign to activate	lam + dcsign_ras → dc_sign_ras_a	k200	1.00E-06
Active DC sign makes SRC	dc_sign_ras_a → src	k201	1.00E-06
SRC activates raf1_p1	src → raf1_p1	k202	1.00E-06
Active DC sign makes makes PAKS	dc_sign_ras_a → paks	k203	1.00E-06
PAKS activates raf1_p2	paks → raf1_p2	k204	1.00E-06
RAF1_p1 combines with RAF1_p2	raf1_p1 + raf1_p2 → raf1_p	k205	1.00E-06
RAF1_p activates NFkb	raf1_p + ikba_nfkb → nfkb_p	k206	1.00E-07
transcription IL-10	2*nfkb→ mrna_il10	k207, km207	1.7e-6, 1.1e-6
translation IL-10	mrna_il10 →IL10	k208	1.00E-06

Table 21. continued

activation of JAK1 TYK2 by IL-10	IL10 + IL10_r → JAK1_TYK2_a	k209	1.00E-06
Stat3 phosphorylation	JAK1_tyk2_a + stat3 → stat3_p	k210	1.00E-06
transport of STAT3 to nucleaus	stat3_p →stat3_p_nu	k211	1.00E-06
transcription of SOCS3	stat3_p_nu → mrna_socs3	k212, km212	1e-7, 4e-6
transport of SOCS3 to cytoplasm	mrna_socs3 →mrna_ socs3_cyt	k213	1.00E-06
Translation of SOCS3	mrna_socs3_cyt → socs3	k214	1.00E-05
Inhibition of NFKb	socs3 + nfkb_p → ikba_nfkb	k215	1.00E-05
Inhibition of IKK	socs3 + ikk_p → ikk_i	k216	1.00E-05
reverse inhibition	ikk_i → ikk	k217	1.00E-06
Transcription of IL-12	2 * nfkb → mrna_il12	k218	1.00E-06
transport IL-12 to cytoplasms	mrna_il12 →mrna_ il12_cyt	km218	4.00E-06
Translation of IL-12	mrna_il12_cyt → il12	k219	1.00E-06
IL-12 binds to its receptro to activate JAK2 and TYK2	il12 + il12_r → jak2_tyk2_a	k220	1.00E-06
JAK2 and TYK2 phosphorylate STAT4	jak2_tyk2_a + stat4 → stat4_p	k221	1.00E-05
transport of STAT3 to nucleaus	stat4_p →stat4_p_nu	k222	1.00E-06
STAT4 transcribes IFN-g	stat4_p_nu → mrna_ifng	k223	1.00E-05
transport IFN-g to cytoplasm	mrna_ifng →mrna_ ifng_cyt	k224, km224	4e-6, 1e-6
translation of IFN-g	mrna_ifng_cyt→ ifng	k225	1.00E-06

Table 22. Initial Concentrations for Model

Condition	Initial Conc.
ivd_alb_ex	650
ivd_ex	0.0005
ivd_dbp_ex	0.0005
ivd_alb_cyt	0
ivd_dbp_cyt	0
ivd_cyt	0
cyp27b1	0
cyp27b1_ivd_cyt	0
avd_alb_ex	16.25
avd_ex	0.0001
avd_dbp_ex	0.0125
avd_alb_cyt	0
avd_dbp_cyt	0
avd_cyt	0
vdr	2.00E-04

Table 22. continued

vdr_avd_cyt	0
vdr_avd_nu	0
rxr_ra	1
vdr_avd_nu_rxr_ra	0
mrna_vdre_nu	0
mrna_vdre_cyt	0
vdre_protein	0
piecemyd88	1.00E+00
myd88	1
myd88_p	0
tak_tab	1
myd88_p_tak_tab	0
ikk	1
ikk_p	0
ikba	1
nfkb_p	1
ikba_nfkb	0
ikk_p_ikba_nfkb	0
mrna_cyp27b1	0
piecemyd88_bound	1
lam	300
il4	0
ifng	0.00E+00
il15	0
cyp24a1	1
cyp24a1_avd_cyt	0
bac	13.25
gqby	1000
gqby_a	0
plcb	1000
plcb_a	0
pip2	1000
ip3	0
ca2	0
dag	0.9
pkc	10
ca2_dag_pkc_cyt	0
ca2_dag_pkc	5
cpla2	1
ca2_cpla2	1

Table 22. continued

aa	1
rhogdi_rac_gdp	1
rhogdi_aa	0
gef	1
gap	1
rac_gdp	0
rac_gtp	0
rac_gdp_gef	0
rac_gtp_gap	0
p40_complex	0
p40_complex_a	0
b558_complex	1.00E+06
nadph_ox_complex	0
nadph	1000
o2	1000
h_cyt	0
nadp	0
o2_neg	0
h_phag	0
h2o2_phag	0.00E+00
h2o2_cyt	0
h2o2_ex	0
no_cyt	0.00E+00
no_ex	0
dcsign_ras	1.00E+00
dcsign_ras_a	1.00E+10
src	0
paks	0
raf1_p1	0
raf1_p2	0
raf1_p	0
mrna_il10	0
il10	0
il10_r	1.00E+03
jak1_tyk2_a	0
stat3	1.00E+03
stat3_p	0
stat3_p_nu	0.00E+00
mrna_socs3	0
mrna_socs3_cyt	0

Table 22. continued

socs3	0
ikk_i	0
mrna_il12	0
il12	0
il12_r	1.00E+03
jak2_tyk2_a	0
stat4	1.00E+03
stat4_p	0
stat4_p_nu	0
mrna_ifng	0
mrna_ifng_cyt	0
no_phag	0.00E+00
mrna_il12_cyt	0

Results

<u>In silico model of the uptake and metabolic use of vitamin D3 to modulate gene regulation.</u>

Our simulation was run utilizing optimized parameters with initial concentrations of vitamin D_3 proportional to that of a healthy adult mouse. Using our model we simulated macrophage response during 16 hours (57600 seconds) of exposure to *M. smegmatis*. The experimentally generated data was consistent with experimental studies, displaying the host cells enhanced ability to produce IL-10 in the presence of vitamin D_3 [26], [31], [32]. *In vitro* host cells exposed to vitamin D_3 showed less cell death, this coincided with increased concentrations of IL-10 detected using ELISA. IL-10 is able to downregulate the proinflammatory immune response to reduce the amount of host cell morbidity and damage [40], [41].

Our model simulated the effector response for a single infected macrophage cell. Since our experimental data was obtained utilizing 5e5 macrophage cells per milliliter, there was a large discrepancy between the experimental and computational results (Figure 24), therefore a normalization scheme was applied to all data sets before comparison (Equation 4). The normalization equation,

$$x_{\kappa} = \frac{x_k}{\bar{x}} \tag{16}$$

x_{κ} = normalized values of x x=conc. of IL-10 k = 0,..,16 (hrs)

was used to rescale empirical and simulated results to comparable levels. The normalized results are shown in Figure 25 (simulation results for sufficient vitamin D in green).

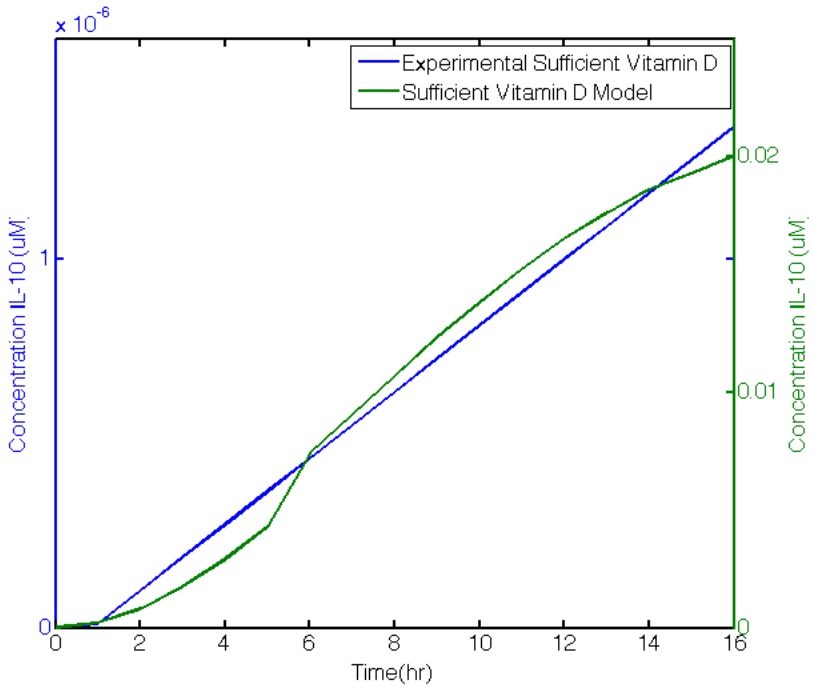

Figure 24. Non-Normalized IL-10 Expression (μM).

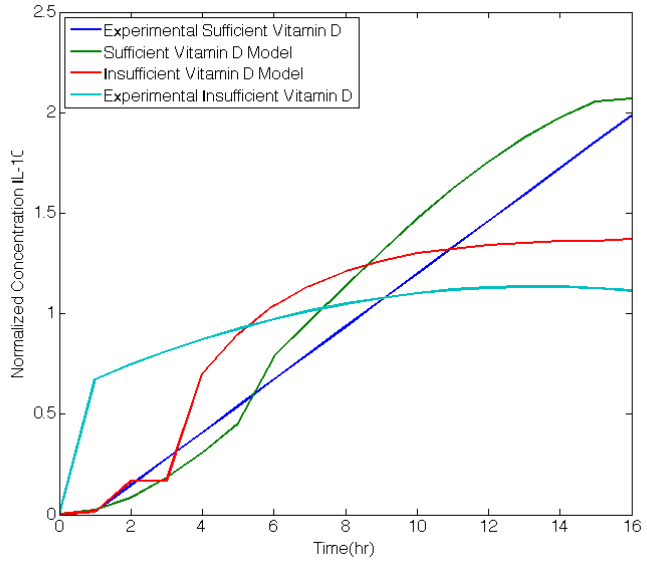

Figure 25. Normalized IL-10 Expression.

To predict IL-10 production in a vitamin D_3 deficient environment, the initial concentrations of vitamin D_3 were decreased by 10-fold to simulate a deficient condition (Figure 25). This decrease was

proportionate to the circulating concentrations of vitamin D_3 found in a deficient adult mouse. The experimental sufficient vitamin D_3 and sufficient vitamin D_3 model results exhibit comparable dynamics, with IL-10 increasing in response to infection. The experimental sufficient vitamin D_3 data set was not found to be significantly different from sufficient vitamin D_3 model using the Matlab provided function two-sample student t test and evaluating at $p<0.05$. Upon application of the student t test against insufficient vitamin D_3 experimental and model data sets, we found no significant difference.

In silico model of vitamin D3 modulated effector molecule production

Our simulation was run utilizing optimized parameters with initial concentrations of vitamin D_3 proportional to that of a healthy adult mouse. Using our model we simulated macrophage response during 74 hours (266400 seconds) of exposure to *M. smegmatis*. The experimentally generated data was consistent with experimental studies, displaying the host cells enhanced ability to produce H_2O_2 in the presence of vitamin D_3 [27], [89]. *In vitro* host cells exposed to vitamin D_3 showed less cell death, which coincided with controlled increases in H_2O_2 production (Figure 26-27).

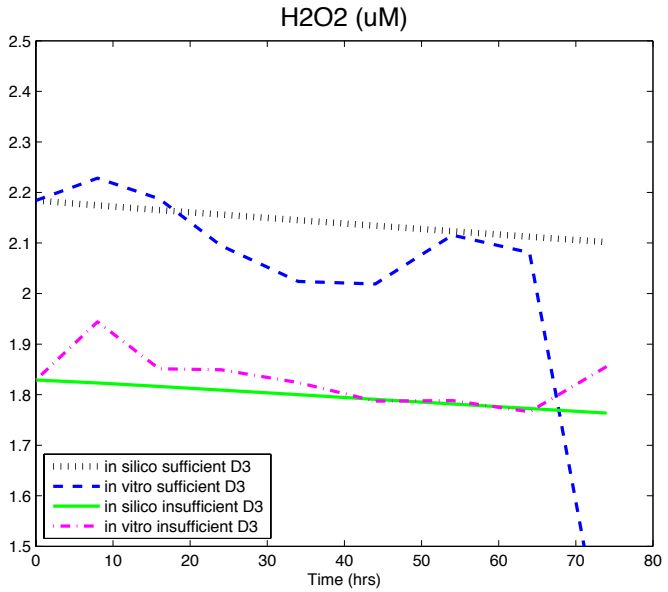

Figure 26. In silico and in vitro H_2O_2 production in Vitamin D_3 Sufficient and Insufficient Host (μM).

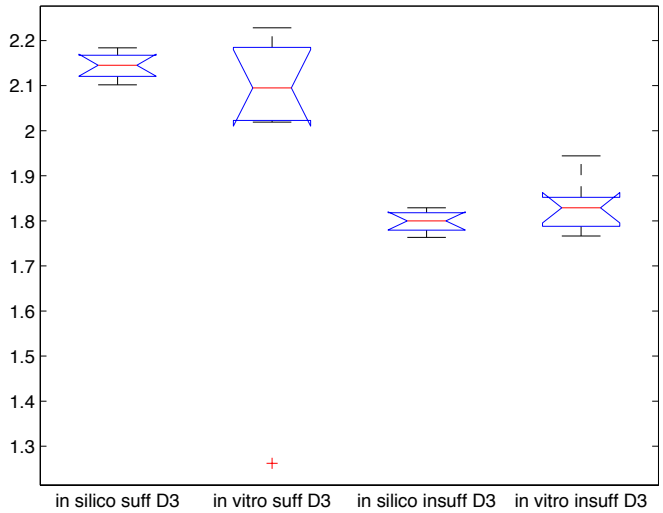

Figure 27. In silico and in vitro H_2O_2 production in Vitamin D_3 Sufficient and Insufficient Host (μM).

To predict H_2O_2 production in a vitamin D_3 deficient environment, the initial concentrations of vitamin D_3 were decreased by 10-fold to simulate a deficient condition. This decrease was proportionate to the circulating concentrations of vitamin D_3 found in a deficient adult mouse. The sufficient vitamin D_3 *in vitro* and *in silico* results exhibit comparable dynamics, with H_2O_2 decreasing over time, with a sharp decline towards the end of infection. The empirical sufficient vitamin D_3 data set was not found to be significantly different from sufficient vitamin D_3 *in silico* model results, using the Matlab provided two-sample student t test function and evaluating at $p<0.05$ (Figure 3, 4). Upon application of the student t test against insufficient vitamin D_3 experimental and model data sets, we found no significant difference from 0 to 74 hours (Figure 3, 4). The relationship between *in silico* vitamin D3 sufficient and insufficient models retained similar characteristics as the relationship observed *in vitro*. We found insufficient D_3 and sufficient D_3 results to be statistically significantly different from each other in both *in silico* and *in vitro* results.

<u>Fully integrated mechanistic model of vitamin D3 immunomodulation</u>

We have integrated our vitamin D3 immunomodulatory model with the Salim et.al model in two distinct ways. First we performed an extremity integration of the two models, tying the production of our vitamin D3 model to the Salim et.al model through the production and consumption of interferon gamma (IFN-g), respectively. Through this extremity integration we utilize the Salim.et.al models production of NO, and feed it back into our vitamin D3 model to further stimulate reactions, through which there is

downstream production of IFN-g. In addition to the extremity integration we further integrated our model with the Salim.et.al model through our shared NFkB metabolism pathway. Both models are heavily dependent on NFkB for the production of several key substrates. We found that upon further integration beyond the extremities the shared model produced significantly higher concentrations of NO and was able to maintain stable availability of NFkB (Figure 30). H2O2, another major output of our model was unperturbed by the dysregulation of NFkB caused by the full integration of NFkB, while vitamin D3 metabolism received a slight increase in availability of active vitamin D3 (avd_cyt) through the conversion from inactive (ivd_cyt).

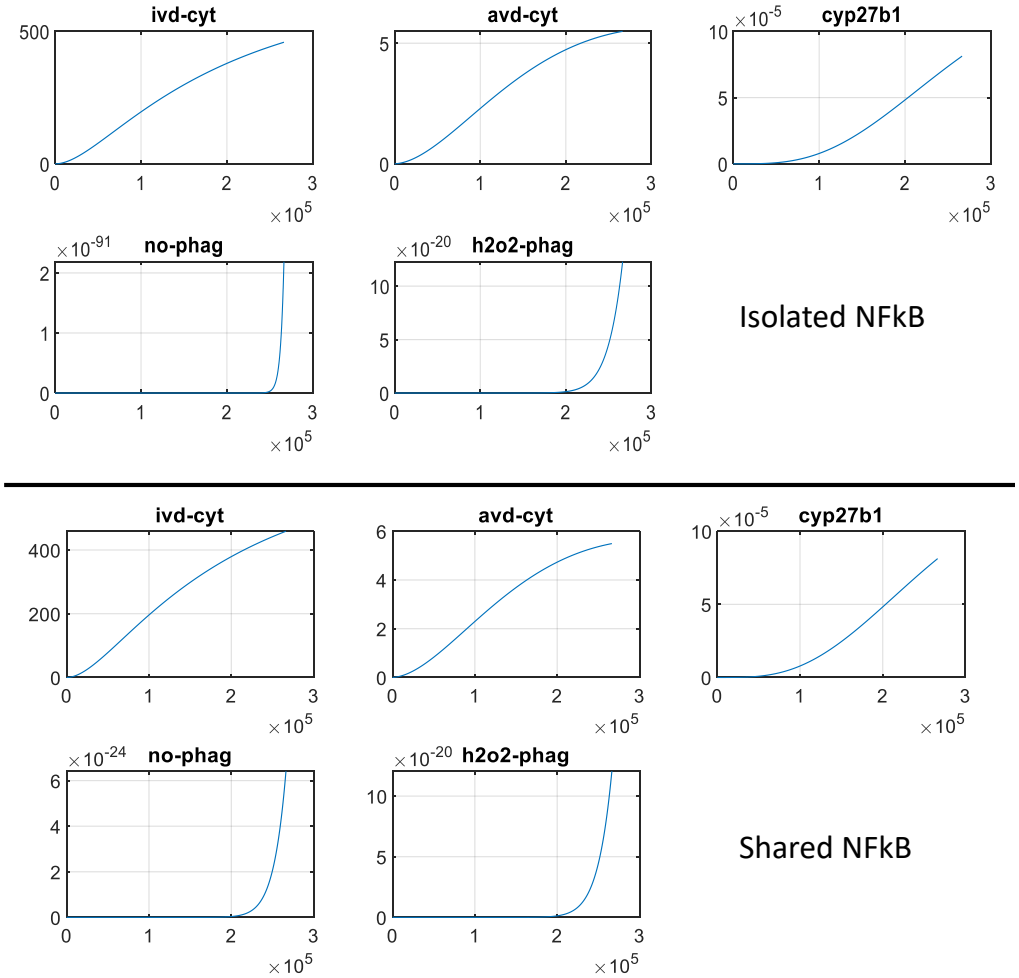

Figure 28. Comparison between in silico model with isolated and shared NFkB metabolism.

Conclusion

In silico model of the uptake and metabolic use of vitamin D3 to modulate gene regulation

We developed a kinetic intracellular model to simulate the effect of vitamin D_3 on the system. Both experimental and simulation derived data sets for insufficient vitamin D_3 display similar dynamics by reaching their max early in infection, while experimental data and sufficient vitamin D_3 model outputs continue to rise. Low concentrations of vitamin D_3 change the dynamics of the macrophage response, resulting in increased production at the beginning of infection, with a premature peak in IL-10 production occurring only shortly after onset of infection. We observed clear similarities in dynamics between the experimental and model generated datasets. Indicating that an adjustment to initial concentrations may provide a closer fit in terms of magnitude and behavior.

Currently there does not exist, a detailed dynamic model that captures the interactions of vitamin D_3 and the intracellular components of the macrophage TLR4 pathway. Previously created models were specific only to humans and limited in their representation of the kinetics of the system due to the limited availability of empirical data for human and non-human primates. Most in vivo studies provide insufficient dynamic data necessary to inform the development of dynamic models capable of predicting response over a period of several hours or days [177]. Our intracellular vitamin D_3 model overcomes many of these limitations through the use of our own experimentally generated data spanning several hours. The results from our simulation can be used to provide a greater understanding of how vitamin D_3 deficiency can impact the immune system during infection, affording us the ability to create a platform for modulating immune response using nutraceuticles

In silico model of vitamin D3 modulated effector molecule production

We developed a complex kinetic intracellular model to simulate the effect of vitamin D_3 and mycobacterium infection on host production of H_2O_2. Further optimization and curation of our *in silico* model is necessary to be able to more closely duplicate *in vitro* results. We have simulated the mechanistic pathway through which vitamin D_3 is able to modulate host assembly of complex structures resulting in the production of immune relevant effector molecule, H_2O_2 and simulated bacterial death. We have accounted for all relevant biological mechanisms within our *in silico* model, allowing for the preservation of biological

and chemical interactions. In our results, both experimental and simulation derived data sets for sufficient and insufficient vitamin D_3 display similar dynamics and maintain statistically significantly different relationships between conditions. All datasets, both *in silico* and *in vitro,* show an overall decrease over time in H_2O_2 concentration. Low concentrations of vitamin D_3 changed the range of H_2O_2 for the majority of infection, resulting in a lower production level than for sufficient conditions and a slower rate of decrease over time. From these results we can conclude that in the presence of vitamin D_3, H_2O_2 concentration starts at a higher concentration than insufficient but very gradually and consistently is depleted over time. In the absence of D_3 we can observed that the behavior is very similar to that of our sufficient condition, with H_2O_2 concentrations consistently depleting over time but we hypothesize that a separate modulatory pathway from what we model here may activate, causing the sharp increase in H_2O_2 at 64 hours that is not seen in vitamin D_3 sufficient cells. Our previous *in silico* model was the first dynamic model to capture the interactions of vitamin D_3 and the macrophage MyD88 pathway, our new model builds upon that foundation.

Fully integrated mechanistic model of vitamin D3 immunomodulation

We have developed a fully integrated model of intracellular infection that captures, vitamin D3 enzymatic processing and transport, cytokine production and signaling, vitamin D dependent and non-dependent gene transcription and translation, and vitamin D3 downstream production of effector molecules. We were able to integrate the Salim et.al IFN-g and TNF-a model with our own vitamin D3 intracellular model, further expanding out network to include TNF-a and IFN-g signaling and subsequent NO and H2O2 production.

Further optimization and curation of our *in silico* model is necessary to be able to more closely duplicate empirical findings. We have accounted for several biological mechanisms within our *in silico* model, allowing for the preservation of biological and chemical interactions. Our *in silico* model is the first dynamic model to capture the interactions of vitamin D_3 and its transcriptional modulation of immune response during infection through NADPH complex formation and cytokine signaling. The complexity of our *in silico* model will allow for further expansion in the future to areas of the immune system not yet computationally elucidated. The results from our simulation can be used to provide a greater understanding

of how vitamin D_3 deficiency can impact the immune system during infection, building a platform to identify and further explore currently unknown immune regulatory pathways.

Chapter 5 In vivo vitamin D3 deficiency and alcohol exposure followed by in vitro BCG infection

Introduction

As an expansion of our earlier experimentation in chapter 3 we pursued full in vivo conditioning of the host for both alcohol and vitamin D3 deficiency. We explored the compounding effects of vitamin D3 and alcohol exposure, as well as the isolated effects of each. Chronic alcohol exposure has been shown to interfere with the functions of essential vitamins and nutrients, such as folic acid and vitamins D, C, and E, but these studies are few and fail to investigate the compounding effect of alcohol exposure, impaired vitamin function, and infection [90]. Malnutrition and alcoholism have long correlated with suboptimal immune function and efficacy. Alcohol is commonly associated with a detrimentally upregulated inflammatory response while vitamin D3 has been associated with an upregulated anti-inflammatory response. One study found that alcohol attributed TB deaths reached about 170,000 globally in 2014[178]. Alcoholism, micronutrient deficiency, and tuberculosis often coexist, and patients with this combination having the most frequent failures of therapy. Alcohol and vitamin D3 deficiency separately have been shown to increase susceptibility to tuberculosis infection, increase risk of reactivation, and alter macrophage behavior and response.

Methods

<u>In vivo alcohol exposure and vitamin D_3 deficiency model</u>

Three-week old C57BL/6J female mice (Jackson Labs) were fed TD89123 vitamin D3 deficient diet (Envigo) or TD89124 vitamin D3 sufficient control diet for 18 weeks. TD.89124 diet is considered to be a normal diet and provides all the necessary nutrients for healthy rodent growth. Mice were weighted once a week and weight was recorded. At 10 weeks of age mice were switched from a solid diet to a liquid diet. Mice were given both solid and liquid food for 3 days as an adjustment period. Mice previously receiving TD89123 vitamin D3 deficient diet received the Lieber-DeCarli liquid diet (cat#F7584SP) and mice previously receiving TD89124 vitamin D3 sufficient control diet received the Lieber-DeCarli liquid diet (cat# F1259SP). After 3 days of receiving the liquid diet, half of the mice on vitamin D3 deficient and sufficient liquid diets were switched to Lieber-DeCarli 7% ethanol liquid (cat#F7585SP, F1258SP) while the other half remained on their non-alcohol liquid diet. This resulted in four host conditions: (1)+vitamin

D3/-ethanol, (2)+vitamin D3/+ethanol, (3)-vitamin D3/-ethanol, (4)-vitamin D3/+ethanol. At 25 weeks of age mice were sacrificed and bone marrow and blood were collected.

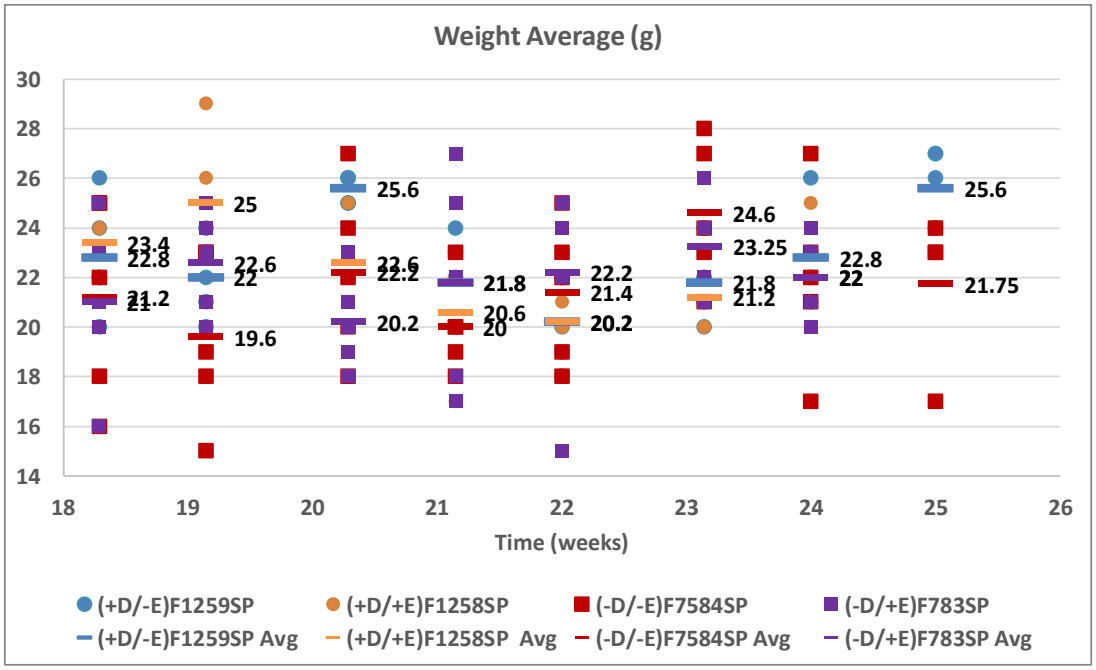

Figure 29. Mouse weight over age in weeks.

Cell Isolation

Peripheral blood mononuclear cells were isolated from the blood of the mice. Whole blood was diluted 1:1 ratio by using DMEM without FBS. An equal volume of Ficoll Paque was layered underneath the blood. After centrifugation, solution separated into three layesr: upper containing plasma, middle containing PBMCs, bottom containing RBC. Layers were carefully separated and resuspended in 10% DMSO, 90%FBS solution, then frozen at -80C. All PBMC isolation was completed thanks to the work of Dr. Jayaraman Tharmalingam.

For isolation of spleenocytes, spleen was cut into two pieces and crushed between sterile glass slides. Splenocytes were then suspended in DMEM media and filtered using 70um filter. Resulting solution was centrifuged for 10 min at 1500rpm. Supernatant was discarded and pellet was resuspended in RBC lysis buffer. Resuspended cells were incubated for 2min at room temperature followed by the

addition of DMEM to neutralize lysis buffer. Resulting splenocytes were centrifuged again and resuspended in 10%DMSO, 90%FBS solution for freezing at -80C. All splenocyte isolation was completed thanks to the work of Dr. Jayaraman Tharmalingam.

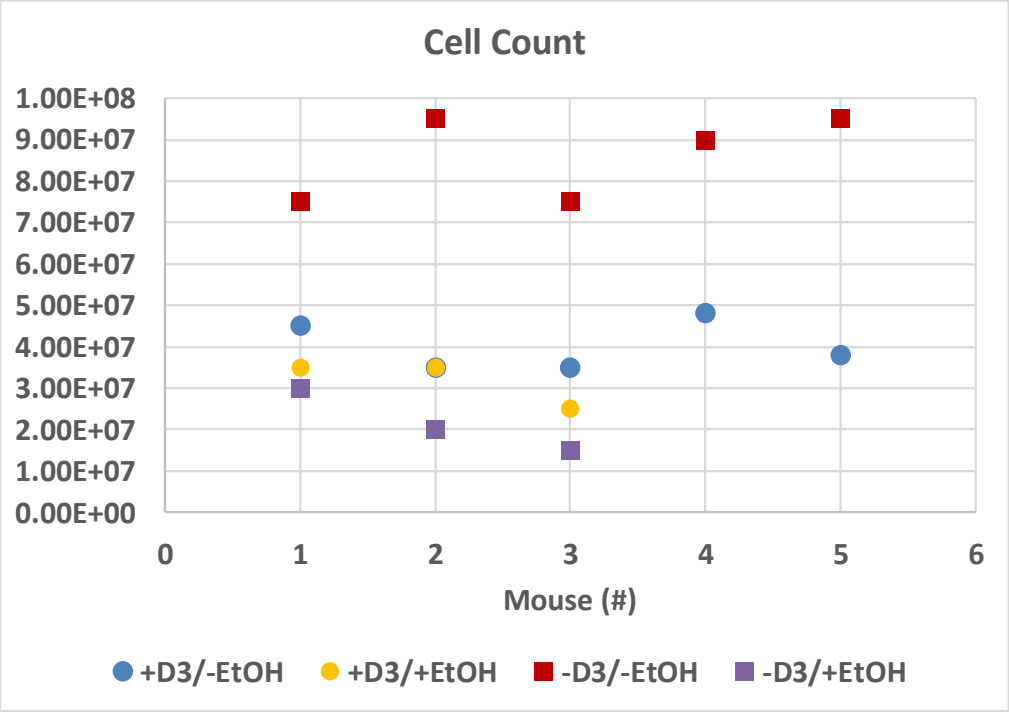

Figure 30. Cell count

Table 23. Cell Counts

	+D3/-EtOH	+D3/+EtOH	-D3/-EtOH	-D3/+EtOH
PBMC: Average	4.00E+06	7.33E+05	2.00E+06	1.33E+06
Splenocyte: Average	4.02E+07	3.17E+07	8.60E+07	2.17E+07
Splenocytes: Mouse 1	4.50E+07	3.50E+07	7.50E+07	3.00E+07
Splenocytes: Mouse 2	3.50E+07	3.50E+07	9.50E+07	2.00E+07
Splenocytes: Mouse 3	3.50E+07	2.50E+07	7.50E+07	1.50E+07
Splenocytes: Mouse 4	4.80E+07		9.00E+07	
Splenocytes: Mouse 5	3.80E+07		9.50E+07	

Cell Maturation

BMDMs were matured for 6-7 days at 37˚C and 5% CO2 in DMEM (Dulbecco's Modified Eagle Medium) containing 10% fetal bovine serum, 1% multi-clonal stimulation factor, 1% penicillin-streptomycin (pen/strep), and 1% L-glutamine. BMDM cells were dislodged from using cell stripper (Corning, 25-056-CI). Adherent cells were incubated with cell stripper for 2 minutes and then dislodged by gentle pipetting and centrifuged at 1500 rpm for 10 minutes and then resuspended in DMEM complete to wash. Centrifuged at 1500 rpm for 10 minutes and then resuspended in DMEM complete to a concentration of $5x10^5$ cells/ml in DMEM complete without pen/strep. Cells were distributed to 24-well and 6-well plates and incubated for 2 hours to allow adherence.

Bacterial culture

M. bovis (BCG; gifted from Graviss Lab, Houston Methodist Research Institute, TX) was grown from frozen stock in Middlebrook 7H9 media (C32, Hardy Diagnostics), containing 0.2% glycerol, 10% OADC and 0.05% Tween-80. After undergoing one subculture bacteria was grown to late log phase, centrifuged, and resuspended to desired concentration.

Ex vivo infection

DMEM complete without pen/strep was prepared. Host BMDM cells were allowed to adhere for 2 hours and then were washed with medi. BCG was centrifuged at 1500rpm for 10 minutes and then resuspended to a desired concentration in the DMEM complete. Resuspended bacteria was utilized to infect at an MOI of 1:5 host cells to bacteria (BCG). Study was performed in triplicate. Cells were then incubated at 37˚C and 5% CO2 for 4 hours with infected media. After infection was complete supernatant was removed and host cells were washed twice with phosphate buffer saline solution (PBS). DMEM media containing 50µg/ml of gentamicin was added to wells followed by 12 hours of incubation to remove extracellular bacteria leftover from infection incubation. After incubation with gentamicin, plates were washed with PBS twice and fresh media was added to cell wells. Cells were then incubated for 120 hours.

Sample collection and immune response quantification

Samples were collected at hour 0, 24, 48, 72, 96 and 120 hours post infection. Imaging occurred using an Olympus CKX41 microscope immediately prior to every sample collection time point (Figure 2D). This experiment was replicated three times, resulting in three trial groups per condition.

Quantification of bacterial load

At hours 0, 24, 48, 72, 96 and 120 post infection, supernatant from the 24-well plate was collected and serially diluted 10-fold. Dilutions were then plated on 7H11 agar plates (W35, Hardy Diagnostics) to quantify the extracellular bacterial load. Wells were washed once with PBS then incubated with 1% Triton X-100 for 10 minutes, to allow cells to lyse. The lysate was then collected, serially diluted 10-fold, and plated on 7H11 agar plates to quantify intracellular bacterial load. After 28 days incubation, countable colony forming units (CFU) were enumerated to determine extracellular and intracellular bacterial load. It should be noted that at hour 0 extracellular counts were present; this may be caused by inefficiency of gentamicin to fully eradicate BCG infection, though it does lower bacterial counts significantly. Supernatant not utilized for CFU counts was stored in -80˚C and later used for cytokine and reactive species quantification. After collection of supernatant from 6-well plates, trizol was added to wells. Trizol lysate was collected from from 6 and 24 well plates and chloroform extraction for the purification of mRNA (Qiagen, 74104) was performed. Samples were frozen in -80C for short term storage. Purified mRNA samples were further process using iScript cDNA kit (#1708891, Bio-Rad), SYBR green universal mix (#1725275, Bio-Rad), and primers (Bio-Rad) to quantify mRNA. RNA processing completed thanks to Dr. J. Tharmalingam.

Assay Quantification

Using supernatant collected from 24-well plates, 25(OH) Vitamin D ELISA (ENZO, ADI-900-215-0001) was performed in accordance with manufacturer's instructions with a sensitivity range 0.5-1010 ng/ml was used to quantify circulating vitamin D3 concentrations and the amount of vitamin D3 present at 0h. Griess reagent (Promega, G2930) was utilized to quantify NO2– concentrations. LDH cytotoxicity assay (Pierce, 88954), performed in accordance with manufacturer's instructions, was used to quantify cell death. Known concentrations of host cells were lysed and their corresponding LDH concentrations used to

generate a linear regression subsequently applied to LDH assay readings from experimental samples to determine amount of cell death. Alcohol colorimetric assay(K620-100, BioVision) was performed in accordance with manufacturer's instructions with a sensitivity range 10-800nM, was used to quantify circulating alcohol concentrations and the amount of alcohol present at 0h. H2O2 colorimetric assay (K265-200 , BioVision) was performed, the sensitivity of the assay is as low as 40nM.

Statistical analysis

Statistical analysis was performed using MATLAB [98]. We performed outlier analysis and normalized the data within their vitamin D state and within their ethanol state to better understand the effects of isolated conditioning as well as combined. Normalization was done at each time point within each assay. After normalization values were averaged together. Welch's t test was performed on non-normalized data for each time point (0-120, 24 hour time window intervals) and for all time points combined (0-120, without windowed intervals) to identify statistically significant variations in immune response between experimental conditions. Rate of change over time was calculated using non-normalized data. Pearson correlation analysis was applied to non-normalized data and rates of change to calculate correlations between cytokines and effector molecules.

Results

Mice receiving our liquid diet maintained a weight between 20 and 25 grams(g), with those diets containing vitamin D3 trending on the higher end, towards 25g, for the first 3 weeks on liquid diet (18-20 week, Figure 31). By week 4 of liquid diet (21 week) there is less skew between the groups and with a range of 20-22. This ranges persists through week 5 (22week) until week 6 (23 week) in which vitamin D3 deficient with and without alcohol rise to a weight of 23.25g and 24.6g, respectively (Figure 31). At 7 weeks after starting liquid diet all alcohol diet mice were sacrificed due to unforeseen health complication, at this time all mice were 22-22.8g. Complications included malocclusion, tail infection, and neurological disorder possibly due to trauma. Though the veterinarian assessments found each incident to be unique and could not attribute it to our diet, incidents occurred only in alcohol containing diets. At 8 weeks post liquid diet initiation the remaining non-alcohol exposed mice were sacrificed. Their weight average was 21.75 for

vitamin D3 deficient and 25.6 for vitamin D3 sufficient. Though we saw differences in response to infection there was no great difference in weight found between any of the conditions. What difference that could be found was in the unusual deaths experienced by four of our alcohol exposed mice. Upon collection of blood and spleen we found differences between cell counts. In the spleen we found that alcohol diet mice regardless of vitamin D status had lower counts of splenocytes than those without alcohol exposure. -D3/-EtOH mice had noticeably higher splenocyte counts than any other condition, 2-6 times higher than other conditions. Previous studies completed using the Lieber-DeCarli alcohol diet have shown that alcohol exposure allows for a dysregulated immune response in splenocytes potentially resulting in lower cell counts [179] (Table 15). We also found that alcohol exposure mice had less PBMC cells counted than their non-alcohol exposed vitamin D3 counterpart. Previous studies have found that alcohol can induce apoptosis in PBMCs causing the lower cell counts we recorded [180] (Table 15).

Cytotoxicity

Cytotoxicity across all conditions saw the most difference at later time points. We can observe from (Figure 33) microscopic images that over time the infection worsens and has not been contained or cleared. At 48h -D3/+EtOH appeared to have the healthiest cells, in the greatest quantity. This agrees with cytotoxicity measurements at this point in which -D3/+EtOH cytotoxicity values are the second lowest. -D3/-EtOH has the lowest measured amount of cytotoxicity but appears based on microscopic images to be carrying a slightly higher bacterial load than -D3/+EtOH. By 96h infection has worsened greatly across all conditions. Most notably -D3/+EtOH now appears to be the second highest measurement. +D3/-EtOH had the highest amount of cytotoxicity, though from the images we can observe less cells present but a healthier appearance to the cells, less bacterial aggregates and cellular debris (Figure 31). From our microscopic images it appears that +D3/+EtOH has the most aggravated infection, with non-alcohol conditions both with and without vitamin D3 having less bacterial clumps.

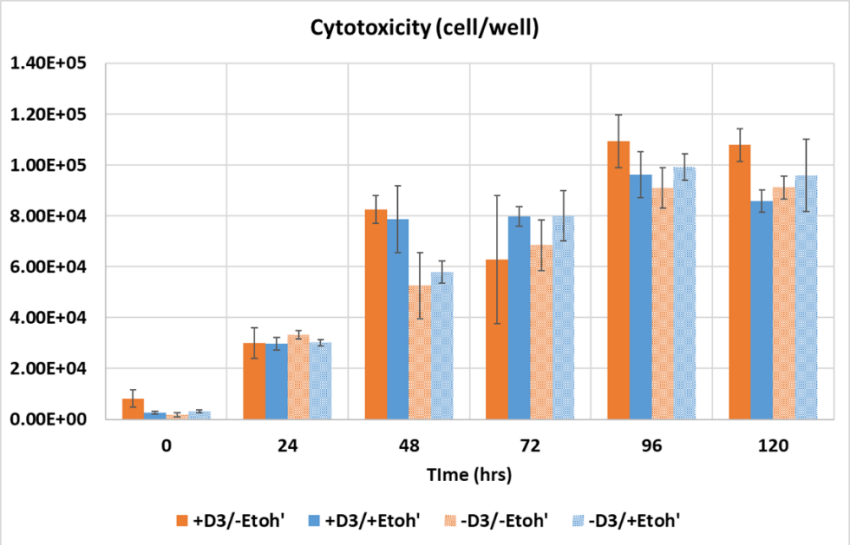

Figure 31. Cytotoxicity.

Table 24. Welch's t Test.

Condition1	Condition2	0	24	48	72	96	120
h2o2.+D.-E	h2o2.+D.+E						0.049
ldh.+D.-E	ldh.+D.+E						0.047
ldh.+D.-E	ldh.-D.+E			0.025			
ldh.uninf	ldh.+D.+E			0.049	0.010	0.008	0.001
ldh.uninf	ldh.+D.-E			0.005		0.005	0.001
ldh.uninf	ldh.-D.+E	0.046			0.023	0.002	0.021
ldh.uninf	ldh.-D.-E		0.045			0.008	0.001
no.+D.+E	no.-D.+E			0.008			
no.+D.-E	no.+D.+E					0.009	
no.+D.-E	no.-D.+E			0.017			
no.uninf	no.+D.+E			0.000	0.001	0.000	0.000
no.uninf	no.+D.-E		0.010	0.001		0.000	0.001
no.uninf	no.-D.+E			0.000	0.000	0.002	0.001
no.uninf	no.-D.-E			0.005	0.007	0.005	0.001

Table 25. Aggregate amount of significant differences as determined by Welch's t test.

Condition	Significant Differences
+D3	6
-D3	3
-EtOH	5
+EtOH	6

Table 26. Welch's t Test for Rate of Change

Condition1	Condition2	0-24	24-48	48-72	72-96	96-120
h2o2.+D.-E	h2o2.-D.-E	0.023				
h2o2.uninf	h2o2.+D.-E			0.012		
h2o2.uninf	h2o2.-D.-E			0.035		
ldh.uninf	ldh.+D.-E		0.026			
ldh.uninf	ldh.-D.-E			0.029		
no.+D.+E	no.-D.+E		0.032			
no.+D.+E	no.-D.-E		0.040			
no.uninf	no.+D.+E	0.008	0.001	0.032		
no.uninf	no.+D.-E		0.003			
no.uninf	no.-D.+E	0.005	0.001	0.010		
no.uninf	no.-D.-E	0.003	0.002			

At all time points except 24h -D3/+EtOH was 1.1 to 2.1-fold higher than -D3/-EtOH. Allowing us to theorize that alcohol consumption in a vitamin D3 deficient host will result in a strong cytotoxic response. In +D3/+EtOH we see the opposite relationship with +D3/-EtOH. At all time points except 24 and 120h +D3/+EtOH has 0.4 to 0.9-fold less cytotoxicity. At 120h +D3/+EtOH was found to be statistically significantly different from +D3/-EtOH (p value 0.047, Table 26); this may indicate a protective effect that ethanol consumption has when consumed by a vitamin D3 sufficient host. This is different from what we have seen in regards to our previous experimentation in chapter 2 and 3. Previously we had exposed host cells directly to 0.8% ethanol, and saw a sizeable increase in cytotoxic response due to this exposure. Now having moved to in vivo alcohol exposure we see that there is some protective effects in the presence of vitamin D3. This may be due to a systemic utilization of alcohol and instead of single cellular processing. BMDMs may not have the necessary functionality to utilize and neutralize alcohol to the extent that the whole body system is capable of.

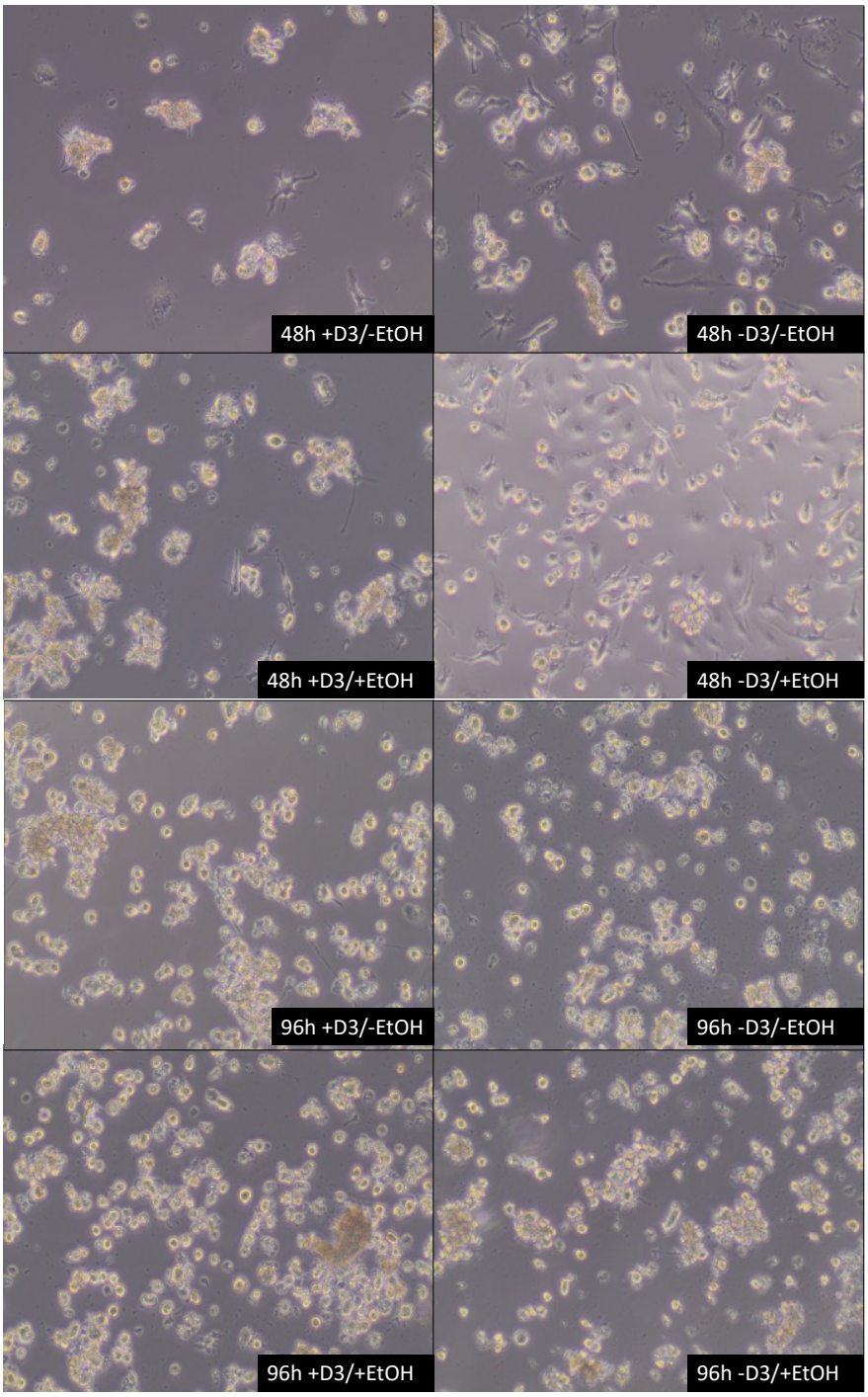

Figure 32. 48 and 96 hour microscopic images of infection.

Nitric Oxide and Hydrogen Peroxide

As with cytotoxicity we see an oscillatory pattern, though it is much more pronounced in NO production than cytotoxicity, with peaks in production at 48 and 96h. . +D3/-EtOH and +D3/+EtOH was

significantly different at 96h (p value 0.009, Figure 33). As with previous experimentation in chapter 2 and 3, NO response is more prevalent at the later time points of infection. Vitamin D3 deficient conditions produce similar levels of NO throughout with the largest differences at 72h, wherein -D3/+EtOH produces 1.1-fold higher than -D3/-EtOH. +D3/+EtOH was significantly different from -D3/+EtOH for both concentration and rate of change, 48h and 23-48h respectively (p value 0.008, 0.032). At later time points 96h and 120h, +E3/+EtOH produces the lowest amount of NO. This once again lends towards the theory that in vivo alcohol consumption in a vitamin D3 sufficient host may actually have positive effects.

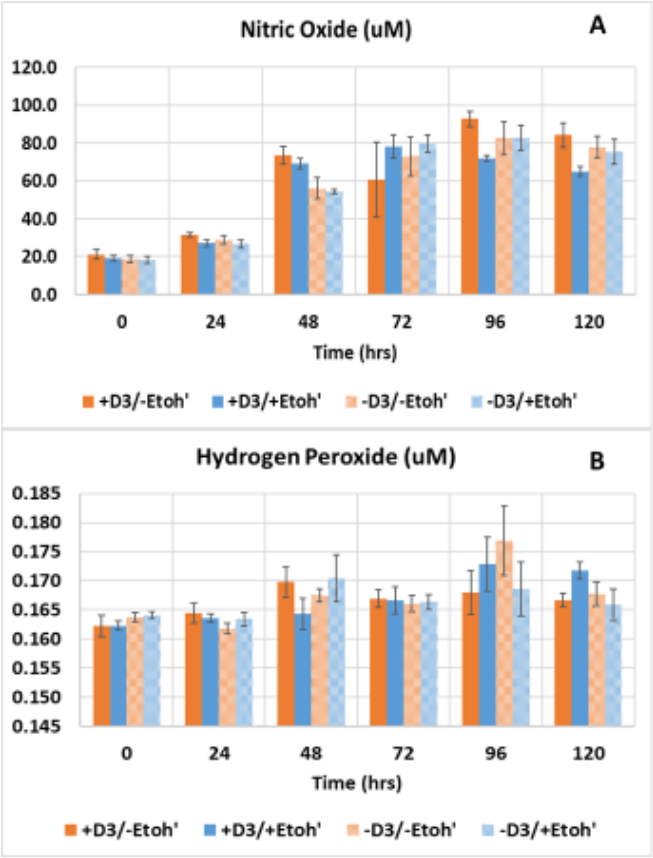

Figure 33. Effector Molecules nitric oxide and hydrogen peroxide.

In the earlier time points (0, 24, 48, 72h) -D3/+EtOH condition consistently produces 1.002-1.017-fold higher than -D3/-EtOH. In previous experimentation in chapter 2 and 3 we found that H2O2 had greater differences in condition at earlier time points while NO had differences later (Figure 33). In this current study we do see some small differences at earlier time points (0, 24h) but the greatest difference -

between conditions is present at 48, 96, and 120h. We found that +D3/-EtOH was significantly different from +D3/+EtOH at 120h (p value 0.049). For rate of change we found that +D3/-EtOH was significantly different from -D3/-EtOH at 0-24h (p value 0.023, Table 28), indicating that at onset of infection without the presence of alcohol vitamin D3 has early regulation of H2O2. When conditioned in vivo we see a much more synergistic and similar production between NO and H2O2 trends between conditions, though the time dependent behavior does remain prevalent in NO especially.

Pearson Correlation Analysis

We found that cytotoxicity and NO had a strong positive correlation across all conditions, including uninfected cells. This is indicative of the acute cytotoxic effect of NO when present in large quantities. As NO goes up with time so does the cytotoxic response. For all infected conditions except -D3/+EtOH cytotoxicity had a positive correlation with H2O2. This may be indicative of the voracity of infection taking place, as evidenced by the cytotoxic- H2O2 positive correlation, the cytotoxic measurements, and the microscopic images. NO and H2O2 have a strong positive correlation in -D3/-EtOH as well, in previous experiments shown in chapter 2, this was also true but only in high level infection (Table 27).

Table 27. Pearson Correlation for conc.

		uninf	+D3/-Etoh'	+D3/+Etoh'	-D3/-Etoh'	-D3/+Etoh'
Cytotox	NO	+	+	+	+	+
Cytotox	H2O2		+	+	+	
NO	H2O2				+	

Discussion

Vitamin D3 sufficiency produces the most distinct response to infection. We found that in vitamin D3 sufficient condition (+D3) there were 9 significant differences as compared to the all other host states. This emphasizes the distinction between the added stress of alcohol exposure and the normative condition, +D3/-EtOH. We compared this model for infection with the one utilized previously in chapter 3. We found that in regards to cytotoxicity our current study utilizing the liquid diet results in higher amounts of

cytotoxicity when compared to our previous study (Figure 36). At all time points except 0 and 120h our liquid diet study had larger amounts of cytotoxicity. At 120h vitamin D3 deficient conditions (Def, Def+VitD, Def+EtOH) were in a similar range to that of our liquid diet study. It is clear based on these results that we achieved a much higher infection level than that of our previous study. Our previous study from chapter 3 was at an MOI 1:1 while in this study we utilized an MOI 1:5, based on these comparisons we can determine that our infection level was higher than MOI 1:1 but we can not definitively state that it was MOI 1:5. When comparing 48h microscopic images in this study to images at 34h from chapter 2 we found at high level infection of *M.smegmatis* ethanol conditioned cells appear to have less cytotoxicity than all other conditions, the same result was observed in the current study.

Similar to our previous *M.smegmatis* experiment in chapter 2, in which we observed that ethanol conditioned cells produced the maximum amount of H2O2 across infection levels, we found that +D3/+EtOH cells produced less H2O2 than -D3/+EtOH. This trend held true across all time points for *M.smegmatis* infection but for BCG infection the trend was observed 0-48h. Difference in observed between the two studies may be due to intrinsic differences between *M.smegmatis* and *BCG* strains or it could be temporally motivated, as BCG infection samples were collected over a greater period of time but less frequently than with *M.smegmatis*.

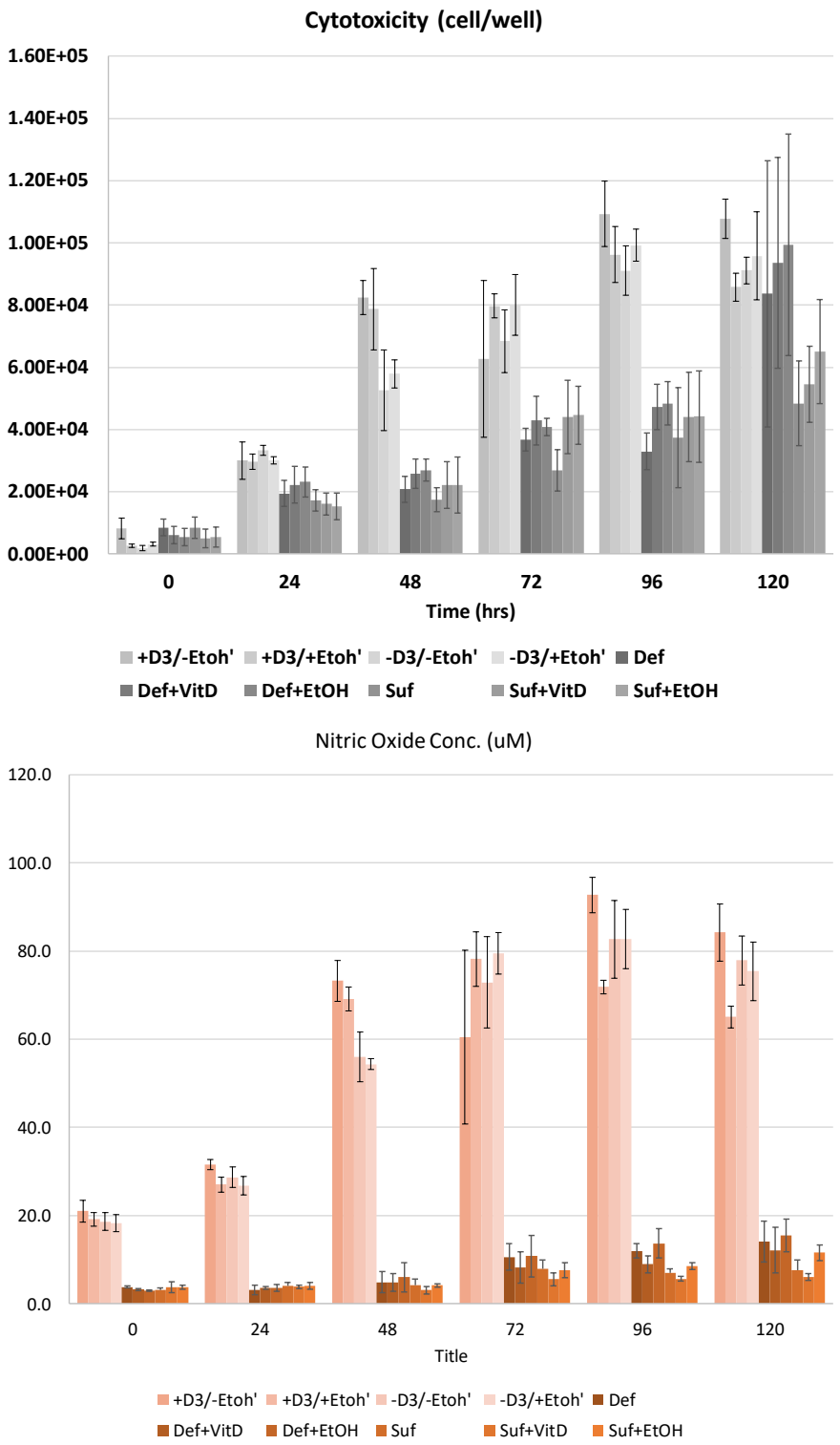

Figure 34. Comparison between ex vivo experiments Cytotoxicity and NO

We also compared the nitric oxide production between this experiment and that of chapter 3 (Figure 34). Cells in the chapter 3 study were infected with a low level amount of BCG, MOI 1:1. We found that this experiment resulted in much higher amounts of NO than of chapter 3. This is indicative of a higher infection load of MOI 1:5 as compared to MOI 1:1 in chapter 3. Though the magnitude is much high in the liquid diet NO production the trend between behavior is the same between both experiments. The presence of both alcohol and vitamin D results in the decrease of NO production. Between both experiments vitamin D3 sufficient mice in both cases produced more NO than their vitamin D3 deficient counterparts. Though we can see that NO production is effected greatly by infection level, there are still some trends that persist in regards to the relationship between vitamin D3 deficient and sufficient production (Figure 34, Table 28).

Table 28. Correlation comparisons within the same assay across different conditions to analyze similarities.

	uninf	+D3/-EtOH	+D3/+EtOH	-D3/-EtOH	-D3/+EtOH
uninf		no, ldh	ldh, h2o2	no, ldh	no, ldh
+D3/-EtOH			no, ldh	no, ldh, h2o2	no, ldh, h2o2
+D3/+EtOH				no, ldh, h2o2	no, ldh
-D3/-EtOH					no, ldh, h2o2
-D3/+EtOH					

When comparing the current study with that of chapter 3 we found that at 96h all similar conditions showed the same trend in behavior with regards to vitamin D3 availability. Suf, Def, Def+EtOH, and Suf +EtOH showed similar trends when compared to their counterpart, +D3/-EtOH, -D3/-EtOH, -D3/+EtOH, and +D3/+EtOH respectively. At 96h ethanol exposed cells had less vitamin D3 available than their non-exposed counterparts, this was true in both studies. At 0 and 48h, +D3/-EtOH and +D3/+EtOH have the same trend in behavior as that of Suf and Suf+EtOH. At 0h +D3/+EtOH vitamin D3 availability exceeds that of +D3/+EtOH and at 48h the opposite is true. For 0 and 48h -D3/-EtOH and -D3/+EtOH have an opposite trend in behavior when compared to Def and Def+EtOH. At 0h -D3/-EtOH and -D3/+EtOH have the same trend at the vitamin D3 sufficient conditions, with ethanol conditioned cells having higher concentrations of available vitamin D3. But in our previous study in chapter 3 the opposite was true, Def had a higher concentration of vitamin D3 than Def+EtOH. The same is true at 48h, -D3/-

EtOH and -D3/+EtOH have the same trend at the vitamin D3 sufficient conditions, with ethanol conditioned cells having lower concentrations of available vitamin D3. But in our previous study in chapter 3 the opposite was true, Def+EtOH had a higher concentration of vitamin D3 than Def. This change in trend may indicate that in vivo deficiency plus alcohol has a larger dyregulatory effect than in vivo deficiency followed by exogenous alcohol exposure.

In this study we found cytotoxicity to be highly positively correlated to NO concentration across all conditions. This correlation held in our previous BCG infection study as well, in chapter 3, but was found only in Def and Def+VitD conditions. This is further indication that infection level in this study is much higher than that of the previous, as the concentration of NO increases in response to infection. In our previous study the correlation was present in cells which carried the highest bacterial load and most cell death, irrespective of exogenous addition of alcohol. We found that rate of change correlated between cytotoxicity and NO across all conditions as well. In previous studies rate of change correlated between cytotoxicity and NO at high level of *M.smegm*atis infection for control and vitamin D3 conditioned cells, and Suf+EtOH condition cells in our previous BCG infection. The correlations between NO and cytotoxicity for rate of change and concentration may be indicative of a dysregulated system either through high bacterial burden, exogenous alcohol, or deficiency H2O2 and NO positively correlated in high level *M.smegmatis* infection in our previous study, in this current study -D3/-EtOH maintained that correlation.

We have developed the first *in vivo* vitamin D3 deficient, alcohol based diet utilizing a murine model of mycobacterium infection. Our study is unique in that we have conditioned mice on a vitamin D3 deficient diet not from adulthood as most others do, but from weanlings (3 week old) [50], [179], [181]. After 15 weeks on the vitamin D3 deficient solid diet we then switch the mice to the alcohol diet for an additional 8 weeks. While several studies regarding the role of alcohol or vitamin D3 deficiency during mycobacterium infection do exist few have characterized infection over time and we found no other models regarding the combined effects of deficiency and alcoholism.

Chapter 6 Examination of differences between M.tuberculosis strains

Introduction

To examine strain-dependent differential growth we performed bacterial growth studies for three strains of M.tuberculosis H37Rv, CDC 1551, and HN3409. The majority of TB research is performed using less virulent M.tb analogs, the most common being M.smegmatis and M.bovis (BCG live vaccine). We utilized these analogs as well the Mtb strains for our studies. Strains were grown in optimal growth broth, in a highly nutritious environment.

H37Rv is the standard lab strain utilized for the study of TB. H37Rv is a virulent subculture from the original H37 strain. H37 was isolated in 1905 and in 1934, H37 was dissociated into virulent(H37Rv) and avirulent(H37Ra) strains.[182], [183]. CDC1551 is a Kentucky - Tennessee outbreak strain. This clinical isolate considered to be hypervirulent, fast growing, and highly transmissible. The CDC1551 strain caused a local outbreak of TB in the Kentucky-Tennessee border region . In 1994, 21 patients were diagnosed with active TB. Among 429 TB patient contacts, 72% had positive (often large) tuberculin reactions. These findings originally implied that the CDC1551 strain is more infectious than other TB strains. In vivo animal models have also supported this claim [184]–[186]. HN3409 was isolated in 2002 from human pulmonary tissue in Texas. HN3409 is multi-drug resistant (MDR) strain of tuberculosis. It has been shown to be resistant to rifampicin, rifabutin, and isoniazid[187].

Following the growth studies we intended to examine cross-generational vitamin D3 deficiency and its effects during H37Rv and HN3409 infection. With further conditioning based on age of host (murine) at onset of infection.

Methods

<u>Bacterial culture</u>

M.tuberculosis strains H37Rv, CDC 1551, and HN3409 were grown from frozen stock on Lowenstein Jensen slants. From the solid culture we inoculated baffle flasks containing 7H9 broth (0.2% glycerol, 10% OADC and 0.05% Tween-80). Flasks were grown to late log. Using the initial liquid culture we inoculated a secondary culture at 1:100 ratio. Our secondary culture was used for all sample

collection and OD600nm readings over time. OD readings and samples were taken every 48 hours for 18 to 28 days. Experiments were performed in triplicate.

BCG and M.smegmatis strains were inoculated from frozen stock into 7H9 broth, contained in aerated glass tubes. Bacteria was grown to late log phase and was used for a secondary inoculation at a 1:100 ratio. Our secondary culture was used for all sample collection and OD600nm readings over time. OD readings and samples were taken for BCG every 24 hours and for M.smegmatis every 6. Colony forming unit (CFU/ml) was quantified by serially diluting collected sample and plating dilutions on 7H11 plates. Experiments were performed in triplicate. Welch's t test was run on CFU/ml and rates of change data.

Results

From the OD600nm curve we can observe very similar growth dynamics between the strains. It is apparent that HN 3409 grew slowest of all mycobacterium strains measured and H37Rv grew the fastest. Though the OD600nm reading for all strains plateaus between 1.2 and 1.5OD600nm, in actuality a death curve has begun. We found that there was no significant difference between the mycobacterium strains when comparing CFU/ml and OD600nm reading, as well as their respective rates of change. We observed that all the strains experience two peaks in their growth curve, a minor and major peak, instead of just the anticipated one. We found that even sampling in the middle of logarithmic phase of growth presented with a decrease in live bacteria compared to earlier time points. This sudden drop in CFU/ml counts happened in H37Rv at 10d, CDC1551 at 6d, BCG at 7d, and HN3409 at 9d. OD600nm readings were not able to detect the change.

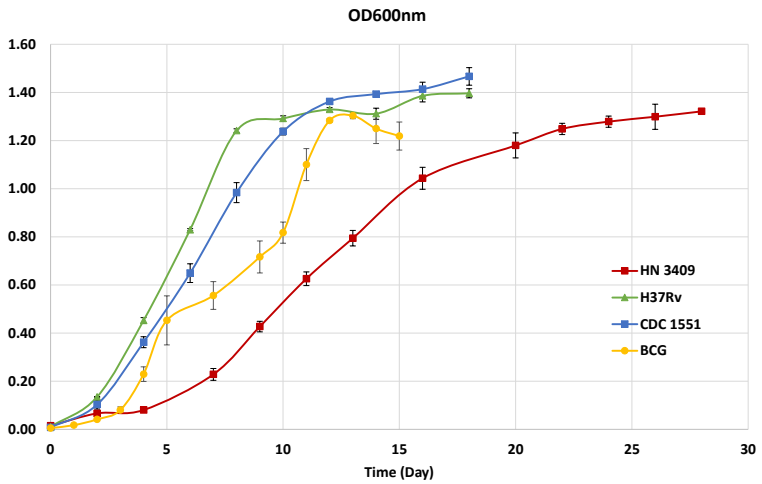

Figure 35. OD600nm readings for different Mycobaterium strains.

In regard to the timing of the peaks, CDC 1551 experienced its first peak, minor, at 4d and its second, major, at 8d. CDC 1551 peaked the fastest of all other strains. The slowest to peak was HN 3409 with its minor peak at 7d, and its minor at 16d. This is to be anticipated from an MDR strain. BCG interestingly, experiences a minor peak similar in magnitude to CDC 1551's minor peak and a major peak similar in magnitude to H37Rv and HN 3409. H37Rv, oddly experiences its major peak before its minor, with its major at 8d, and its minor at 12d. This is unlike any of the other strains (Figure 35).

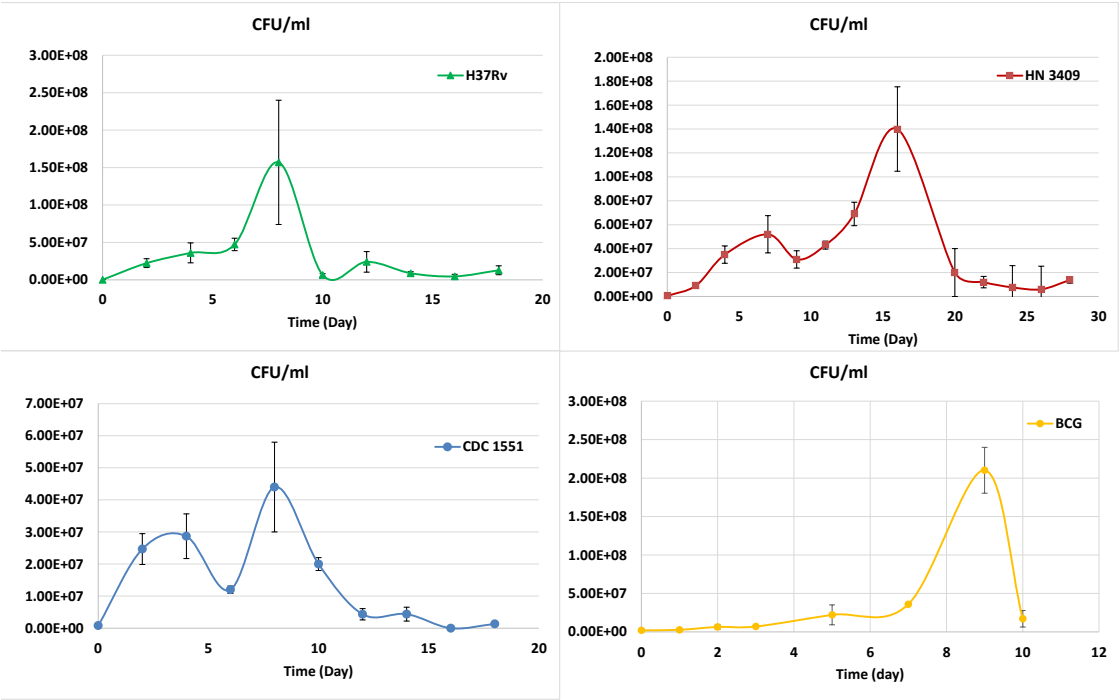

Figure 36. Colony forming units per ml for different Mycobacterium strains.

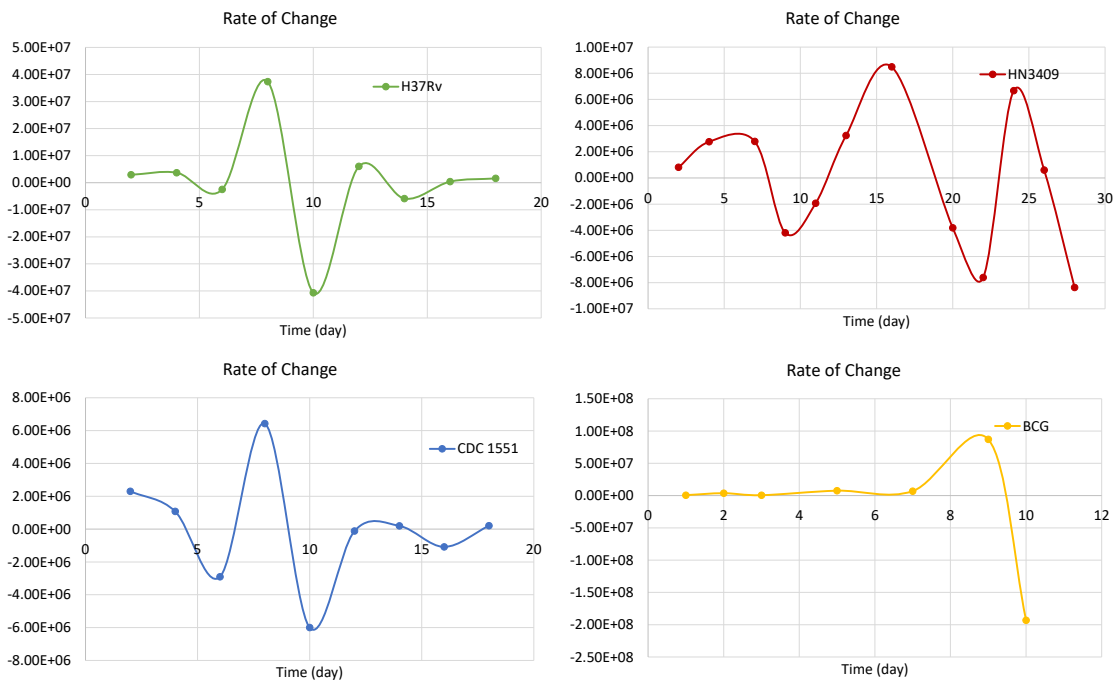

Figure 37. Rate of Change for different Mycobacterium strains

We observed interesting differences between strains in regards to the minimum and maximum CFU/ml. We did not consider counts taken at 0h as those were more dependent on the previous inoculate and less so on the growth over time. CDC 1551 produced the smallest minimum CFU/ml at 18d (1.33e6 CFU/ml), followed by H37Rv (14d, 4.67e8 CFU/ml), BCG (1d, 2.71e6 CFU/ml), and HN 3409 (16d, 6e6 CFU/ml, Figure 36-37). CDC 1551 also produced the smallest maximal measurement at 8d (4.4e7 CFU/ml), followed by HN3409 (16d, 1.4e8 CFU/ml), H37Rv (8d, 1.47e8), and BCG (9d, 2.10e8 CFU/ml). For all Mtb strains the minimum occurs between 14d and 26d, but with BCG its minimum occurs at 1d. BCG appears to maintain very low quantities of mycobacterium and remain in the log phase for 7d, at which point it enters the log phase. BCG has the longest lag phase of all the mycobacterium observed, while CDC 1551 has the shortest lag phase. CDC 1551 enters into the logarithmic phase by 2d.

Discussion

BCG and H37Rv are two of the most common bacterium used for the study of clinical TB. What we have shown through our growth studies is the similarities and differences between clinical strains, CDC 1551 and HN 3409, and laboratory strains, H37Rv and BCG. From our discovery of the two peaks in CFU

growth we are able to ascertain that a mid-logarithmic phase the live-dead ratio of the bacteria is such that the OD600nm reading continues to increase but the bacterial growth is actually in decline. We see a similar effect when the bacterium enter the stationary phase. In the stationary phase the OD600nm reading plateaus but the bacterium have entered their death curve and are in sharp decline. Though we did not find a significant difference between strains when comparing CFU/ml and rate of change. From these results we can determine that early log phase is best when utilizing OD600nm readings to predict CFU/ml. Specifically H37Rv is best collected between day 3-6 at an OD600nm reading of 0.1-0.8, HN 3409 at day 9-16 with an OD600nm reading of 0.4 to 1, BCG at day 2-6 with an OD600nm of 0.06-0.7, and due to its fast growth rate CDC 1551 at day 0-4 at an OD600nm reading 0.01-0.4.

Chapter 7 Future work and conclusions

In utero vitamin D3 deficiency to be used for future studies

There are many strains of mycobacterium, each expressing their own unique phenotype. Studies have shown large genetic variation among strains of Mtb. Genetic variation is the cause of strain-based differential immune response and is often overlooked in studies utilizing only H37Rv, Erdman, H37Ra, or BCG strains. Strains which have been cultivated in a lab setting sometimes lack virulence factors, present in clinical isolates collected from an infected human host. These genetic variations will most assuredly result in differences in immune response which will in turn effect many aspects of treatment, diagnostics, and scientific study.

Utilizing *Mycobacterium tuberculosis* standard lab strain (H37Rv) and MDR clinical strain (HN3409) we intended to investigate the effects of age, vitamin D_3 deficiency and bacterial strain on outcome of disease. By feeding weanling females vitamin D_3 deficient diet (Envigo, TD89123) for greater than 5 weeks and then breeding those females we will able to obtain *in utero* vitamin D_3 deficient pups. The subsequent pups will also be fed the vitamin D_3 deficient diet and sacrificed at 4 and 10 weeks of age, equivalent to 5 and 12 human years. BMDM cells will be extracted and infected with H37Rv or HN3409. Samples will be collected every 24 hours and assay analysis will be performed. Our *in utero* vitamin D_3 deficiency is currently underway, several litters have been born from this process. Their cells have been collected and frozen for future use. We observed problems with diet during breeding. The Envigo diet is intended for colony maintenance not breeding and so pups were often undersized or did not survive to weaning age. We also observed that the pups bred on both Envigo diets had greasy, thinning fur. Breeding females on the Envigo diets exhibited higher amounts of aggression and killed most of the litters they carried to term. It is recommended that only the first litter from Envigo diet conditioned breeding female is utilized. Two or more litters from the same breeding female exacerbate anomalous effects of diet.

Quantifying the effect of vitamin D deficiency and alcohol exposure on immune response to mycobacterium infection

Our preliminary results utilizing *M.smegmatis* found that exogenous addition of vitamin D3 modulated host response in an infection level dependent manner. It is evident that modulation occurred on

a genetic level. In both high and low level infection vitamin D3 reduced the concentreation of NO and H2O2 below that of the ethanol conditioned cells. We found NO to be an infection level dependent response. We concluded from our preliminary *M.smegmatis* study that ethanol, even in small quantities, dysregulates immune response.

With the application of our previous methodology to ex vivo infection, with in vivo vitamin D3 deficiency we found that alcohol had an acute effect on immune response when added exogenously to primary mouse macrophage cells during BCG infection. Alcohol caused the upregulation of all cytokines and effector molecules measured. Both *in vivo and ex vivo* conditioning effected cytokine production, with *in vivo* conditioning having the greatest effect on macrophage immune response. Overall sufficient vitamin D3 in vivo diet caused a down-regulation of cytokines and effector molecules, as well as a down-regulation of host cytotoxicity while maintaining a bacterial load that was comparable or lower than that of deficient.

We have built a simulation comprised of four host cellular compartments: the immediate extracellular area, the cytoplasmic compartment, the nuclear compartment and the phagocytic compartment. Our model was able to simulate several primary immune response functions, such as the mycobacterium small protein-induced production of Cyp27B1 enzyme, the vitamin D_3 mediated production of H_2O_2, the signal transduction of cytokines IL-12 and IFN-g, the metabolism of NO, and several others. We were able to capture vitamin D3 enzymatic processing and transport, cytokine production and signaling, vitamin D3 downstream production of effector molecules, as well as integrate the Salim et.al. IFN-g and TNF-a model with our own intracellular model. We were able to make comparisons between in silico and in vitro/ex vivo in our earlier models and found our computational models were not significantly different from our empirical. In the future we will compare the behavior of our fully integrated model to that of its empirical counterpart.

We further expanded our empirical model to perform all host cell conditioning *in vivo*. Mouse were given a vitamin D3 deficient or sufficient diet and administered alcohol or water depending on assigned condition. We found that in vitamin D3 deficient mice alcohol consumption causes higher amounts of cytotoxicity, as evidenced by our LDH concentration and cell counts. In a vitamin D3 sufficient mice alcohol consumption was sometimes beneficial in host cell preservation, if vitamin D3 is

present. The presence of vitamin D3 causes a faster, earlier upregulation of H2O2 while the presence of ethanol depresses NO production.

We found that vitamin D3 and ethanol exposure differentially modulate immune response to infection, this response is contingent on a number of factors. Factors such as, infection level, in vivo or in vitro exposure to vitamin D3 and/or ethanol, sampling time, and bacterial strain. We were able to quantify the effects of vitamin D3 deficiency and alcohol exposure through the exploration and manipulation of all the listed factors. We were able to the combined and isolated effects of each factor, and its subsequent modulation of immune response.

References

[1] "WHO | Global tuberculosis report 2018," *WHO*. [Online]. Available: http://www.who.int/tb/publications/global_report/en/. [Accessed: 23-Apr-2019].

[2] J. K. Sia, M. Georgieva, and J. Rengarajan, "Innate Immune Defenses in Human Tuberculosis: An Overview of the Interactions between Mycobacterium tuberculosis and Innate Immune Cells," *J. Immunol. Res.*, vol. 2015, p. e747543, Jul. 2015.

[3] J. D. Ernst, "Macrophage Receptors for Mycobacterium tuberculosis," *Infect. Immun.*, vol. 66, no. 4, pp. 1277–1281, Apr. 1998.

[4] A. R. Martineau, F. U. Honecker, R. J. Wilkinson, and C. J. Griffiths, "Vitamin D in the treatment of pulmonary tuberculosis," *J. Steroid Biochem. Mol. Biol.*, vol. 103, no. 3–5, pp. 793–798, Mar. 2007.

[5] M. Verway, M. Bouttier, T.-T. Wang, M. Carrier, M. Calderon, B.-S. An, E. Devemy, F. McIntosh, M. Divangahi, M. A. Behr, and J. H. White, "Vitamin D Induces Interleukin-1β Expression: Paracrine Macrophage Epithelial Signaling Controls M. tuberculosis Infection," *PLoS Pathog.*, vol. 9, no. 6, p. e1003407, Jun. 2013.

[6] CDC, "Center for Disease Control and Prevention," Apr-2016. .

[7] "CDC | TB | Treatment." [Online]. Available: https://www.cdc.gov/tb/topic/treatment/default.htm. [Accessed: 10-Feb-2017].

[8] J. Liu, V. Tran, A. S. Leung, D. C. Alexander, and B. Zhu, "BCG Vaccines: Their mechanisms of attenuation and impact on safety and protective efficacy," *Hum. Vaccin.*, vol. 5, no. 2, pp. 70–78, Feb. 2009.

[9] X. Jia, L. Yang, M. Dong, S. Chen, L. Lv, D. Cao, J. Fu, T. Yang, J. Zhang, X. Zhang, Y. Shang, G. Wang, Y. Sheng, H. Huang, and F. Chen, "The Bioinformatics Analysis of Comparative Genomics of Mycobacterium tuberculosis Complex (MTBC) Provides Insight into Dissimilarities between Intraspecific Groups Differing in Host Association, Virulence, and Epitope Diversity," *Front. Cell. Infect. Microbiol.*, vol. 7, Mar. 2017.

[10] A. Roy, M. Eisenhut, R. J. Harris, L. C. Rodrigues, S. Sridhar, S. Habermann, L. Snell, P. Mangtani, I. Adetifa, A. Lalvani, and I. Abubakar, "Effect of BCG vaccination against Mycobacterium tuberculosis infection in children: systematic review and meta-analysis," *BMJ*, vol. 349, no. aug04 5, pp. g4643–g4643, Aug. 2014.

[11] B. B. Trunz, P. Fine, and C. Dye, "Effect of BCG vaccination on childhood tuberculous meningitis and miliary tuberculosis worldwide: a meta-analysis and assessment of cost-effectiveness," *The Lancet*, vol. 367, no. 9517, pp. 1173–1180, Apr. 2006.

[12] G. A. Colditz, C. S. Berkey, F. Mosteller, T. F. Brewer, M. E. Wilson, E. Burdick, and H. V. Fineberg, "The efficacy of bacillus Calmette-Guérin vaccination of newborns and infants in the prevention of tuberculosis: meta-analyses of the published literature," *Pediatrics*, vol. 96, no. 1 Pt 1, pp. 29–35, Jul. 1995.

[13] T. F. Brewer, "Preventing Tuberculosis with Bacillus Calmette-Guérin Vaccine: A Meta-Analysis of the Literature," *Clin. Infect. Dis.*, vol. 31, no. Supplement_3, pp. S64–S67, Sep. 2000.

[14] G. A. Colditz, T. F. Brewer, C. S. Berkey, M. E. Wilson, E. Burdick, H. V. Fineberg, and F. Mosteller, “Efficacy of BCG vaccine in the prevention of tuberculosis. Meta-analysis of the published literature,” *JAMA*, vol. 271, no. 9, pp. 698–702, Mar. 1994.

[15] E. Anes, P. Peyron, L. Staali, L. Jordao, M. G. Gutierrez, H. Kress, M. Hagedorn, I. Maridonneau-Parini, M. A. Skinner, A. G. Wildeman, S. A. Kalamidas, M. Kuehnel, and G. Griffiths, “Dynamic life and death interactions between Mycobacterium smegmatis and J774 macrophages,” *Cell. Microbiol.*, vol. 8, no. 6, pp. 939–960, Jun. 2006.

[16] W. L. Gluck and J. la Weinberg, “1 alpha, 25 Dihydroxyvitamin D3 and mononuclear phagocytes: enhancement of mouse macrophage and human monocyte hydrogen peroxide production without alteration of tumor cytolysis.,” *J. Leukoc. Biol.*, vol. 42, no. 5, pp. 498–503, 1987.

[17] C. Deb, C.-M. Lee, V. S. Dubey, J. Daniel, B. Abomoelak, T. D. Sirakova, S. Pawar, L. Rogers, and P. E. Kolattukudy, “A Novel In Vitro Multiple-Stress Dormancy Model for Mycobacterium tuberculosis Generates a Lipid-Loaded, Drug-Tolerant, Dormant Pathogen,” *PLoS ONE*, vol. 4, no. 6, p. e6077, Jun. 2009.

[18] J. M. DiChiara, L. M. Contreras-Martinez, J. Livny, D. Smith, K. A. McDonough, and M. Belfort, “Multiple small RNAs identified in Mycobacterium bovis BCG are also expressed in Mycobacterium tuberculosis and Mycobacterium smegmatis,” *Nucleic Acids Res.*, vol. 38, no. 12, pp. 4067–4078, Jul. 2010.

[19] J. Mattow, P. R. Jungblut, U. E. Schaible, H.-J. Mollenkopf, S. Lamer, U. Zimny-Arndt, K. Hagens, E.-C. Müller, and S. H. E. Kaufmann, “Identification of proteins

from Mycobacterium tuberculosis missing in attenuated Mycobacterium bovis BCG strains," *ELECTROPHORESIS*, vol. 22, no. 14, pp. 2936–2946.

[20] K. Takayama, C. Wang, and G. S. Besra, "Pathway to Synthesis and Processing of Mycolic Acids in Mycobacterium tuberculosis," *Clin. Microbiol. Rev.*, vol. 18, no. 1, pp. 81–101, Jan. 2005.

[21] P. R. Jungblut, U. E. Schaible, H.-J. Mollenkopf, U. Zimny-Arndt, B. Raupach, J. Mattow, P. Halada, S. Lamer, K. Hagens, and S. H. E. Kaufmann, "Comparative proteome analysis of Mycobacterium tuberculosis and Mycobacterium bovis BCG strains: towards functional genomics of microbial pathogens," *Mol. Microbiol.*, vol. 33, no. 6, pp. 1103–1117, Sep. 1999.

[22] C. Espitia, R. Espinosa, R. Saavedra, R. Mancilla, F. Romain, A. Laqueyrerie, and C. Moreno, "Antigenic and structural similarities between Mycobacterium tuberculosis 50- to 55-kilodalton and Mycobacterium bovis BCG 45- to 47-kilodalton antigens.," *Infect. Immun.*, vol. 63, no. 2, pp. 580–584, Feb. 1995.

[23] C. J. B. Williams, "Cod-liver Oil in Phthisis," *Lond. J. Med.*, vol. 1, no. 1, pp. 1–18, Jan. 1849.

[24] A.-L. Khoo, L. Y. A. Chai, H. J. P. M. Koenen, M. Oosting, A. Steinmeyer, U. Zuegel, I. Joosten, M. G. Netea, and A. J. A. M. van der Ven, "Vitamin D3 down-regulates proinflammatory cytokine response to Mycobacterium tuberculosis through pattern recognition receptors while inducing protective cathelicidin production," *Cytokine*, vol. 55, no. 2, pp. 294–300, Aug. 2011.

[25] M. Vidyarani, P. Selvaraj, M. S. Jawahar, and P. R. Narayanan, “1, 25 Dihydroxyvitamin D3 modulated cytokine response in pulmonary tuberculosis,” *Cytokine*, vol. 40, no. 2, pp. 128–134, Nov. 2007.

[26] J. L. Estrella, C. Kan-Sutton, X. Gong, M. Rajagopalan, D. E. Lewis, R. L. Hunter, N. T. Eissa, and C. Jagannath, “A Novel in vitro Human Macrophage Model to Study the Persistence of Mycobacterium tuberculosis Using Vitamin D3 and Retinoic Acid Activated THP-1 Macrophages,” *Front. Microbiol.*, vol. 2, 2011.

[27] M. E. Gough, E. A. Graviss, and E. E. May, “The dynamic immunomodulatory effects of vitamin D3 during Mycobacterium infection,” *Innate Immun.*, vol. 23, no. 6, pp. 506–523, Aug. 2017.

[28] M. Gough and E. May, “An in silico model of the effects of vitamin D3 on mycobacterium infected macrophage,” in *2016 38th Annual International Conference of the IEEE Engineering in Medicine and Biology Society (EMBC)*, 2016, pp. 1443–1446.

[29] E. Abe, Y. Shiina, C. Miyaura, H. Tanaka, T. Hayashi, S. Kanegasaki, M. Saito, Y. Nishii, H. F. DeLuca, and T. Suda, “Activation and fusion induced by 1 alpha, 25-dihydroxyvitamin D3 and their relation in alveolar macrophages,” *Proc. Natl. Acad. Sci.*, vol. 81, no. 22, pp. 7112–7116, 1984.

[30] S. Christakos, L. Lieben, R. Masuyama, and G. Carmeliet, “Vitamin D endocrine system and the intestine,” *BoneKEy Rep.*, vol. 3, Feb. 2014.

[31] D. Bikle, “Nonclassic Actions of Vitamin D,” *J. Clin. Endocrinol. Metab.*, vol. 94, no. 1, pp. 26–34, Jan. 2009.

[32] R. F. Chun, P. T. Liu, R. L. Modlin, J. S. Adams, and M. Hewison, “Impact of vitamin D on immune function: lessons learned from genome-wide analysis,” *Front. Physiol.*, vol. 5, Apr. 2014.

[33] M. F. Holick, “Vitamin D deficiency,” *N. Engl. J. Med.*, vol. 357, no. 3, pp. 266–281, 2007.

[34] P. T. Liu, M. Schenk, V. P. Walker, P. W. Dempsey, M. Kanchanapoomi, M. Wheelwright, A. Vazirnia, X. Zhang, A. Steinmeyer, U. Zügel, B. W. Hollis, G. Cheng, and R. L. Modlin, “Convergence of IL-1β and VDR Activation Pathways in Human TLR2/1-Induced Antimicrobial Responses,” *PLoS ONE*, vol. 4, no. 6, p. e5810, Jun. 2009.

[35] A. S. Dusso, “Vitamin D,” *AJP Ren. Physiol.*, vol. 289, no. 1, pp. F8–F28, Jul. 2005.

[36] M. L. Cohen, A. Douvdevani, C. Chaimovitz, and S. Shany, “Regulation of TNF-α; by 1α;, 25-dihydroxyvitamin D3 in human macrophages from CAPD patients,” *Kidney Int.*, vol. 59, no. 1, pp. 69–75, 2001.

[37] A. Sonawane, J. C. Santos, B. B. Mishra, P. Jena, C. Progida, O. E. Sorensen, R. Gallo, R. Appelberg, and G. Griffiths, “Cathelicidin is involved in the intracellular killing of mycobacteria in macrophages: The role of cathelicidin in mycobacteria killing,” *Cell. Microbiol.*, vol. 13, no. 10, pp. 1601–1617, Oct. 2011.

[38] A. F. Gombart, “The vitamin D–antimicrobial peptide pathway and its role in protection against infection,” *Future Microbiol.*, vol. 4, no. 9, pp. 1151–1165, Nov. 2009.

[39] Z. Xing, A. Zganiacz, and M. Santosuosso, “Role of IL-12 in macrophage activation during intracellular infection: IL-12 and mycobacteria synergistically release TNF-a and nitric oxide from macrophages via IFN-g induction,” *J. Leukoc. Biol.*, vol. 68, pp. 897–902, 2000.

[40] D. S. Shouval, A. Biswas, J. A. Goettel, K. McCann, E. Conaway, N. S. Redhu, I. D. Mascanfroni, Z. Al Adham, S. Lavoie, M. Ibourk, D. D. Nguyen, J. N. Samsom, J. C. Escher, R. Somech, B. Weiss, R. Beier, L. S. Conklin, C. L. Ebens, F. G. M. S. Santos, A. R. Ferreira, M. Sherlock, A. K. Bhan, W. Müller, J. R. Mora, F. J. Quintana, C. Klein, A. M. Muise, B. H. Horwitz, and S. B. Snapper, “Interleukin-10 Receptor Signaling in Innate Immune Cells Regulates Mucosal Immune Tolerance and Anti-Inflammatory Macrophage Function,” *Immunity*, vol. 40, no. 5, pp. 706–719, May 2014.

[41] K. Moore, R. de Waal Malefyt, R. Coffman, and A. O’Garra, “Interleukin-10 and the interleukin-10 receptor,” *Annu. Rev. Immunol.*, vol. 19, pp. 683–765, 2001.

[42] Z. Bar-Shavit, D. Noff, S. Edelstein, M. Meyer, S. Shibolet, and R. Goldman, “1, 25-dihydroxyvitamin D3 and the regulation of macrophage function,” *Calcif. Tissue Int.*, vol. 33, no. 1, pp. 673–676, 1981.

[43] M. Cohen, D. Mesler, R. Snipes, and T. Gray, “1,25-Dihydroxyvitamin D3 activates secretion of hydrogen peroxide by human monocytes,” vol. 136, no. 3, pp. 1049–53, 1986.

[44] S. Józefowski, A. Sobota, B. Hamasur, A. Pawłowski, and K. Kwiatkowska, “Mycobacterium tuberculosis lipoarabinomannan enhances LPS-induced TNF-α

production and inhibits NO secretion by engaging scavenger receptors," *Microb. Pathog.*, vol. 50, no. 6, pp. 350–359, Jun. 2011.

[45] H. Choi, P. Rai, H. Chu, C. Cool, and E. Chan, "Analysis of nitric oxide synthase and nitrotyrosine expression in human pulmonary tuberculosis," *Am J Respir Crit Care Med*, vol. 166, no. 2, pp. 178–86, Jul. 2002.

[46] S. M. Simet and J. H. Sisson, "Alcohol's Effects on Lung Health and Immunity," *Alcohol Res. Curr. Rev.*, vol. 37, no. 2, pp. 199–208, 2015.

[47] D. Sarkar, M. K. Jung, and H. J. Wang, "Alcohol and the Immune System," *Alcohol Res. Curr. Rev.*, vol. 37, no. 2, pp. 153–155, 2015.

[48] N. B. D'Souza, S. Nelson, W. R. Summer, and I. V. Deaciuc, "Alcohol modulates alveolar macrophage tumor necrosis factor-alpha, superoxide anion, and nitric oxide secretion in the rat," *Alcohol. Clin. Exp. Res.*, vol. 20, no. 1, pp. 156–163, Feb. 1996.

[49] V. B. Antony, S. W. Godbey, J. W. Hott, and S. F. Queener, "Alcohol-induced inhibition of alveolar macrophage oxidant release in vivo and in vitro," *Alcohol. Clin. Exp. Res.*, vol. 17, no. 2, pp. 389–393, Apr. 1993.

[50] E. Porretta, K. I. Happel, X. S. Teng, A. Ramsay, and C. M. Mason, "The Impact of Alcohol on BCG-Induced Immunity Against Mycobacterium tuberculosis," *Alcohol. Clin. Exp. Res.*, vol. 36, no. 2, pp. 310–317, Feb. 2012.

[51] W. R. Waters, M. V. Palmer, B. J. Nonnecke, D. L. Whipple, and R. L. Horst, "Mycobacterium bovis infection of vitamin D-deficient NOS2−/− mice," *Microb. Pathog.*, vol. 36, no. 1, pp. 11–17, Jan. 2004.

[52] K. A. Rockett, R. Brookes, I. Udalova, V. Vidal, A. V. S. Hill, and D. Kwiatkowski, "1,25-Dihydroxyvitamin D3 Induces Nitric Oxide Synthase and Suppresses Growth of Mycobacterium tuberculosis in a Human Macrophage-Like Cell Line," *Infect. Immun.*, vol. 66, no. 11, pp. 5314–5321, Nov. 1998.

[53] X. Deng and R. A. Deitrich, "Ethanol Metabolism and Effects: Nitric Oxide and its Interaction," *Curr. Clin. Pharmacol.*, vol. 2, no. 2, pp. 145–153, May 2007.

[54] N. Toda and K. Ayajiki, "Vascular Actions of Nitric Oxide as Affected by Exposure to Alcohol," *Alcohol Alcohol*, vol. 45, no. 4, pp. 347–355, Jul. 2010.

[55] T. K. Wöbke, B. L. Sorg, and D. Steinhilber, "Vitamin D in inflammatory diseases," *Front. Physiol.*, vol. 5, Jul. 2014.

[56] J. Lemire, "1, 25-Dihydroxyvitamin D3–a hormone with immunomodulatory properties," *Z. Für Rheumatol.*, vol. 59, no. 1, pp. I24–I27, 2000.

[57] J. M. Lemire, D. C. Archer, L. Beck, and H. L. Spiegelberg, "Immunosuppressive actions of 1,25-dihydroxyvitamin D3: preferential inhibition of Th1 functions," *J. Nutr.*, vol. 125, no. 6 Suppl, pp. 1704S-1708S, Jun. 1995.

[58] K. Edfeldt, P. T. Liu, R. Chun, M. Fabri, M. Schenk, M. Wheelwright, C. Keegan, S. R. Krutzik, J. S. Adams, M. Hewison, and R. L. Modlin, "T-cell cytokines differentially control human monocyte antimicrobial responses by regulating vitamin D metabolism," *Proc. Natl. Acad. Sci.*, vol. 107, no. 52, pp. 22593–22598, Dec. 2010.

[59] C. J. Bemiss, B. D. Mahon, A. Henry, V. Weaver, and M. T. Cantorna, "Interleukin-2 is one of the targets of 1,25-dihydroxyvitamin D3 in the immune system," *Arch. Biochem. Biophys.*, vol. 402, no. 2, pp. 249–254, Jun. 2002.

[60] N. Lanzke, R. Kleinwächter, S. Kerschischnik, L. Sargsyan, D. A. Groneberg, T. Kamradt, O. Liesenfeld, V. Krenn, M. Sander, and C. Spies, "Differential effects of ethanol on IFN-gamma- and TNF-alpha-producing splenic T lymphocytes in a murine model of gram-negative pneumonia," *Addict. Biol.*, vol. 12, no. 1, pp. 59–68, Mar. 2007.

[61] G. Szabo, P. Mandrekar, A. Dolganiuc, D. Catalano, and K. Kodys, "Reduced Alloreactive T-Cell Activation After Alcohol Intake is Due to Impaired Monocyte Accessory Cell Function and Correlates With Elevated IL-10, IL-13, and Decreased IFNγ Levels," *Alcohol. Clin. Exp. Res.*, vol. 25, no. 12, pp. 1766–1772, Dec. 2001.

[62] S. Joshi, L.-C. Pantalena, X. K. Liu, S. L. Gaffen, H. Liu, C. Rohowsky-Kochan, K. Ichiyama, A. Yoshimura, L. Steinman, S. Christakos, and S. Youssef, "1,25-Dihydroxyvitamin D3 Ameliorates Th17 Autoimmunity via Transcriptional Modulation of Interleukin-17A," *Mol. Cell. Biol.*, vol. 31, no. 17, pp. 3653–3669, Sep. 2011.

[63] M. Vidyarani, P. Selvaraj, M. S. Jawahar, and P. R. Narayanan, "1, 25 Dihydroxyvitamin D3 modulated cytokine response in pulmonary tuberculosis," *Cytokine*, vol. 40, no. 2, pp. 128–134, Nov. 2007.

[64] M. Di Rosa, M. Malaguarnera, F. Nicoletti, and L. Malaguarnera, "Vitamin D3: a helpful immuno-modulator," *Immunology*, vol. 134, no. 2, pp. 123–139, Oct. 2011.

[65] Z. Urry, E. Xystrakis, D. F. Richards, J. McDonald, Z. Sattar, D. J. Cousins, C. J. Corrigan, E. Hickman, Z. Brown, and C. M. Hawrylowicz, "Ligation of TLR9

induced on human IL-10–secreting Tregs by 1α,25-dihydroxyvitamin D3 abrogates regulatory function," *J. Clin. Invest.*, vol. 119, no. 2, pp. 387–398, Feb. 2009.

[66] K.-H. Tung, Y.-S. Huang, K.-C. Yang, C.-L. Perng, H.-C. Lin, and S.-D. Lee, "Serum Interleukin-12 Levels in Alcoholic Liver Disease," *J. Chin. Med. Assoc.*, vol. 73, no. 2, pp. 67–71, Feb. 2010.

[67] W. F. Rigby, B. J. Hamilton, and M. G. Waugh, "1,25-Dihydroxyvitamin D3 modulates the effects of interleukin 2 independent of IL-2 receptor binding.," *Cell. Immunol.*, vol. 125, no. 2, pp. 396–414, Feb. 1990.

[68] M. Kankova, W. Luini, M. Pedrazzoni, F. Riganti, M. Sironi, B. Bottazzi, A. Mantovani, and A. Vecchi, "Impairment of cytokine production in mice fed a vitamin D3-deficient diet.," *Immunology*, vol. 73, no. 4, pp. 466–471, Aug. 1991.

[69] M. B. Asplund, C. Coelho, R. J. Cordero, and L. R. Martinez, "Alcohol impairs J774.16 macrophage-like cell antimicrobial functions in Acinetobacter baumannii infection," *Virulence*, vol. 4, no. 6, pp. 467–472, Aug. 2013.

[70] W. F. Rigby, T. Stacy, and M. W. Fanger, "Inhibition of T lymphocyte mitogenesis by 1,25-dihydroxyvitamin D3 (calcitriol).," *J. Clin. Invest.*, vol. 74, no. 4, pp. 1451–1455, Oct. 1984.

[71] C. D. Tsoukas, D. M. Provvedini, and S. C. Manolagas, "1,25-dihydroxyvitamin D3: a novel immunoregulatory hormone," *Science*, vol. 224, no. 4656, pp. 1438–1440, Jun. 1984.

[72] G. Saggese, G. Federico, M. Balestri, and A. Toniolo, "Calcitriol inhibits the PHA-induced production of IL-2 and IFN-γ and the proliferation of human peripheral

blood leukocytes while enhancing the surface expression of HLA class II molecules," *J. Endocrinol. Invest.*, vol. 12, no. 5, pp. 329–335, May 1989.

[73] A. K. Bhalla, E. P. Amento, and S. M. Krane, "Differential effects of 1,25-dihydroxyvitamin D3 on human lymphocytes and monocyte/macrophages: inhibition of interleukin-2 and augmentation of interleukin-1 production.," *Cell. Immunol.*, vol. 98, no. 2, pp. 311–322, Apr. 1986.

[74] T. Matsui, R. Takahashi, Y. Nakao, T. Koizumi, Y. Katakami, K. Mihara, T. Sugiyama, and T. Fujita, "1,25-Dihydroxyvitamin D3-regulated Expression of Genes Involved in Human T-Lymphocyte Proliferation and Differentiation," *Cancer Res.*, vol. 46, no. 11, pp. 5827–5831, Nov. 1986.

[75] T. Zhang, C.-J. Guo, S. D. Douglas, D. S. Metzger, C. P. O'Brien, Y. Li, Y.-J. Wang, X. Wang, and W.-Z. Ho, "Alcohol Suppresses IL-2–Induced CC Chemokine Production by Natural Killer Cells," *Alcohol. Clin. Exp. Res.*, vol. 29, no. 9, pp. 1559–1567, Sep. 2005.

[76] M. T. Cantorna, L. Snyder, Y.-D. Lin, and L. Yang, "Vitamin D and 1,25(OH)2D Regulation of T cells," *Nutrients*, vol. 7, no. 4, pp. 3011–3021, Apr. 2015.

[77] S. Yu, J. Zhao, and M. T. Cantorna, "Invariant NKT Cell Defects in Vitamin D Receptor Knockout Mice Prevents Experimental Lung Inflammation," *J. Immunol. Baltim. Md 1950*, vol. 187, no. 9, pp. 4907–4912, Nov. 2011.

[78] A. Waddell, J. Zhao, and M. T. Cantorna, "NKT cells can help mediate the protective effects of 1,25-dihydroxyvitamin D3 in experimental autoimmune encephalomyelitis in mice," *Int. Immunol.*, vol. 27, no. 5, pp. 237–244, May 2015.

[79] T. Barker, T. B. Martins, H. R. Hill, C. R. Kjeldsberg, V. T. Henriksen, B. M. Dixon, E. D. Schneider, A. Dern, and L. K. Weaver, "Different doses of supplemental vitamin D maintain interleukin-5 without altering skeletal muscle strength: a randomized, double-blind, placebo-controlled study in vitamin D sufficient adults," *Nutr. Metab.*, vol. 9, p. 16, Mar. 2012.

[80] F. Santolaria, C. Rodríguez-López, B. Martín-Hernández, M.-R. Alemán-Valls, E. González-Reimers, R. Ros, and J.-J. Viña, "Similar inflammatory response in alcoholic and non-alcoholic sepsis patients," *Eur. Cytokine Netw.*, vol. 22, no. 1, pp. 1–4, 2011.

[81] F. T. Crews, R. Bechara, L. A. Brown, D. M. Guidot, P. Mandrekar, S. Oak, L. Qin, G. Szabo, M. Wheeler, and J. Zou, "Cytokines and Alcohol," *Alcohol. Clin. Exp. Res.*, vol. 30, no. 4, pp. 720–730, Apr. 2006.

[82] M. Inoue, T. Matsui, A. Nishibu, Y. Nihei, K. Iwatsuki, and F. Kaneko, "Regulatory effects of 1alpha,25-dihydroxyvitamin D3 on inflammatory responses in psoriasis.," *Eur. J. Dermatol. EJD*, vol. 8, no. 1, pp. 16–20, 1998.

[83] D. A. Sibley, N. Osna, C. Kusynski, L. Wilkie, and T. R. Jerrells, "Alcohol consumption is associated with alterations in macrophage responses to interferon-gamma and infection by Salmonella typhimurium," *FEMS Immunol. Med. Microbiol.*, vol. 32, no. 1, pp. 73–83, Dec. 2001.

[84] J. Ryynänen and C. Carlberg, "Primary 1,25-Dihydroxyvitamin D3 Response of the Interleukin 8 Gene Cluster in Human Monocyte- and Macrophage-Like Cells," *PLOS ONE*, vol. 8, no. 10, p. e78170, Oct. 2013.

[85] A. M. Manzardo, A. B. Poje, E. C. Penick, and M. G. Butler, “Multiplex Immunoassay of Plasma Cytokine Levels in Men with Alcoholism and the Relationship to Psychiatric Assessments,” *Int. J. Mol. Sci.*, vol. 17, no. 4, Mar. 2016.

[86] S. Arbabi, I. Garcia, G. J. Bauer, and R. V. Maier, “Alcohol (Ethanol) Inhibits IL-8 and TNF: Role of the p38 Pathway,” *J. Immunol.*, vol. 162, no. 12, pp. 7441–7445, Jun. 1999.

[87] C. E. Creeley and J. W. Olney, “Drug-Induced Apoptosis: Mechanism by which Alcohol and Many Other Drugs can Disrupt Brain Development,” *Brain Sci.*, vol. 3, no. 3, pp. 1153–1181, Jul. 2013.

[88] Z. Hmama, “Quantitative analysis of phagolysosome fusion in intact cells: inhibition by mycobacterial lipoarabinomannan and rescue by an 1 ,25-dihydroxyvitamin D3-phosphoinositide 3-kinase pathway,” *J. Cell Sci.*, vol. 117, no. 10, pp. 2131–2140, Mar. 2004.

[89] L. M. Sly, M. Lopez, W. M. Nauseef, and N. E. Reiner, “1 ,25-Dihydroxyvitamin D3-induced Monocyte Antimycobacterial Activity Is Regulated by Phosphatidylinositol 3-Kinase and Mediated by the NADPH-dependent Phagocyte Oxidase,” *J. Biol. Chem.*, vol. 276, no. 38, pp. 35482–35493, Sep. 2001.

[90] O. Ogunsakin, T. Hottor, A. Mehta, M. Lichtveld, and M. McCaskill, “Chronic Ethanol Exposure Effects on Vitamin D Levels Among Subjects with Alcohol Use Disorder,” *Environ. Health Insights*, vol. 10, pp. 191–199, Oct. 2016.

[91] K. E. Mercer, R. A. Wynne, O. P. Lazarenko, C. K. Lumpkin, W. R. Hogue, L. J. Suva, J.-R. Chen, A. Z. Mason, T. M. Badger, and M. J. J. Ronis, “Vitamin D

Supplementation Protects against Bone Loss Associated with Chronic Alcohol Administration in Female Mice," *J. Pharmacol. Exp. Ther.*, vol. 343, no. 2, pp. 401–412, Nov. 2012.

[92] C. M. Leevy and Ş. A. Moroianu, "Nutritional Aspects of Alcoholic Liver Disease," *Clin. Liver Dis.*, vol. 9, no. 1, pp. 67–81, Feb. 2005.

[93] J. C. Kent, R. D. Devlin, D. H. Gutteridge, and R. W. Retallack, "Effect of alcohol on renal vitamin D metabolism in chickens," *Biochem. Biophys. Res. Commun. USA*, 1979.

[94] O. Levy, "Innate immunity of the newborn: basic mechanisms and clinical correlates," *Nat. Rev. Immunol.*, vol. 7, no. 5, pp. 379–390, May 2007.

[95] K.-S. Tsai, H.-L. Chang, S.-T. Chien, K.-L. Chen, K.-H. Chen, M.-H. Mai, and K.-T. Chen, "Childhood Tuberculosis: Epidemiology, Diagnosis, Treatment, and Vaccination," *Pediatr. Neonatol.*, vol. 54, no. 5, pp. 295–302, Oct. 2013.

[96] G. Szabo, "CONSEQUENCES OF ALCOHOL CONSUMPTION ON HOST DEFENCE," *Alcohol Alcohol*, vol. 34, no. 6, pp. 830–841, Nov. 1999.

[97] T. Salim, C. L. Sershen, and E. E. May, "Investigating the Role of TNF-α and IFN-γ Activation on the Dynamics of iNOS Gene Expression in LPS Stimulated Macrophages," *PLOS ONE*, vol. 11, no. 6, p. e0153289, Jun. 2016.

[98] *Matlab version 8.3.0.532. Natick, Massachusetts: The MathWorks Inc., 2014.* .

[99] M. Young, T. Radcliffe, P. St.John, and M. Chatterley, "Normalization Overview," *Improved Outcomes Software*. [Online]. Available: http://www.improvedoutcomes.com/docs/WebSiteDocs/PreProcessing/Normalization/Normalization_Overview.htm. [Accessed: 12-Jul-2016].

[100] D. D'Ambrosio, M. Cippitelli, M. G. Cocciolo, D. Mazzeo, P. Di Lucia, R. Lang, F. Sinigaglia, and P. Panina-Bordignon, "Inhibition of IL-12 production by 1, 25-dihydroxyvitamin D3. Involvement of NF-kappaB downregulation in transcriptional repression of the p40 gene.," *J. Clin. Invest.*, vol. 101, no. 1, p. 252, 1998.

[101] J. M. Matilainen, A. Räsänen, P. Gynther, and S. Väisänen, "The genes encoding cytokines IL-2, IL-10 and IL-12B are primary 1α,25(OH)2D3 target genes," *J. Steroid Biochem. Mol. Biol.*, vol. 121, no. 1–2, pp. 142–145, Jul. 2010.

[102] P. T. Liu, "Toll-Like Receptor Triggering of a Vitamin D-Mediated Human Antimicrobial Response," *Science*, vol. 311, no. 5768, pp. 1770–1773, Mar. 2006.

[103] D. J. Kusner and J. Adams, "ATP-Induced Killing of Virulent Mycobacterium tuberculosis Within Human Macrophages Requires Phospholipase D," *J. Immunol.*, vol. 164, no. 1, pp. 379–388, Jan. 2000.

[104] N. F. Kapasi, R. Ranjan, and E. Izuchukwu, "Ethanol-Induced Macrophage Apoptosis: The," *J Immunol*, vol. 162, pp. 3031–3036, 1999.

[105] J.-M. Chang, M.-C. Kuo, H.-T. Kuo, S.-J. Hwang, J.-C. Tsai, H.-C. Chen, and Y.-H. Lai, "1-α,25-Dihydroxyvitamin D3 regulates inducible nitric oxide synthase messenger RNA expression and nitric oxide release in macrophage-like RAW 264.7 cells," *J. Lab. Clin. Med.*, vol. 143, no. 1, pp. 14–22, Jan. 2004.

[106] J. Alblas, H. Honing, C. Renardel de Lavalette, M. H. Brown, C. D. Dijkstra, and T. K. van den Berg, "Signal Regulatory Protein Ligation Induces Macrophage Nitric Oxide Production through JAK/STAT- and Phosphatidylinositol 3-

Kinase/Rac1/NAPDH Oxidase/H2O2-Dependent Pathways," *Mol. Cell. Biol.*, vol. 25, no. 16, pp. 7181–7192, Aug. 2005.

[107] S. Shimizu, M. Ishii, T. Yamamoto, and K. Momose, "Mechanism of nitric oxide production induced by H2O2 in cultured endothelial cells," *Res. Commun. Mol. Pathol. Pharmacol.*, vol. 95, no. 3, pp. 227–239, Mar. 1997.

[108] M. G. Schwacha and T. K. Eisenstein, "Interleukin-12 is critical for induction of nitric oxide-mediated immunosuppression following vaccination of mice with attenuated Salmonella typhimurium.," *Infect. Immun.*, vol. 65, no. 12, pp. 4897–4903, 1997.

[109] S. Brahmachari and K. Pahan, "Suppression of Regulatory T Cells by IL-12p40 Homodimer via Nitric Oxide," *J. Immunol.*, vol. 183, no. 3, pp. 2045–2058, Aug. 2009.

[110] K. R. B. Bastos, R. Barboza, L. Sardinha, M. Russo, J. M. Alvarez, and M. R. D. Lima, "Role of Endogenous IFN-γ in Macrophage Programming Induced by IL-12 and IL-18," *J. Interferon Cytokine Res.*, vol. 27, no. 5, pp. 399–410, May 2007.

[111] Y. Chen, W. Liu, T. Sun, Y. Huang, Y. Wang, D. K. Deb, D. Yoon, J. Kong, R. Thadhani, and Y. C. Li, "1,25-Dihydroxyvitamin D Promotes Negative Feedback Regulation of TLR Signaling via Targeting MicroRNA-155-SOCS1 in Macrophages," *J. Immunol.*, vol. 190, no. 7, pp. 3687–3695, Apr. 2013.

[112] G. Jones, D. E. Prosser, and M. Kaufmann, "25-Hydroxyvitamin D-24-hydroxylase (CYP24A1): Its important role in the degradation of vitamin D," *Arch. Biochem. Biophys.*, vol. 523, no. 1, pp. 9–18, Jul. 2012.

[113] R. F. Chun, J. S. Adams, and M. Hewison, “Immunomodulation by vitamin D: implications for TB,” *Expert Rev. Clin. Pharmacol.*, vol. 4, no. 5, pp. 583–591, Sep. 2011.

[114] H. Schindler, M. B. Lutz, M. Rollinghoff, and C. Bogdan, “The Production of IFN- by IL-12/IL-18-Activated Macrophages Requires STAT4 Signaling and Is Inhibited by IL-4,” *J. Immunol.*, vol. 166, no. 5, pp. 3075–3082, Mar. 2001.

[115] L. Armstrong, N. Jordan, and A. Millar, “Interleukin 10 (IL-10) regulation of tumour necrosis factor alpha (TNF-alpha) from human alveolar macrophages and peripheral blood monocytes.,” *Thorax*, vol. 51, no. 2, pp. 143–149, 1996.

[116] J. Dagvadorj, Y. Naiki, G. Tumurkhuu, F. Hassan, S. Islam, N. Koide, I. Mori, T. Yoshida, and T. Yokochi, “Interleukin-10 inhibits tumor necrosis factor- production in lipopolysaccharide-stimulated RAW 264.7 cells through reduced MyD88 expression,” *Innate Immun.*, vol. 14, no. 2, pp. 109–115, Apr. 2008.

[117] K. R. Walley, N. W. Lukacs, T. J. Standiford, R. M. Strieter, and S. L. Kunkel, “Balance of inflammatory cytokines related to severity and mortality of murine sepsis.,” *Infect. Immun.*, vol. 64, no. 11, pp. 4733–4738, 1996.

[118] H. Iwasaki, J. Mizoguchi, N. Takada, K. Tai, S. Ikegaya, and T. Ueda, “Correlation between the concentrations of tumor necrosis factor-α and the severity of disease in patients infected with Orientia tsutsugamushi,” *Int. J. Infect. Dis.*, vol. 14, no. 4, pp. e328–e333, Apr. 2010.

[119] A. L. Pukhalsky, G. V. Shmarina, M. S. Bliacher, I. M. Fedorova, A. P. Toptygina, J. J. Fisenko, and V. A. Alioshkin, “Cytokine profile after rubella vaccine

inoculation: evidence of the immunosuppressive effect of vaccination," *Mediators Inflamm.*, vol. 12, no. 4, pp. 203–207, 2003.

[120] G. V. Shmarina, A. L. Pukhalsky, S. N. Kokarovtseva, D. A. Pukhalskaya, L. A. Shabalova, N. I. Kapranov, and N. J. Kashirskaja, "Tumor necrosis factor-α/interleukin-10 balance in normal and cystic fibrosis children," *Mediators Inflamm.*, vol. 10, no. 4, pp. 191–197, 2001.

[121] H. Clay, H. E. Volkman, and L. Ramakrishnan, "Tumor Necrosis Factor Signaling Mediates Resistance to Mycobacteria by Inhibiting Bacterial Growth and Macrophage Death," *Immunity*, vol. 29, no. 2, pp. 283–294, Aug. 2008.

[122] K. Kandasamy, S. S. Mohan, R. Raju, S. Keerthikumar, G. S. S. Kumar, A. K. Venugopal, D. Telikicherla, J. D. Navarro, S. Mathivanan, C. Pecquet, S. K. Gollapudi, S. G. Tattikota, S. Mohan, H. Padhukasahasram, Y. Subbannayya, R. Goel, H. K. Jacob, J. Zhong, R. Sekhar, V. Nanjappa, L. Balakrishnan, R. Subbaiah, Y. Ramachandra, B. A. Rahiman, T. K. Prasad, J.-X. Lin, J. C. Houtman, S. Desiderio, J.-C. Renauld, S. N. Constantinescu, O. Ohara, T. Hirano, M. Kubo, S. Singh, P. Khatri, S. Draghici, G. D. Bader, C. Sander, W. J. Leonard, and A. Pandey, "NetPath: a public resource of curated signal transduction pathways," *Genome Biol.*, vol. 11, no. 1, p. R3, 2010.

[123] "How Does Type 1 Diabetes Develop? | Diabetes." [Online]. Available: http://diabetes.diabetesjournals.org/content/60/5/1370. [Accessed: 13-Oct-2018].

[124] P. Mandrekar, D. Catalano, and G. Szabo, "Alcohol-Induced Regulation of Nuclear Regulatory Factor-Kβ in Human Monocytes," *Alcohol. Clin. Exp. Res.*, vol. 21, no. 6, pp. 988–994, Sep. 1997.

[125] Y. Chen, J. Zhang, X. Ge, J. Du, D. K. Deb, and Y. C. Li, "Vitamin D Receptor Inhibits NF-κB Activation by Interacting with IKKβ Protein," *J. Biol. Chem.*, p. jbc.M113.467670, May 2013.

[126] L. Huang, B. Hu, J. Ni, J. Wu, W. Jiang, C. Chen, L. Yang, Y. Zeng, R. Wan, G. Hu, and X. Wang, "Transcriptional repression of SOCS3 mediated by IL-6/STAT3 signaling via DNMT1 promotes pancreatic cancer growth and metastasis," *J. Exp. Clin. Cancer Res.*, vol. 35, no. 1, p. 27, Feb. 2016.

[127] D. P. Larner, J. S. Adams, and M. Hewison, "Chapter 8 - Regulation of Renal and Extrarenal 1α-Hydroxylase," in *Vitamin D (Fourth Edition)*, D. Feldman, Ed. Academic Press, 2018, pp. 117–137.

[128] K. Ohbo, T. Suda, M. Hashiyama, A. Mantani, M. Ikebe, K. Miyakawa, M. Moriyama, M. Nakamura, M. Katsuki, and K. Takahashi, "Modulation of hematopoiesis in mice with a truncated mutant of the interleukin-2 receptor gamma chain," *Blood*, vol. 87, no. 3, pp. 956–967, 1996.

[129] D. Magaña, G. Aguilar, M. Linares, J. Ayala-Balboa, C. Santacruz, R. Chávez, S. Estrada-Parra, Y. Garfias, R. Lascurain, and M. C. Jiménez-Martínez, "Intracellular IL-4, IL-5, and IFN-γ as the main characteristic of CD4+CD30+ T cells after allergen stimulation in patients with vernal keratoconjunctivitis," *Mol. Vis.*, vol. 21, pp. 443–450, Apr. 2015.

[130] U. Grohmann, M. L. Belladonna, C. Vacca, R. Bianchi, F. Fallarino, C. Orabona, M. C. Fioretti, and P. Puccetti, "Positive Regulatory Role of IL-12 in Macrophages and Modulation by IFN-γ," *J. Immunol.*, vol. 167, no. 1, pp. 221–227, Jul. 2001.

[131] N. Pendás-Franco, Ó. Aguilera, F. Pereira, J. M. González-Sancho, and A. Muñoz, "Vitamin D and Wnt/β-catenin Pathway in Colon Cancer: Role and Regulation of DICKKOPF Genes," *Anticancer Res.*, vol. 28, no. 5A, pp. 2613–2623, Sep. 2008.

[132] M. Babina, M. Krautheim, A. Grützkau, and B. M. Henz, "Human Leukemic (HMC-1) Mast Cells Are Responsive to 1α,25-Dihydroxyvitamin D3: Selective Promotion of ICAM-3 Expression and Constitutive Presence of Vitamin D3 Receptor," *Biochem. Biophys. Res. Commun.*, vol. 273, no. 3, pp. 1104–1110, Jul. 2000.

[133] J. Karavitis, E. L. Murdoch, C. Deburghgraeve, L. Ramirez, and E. J. Kovacs, "Ethanol Suppresses Phagosomal Adhesion Maturation, Rac Activation, and Subsequent Actin Polymerization During FcγR-Mediated Phagocytosis," *Cell. Immunol.*, vol. 274, no. 1–2, pp. 61–71, 2012.

[134] J.-W. Lee and J.-H. Kim, "Activation of the leukotriene B4 receptor 2-reactive oxygen species (BLT2-ROS) cascade following detachment confers anoikis resistance in prostate cancer cells," *J. Biol. Chem.*, vol. 288, no. 42, pp. 30054–30063, Oct. 2013.

[135] S. A. Tersey, E. Bolanis, T. R. Holman, D. J. Maloney, J. L. Nadler, and R. G. Mirmira, "Minireview: 12-Lipoxygenase and Islet β-Cell Dysfunction in Diabetes," *Mol. Endocrinol.*, vol. 29, no. 6, pp. 791–800, Jun. 2015.

[136] A. Linkous and E. Yazlovitskaya, "PLA2G4A (phospholipase A2, group IVA (cytosolic, calcium-dependent))," *Atlas Genet. Cytogenet. Oncol. Haematol.*, no. 10, Nov. 2011.

[137] S. N. Kariuki, J. D. Blischak, S. Nakagome, D. B. Witonsky, and A. Di Rienzo, "Patterns of Transcriptional Response to 1,25-Dihydroxyvitamin D3 and Bacterial Lipopolysaccharide in Primary Human Monocytes," *G3amp58 GenesGenomesGenetics*, vol. 6, no. 5, pp. 1345–1355, May 2016.

[138] X. Zhang and L. P. Zanello, "Vitamin D Receptor–Dependent 1α,25(OH)2 Vitamin D3–Induced Anti-Apoptotic PI3K/AKT Signaling in Osteoblasts," *J. Bone Miner. Res.*, vol. 23, no. 8, pp. 1238–1248, Aug. 2008.

[139] H. Haddad Kashani, E. Seyed Hosseini, H. Nikzad, A. Soleimani, M. Soleimani, M. R. Tamadon, F. Keneshlou, and Z. Asemi, "The Effects of Vitamin D Supplementation on Signaling Pathway of Inflammation and Oxidative Stress in Diabetic Hemodialysis: A Randomized, Double-Blind, Placebo-Controlled Trial," *Front. Pharmacol.*, vol. 9, Feb. 2018.

[140] J. S. L. Yu and W. Cui, "Proliferation, survival and metabolism: the role of PI3K/AKT/mTOR signalling in pluripotency and cell fate determination," *Development*, vol. 143, no. 17, pp. 3050–3060, Sep. 2016.

[141] G. Chan, L. S. Cheung, W. Yang, M. Milyavsky, A. D. Sanders, S. Gu, W. X. Hong, A. X. Liu, X. Wang, M. Barbara, T. Sharma, J. Gavin, J. L. Kutok, N. N. Iscove, K. M. Shannon, J. E. Dick, B. G. Neel, and B. S. Braun, "Essential role for Ptpn11 in survival of hematopoietic stem and progenitor cells," *Blood*, vol. 117, no. 16, pp. 4253–4261, Apr. 2011.

[142] H. Zheng, S. Li, P. Hsu, and C.-K. Qu, "Induction of a Tumor-associated Activating Mutation in Protein Tyrosine Phosphatase Ptpn11 (Shp2) Enhances

Mitochondrial Metabolism, Leading to Oxidative Stress and Senescence," *J. Biol. Chem.*, vol. 288, no. 36, pp. 25727–25738, Sep. 2013.

[143] D. Upadhya, M. Ogata, and L. W. Reneker, "MAPK1 is required for establishing the pattern of cell proliferation and for cell survival during lens development," *Dev. Camb. Engl.*, vol. 140, no. 7, pp. 1573–1582, Apr. 2013.

[144] G. Dewson, G. M. Cohen, and A. J. Wardlaw, "Interleukin-5 inhibits translocation of Bax to the mitochondria, cytochrome c release, and activation of caspases in human eosinophils," *Blood*, vol. 98, no. 7, pp. 2239–2247, Oct. 2001.

[145] L. Cai, H. Wang, and Q. Yang, "CRKL overexpression promotes cell proliferation and inhibits apoptosis in endometrial carcinoma," *Oncol. Lett.*, vol. 13, no. 1, pp. 51–56, Jan. 2017.

[146] W. Hur, H. Rhim, C. K. Jung, J. D. Kim, S. H. Bae, J. W. Jang, J. M. Yang, S.-T. Oh, D. G. Kim, H. J. Wang, S. B. Lee, and S. K. Yoon, "SOX4 overexpression regulates the p53-mediated apoptosis in hepatocellular carcinoma: clinical implication and functional analysis in vitro," *Carcinogenesis*, vol. 31, no. 7, pp. 1298–1307, Jul. 2010.

[147] F. Chen, "MAPK9 (mitogen-activated protein kinase 9)," *Atlas Genet. Cytogenet. Oncol. Haematol.*, no. 2, Feb. 2011.

[148] S. Cagnol and J.-C. Chambard, "ERK and cell death: Mechanisms of ERK-induced cell death – apoptosis, autophagy and senescence," *FEBS J.*, vol. 277, no. 1, pp. 2–21, Jan. 2010.

[149] R. Wisdom, R. S. Johnson, and C. Moore, “c-Jun regulates cell cycle progression and apoptosis by distinct mechanisms,” *EMBO J.*, vol. 18, no. 1, pp. 188–197, Jan. 1999.

[150] B. P. Ingalls, *Mathematical modeling in systems biology: an introduction*. MIT press, 2013.

[151] R. F. Chun, B. E. Peercy, E. S. Orwoll, C. M. Nielson, J. S. Adams, and M. Hewison, “Vitamin D and DBP: The free hormone hypothesis revisited,” *J. Steroid Biochem. Mol. Biol.*, vol. 144, pp. 132–137, Oct. 2014.

[152] R. F. Chun, B. E. Peercy, J. S. Adams, and M. Hewison, “Vitamin D Binding Protein and Monocyte Response to 25-Hydroxyvitamin D and 1,25-Dihydroxyvitamin D: Analysis by Mathematical Modeling,” *PLoS ONE*, vol. 7, no. 1, p. e30773, Jan. 2012.

[153] Y. Chen, W. Liu, T. Sun, Y. Huang, Y. Wang, D. K. Deb, D. Yoon, J. Kong, R. Thadhani, and Y. C. Li, “1,25-Dihydroxyvitamin D Promotes Negative Feedback Regulation of TLR Signaling via Targeting MicroRNA-155-SOCS1 in Macrophages,” *J. Immunol.*, vol. 190, no. 7, pp. 3687–3695, Apr. 2013.

[154] B. Zordoky and A. El-Kadi, “Role of NF-κB in the Regulation of Cytochrome P450 Enzymes,” *Curr. Drug Metab.*, vol. 10, no. 2, pp. 164–178, 2009.

[155] E. A. Shipton and E. E. Shipton, “Vitamin D and Pain: Vitamin D and Its Role in the Aetiology and Maintenance of Chronic Pain States and Associated Comorbidities,” *Pain Res. Treat.*, vol. 2015, pp. 1–12, 2015.

[156] J. Bacchetta, J. J. Zaritsky, J. L. Sea, R. F. Chun, T. S. Lisse, K. Zavala, A. Nayak, K. Wesseling-Perry, M. Westerman, B. W. Hollis, I. B. Salusky, and M. Hewison,

"Suppression of Iron-Regulatory Hepcidin by Vitamin D," *J. Am. Soc. Nephrol.*, vol. 25, no. 3, pp. 564–572, Mar. 2014.

[157] T.-T. Wang, F. P. Nestel, V. Bourdeau, Y. Nagai, Q. Wang, J. Liao, L. Tavera-Mendoza, R. Lin, J. H. Hanrahan, S. Mader, and J. H. White, "Cutting Edge: 1,25-Dihydroxyvitamin D3 Is a Direct Inducer of Antimicrobial Peptide Gene Expression," *J. Immunol.*, vol. 173, no. 5, pp. 2909–2912, Sep. 2004.

[158] J. M. Slauch, "How does the oxidative burst of macrophages kill bacteria? Still an open question," *Mol. Microbiol.*, vol. 80, no. 3, pp. 580–583, May 2011.

[159] J. A. Imlay, "Oxidative Stress," *EcoSal Plus*, vol. 3, no. 2, Sep. 2009.

[160] Y. Groemping and K. Rittinger, "Activation and assembly of the NADPH oxidase: a structural perspective," *Biochem. J.*, vol. 386, no. Pt 3, pp. 401–416, Mar. 2005.

[161] C. C. Winterbourn, M. B. Hampton, J. H. Livesey, and A. J. Kettle, "Modeling the Reactions of Superoxide and Myeloperoxidase in the Neutrophil Phagosome IMPLICATIONS FOR MICROBIAL KILLING," *J. Biol. Chem.*, vol. 281, no. 52, pp. 39860–39869, Dec. 2006.

[162] A. Maeda, Y. Ozaki, S. Sivakumaran, T. Akiyama, H. Urakubo, A. Usami, M. Sato, K. Kaibuchi, and S. Kuroda, "Ca2+-independent phospholipase A2-dependent sustained Rho-kinase activation exhibits all-or-none response," *Genes Cells*, vol. 11, no. 9, pp. 1071–1083, Sep. 2006.

[163] S. Yamada, S. Shiono, A. Joo, and A. Yoshimura, "Control mechanism of JAK/STAT signal transduction pathway," *FEBS Lett.*, vol. 534, no. 1–3, pp. 190–196, Jan. 2003.

[164] G. C. Sharp, H. Ma, P. T. K. Saunders, and J. E. Norman, “A Computational Model of Lipopolysaccharide-Induced Nuclear Factor Kappa B Activation: A Key Signalling Pathway in Infection-Induced Preterm Labour,” *PLoS ONE*, vol. 8, no. 7, p. e70180, Jul. 2013.

[165] R. F. Chun, B. E. Peercy, J. S. Adams, and M. Hewison, “Vitamin D Binding Protein and Monocyte Response to 25-Hydroxyvitamin D and 1,25-Dihydroxyvitamin D: Analysis by Mathematical Modeling,” *PLoS ONE*, vol. 7, no. 1, p. e30773, Jan. 2012.

[166] M. Gough and E. May, “In Silico Model of Vitamin D3Dependent NADPH Oxidase Complex Activation During Mycobacterium Infection,” in *2018 40th Annual International Conference of the IEEE Engineering in Medicine and Biology Society (EMBC)*, 2018, pp. 2382–2385.

[167] R. Milo, P. Jorgensen, and M. Springer, “BioNumbers,” *Nucl. Acids Res.*, no. 38 (suppl 1), pp. D750–D753, 2010.

[168] I. Schomburg, A. Chang, and D. Schomburg, “BRENDA, enzyme data and metabolic information,” *Nucl. Acids Res.*, vol. 30, no. 1, pp. 47–9, 2002.

[169] B. Adams, L. Bauman, W. Bohnhoff, K. Dalbey, M. Ebeida, J. Eddy, M. Eldred, P. Hough, K. Hu, J. Jakeman, L. Swiler, and D. Vigil, *DAKOTA, A Multilevel Parallel Object-Oriented Framework for Design Optimization, Parameter Estimation, Uncertainty Quantification, and Sensitivity Analysis: Version 5.4 User’s Manual*. Sandia Technical Report SAND2010-2183, 2009.

[170] A. Panday, M. K. Sahoo, D. Osorio, and S. Batra, “NADPH oxidases: an overview from structure to innate immunity-associated pathologies,” *Cell. Mol. Immunol.*, vol. 12, no. 1, p. cmi201489, Sep. 2014.

[171] I. Aviram and M. Sharabani, “Kinetics of cell-free activation of neutrophil NADPH oxidase. Effects of neomycin and guanine nucleotides.,” *Biochem. J.*, vol. 261, no. 2, pp. 477–482, Jul. 1989.

[172] M. E. Gough, E. A. Graviss, and E. E. May, “The dynamic immunomodulatory effects of vitamin D_3 during *Mycobacterium* infection,” *Innate Immun.*, vol. 23, no. 6, pp. 506–523, Aug. 2017.

[173] M. E. Gough, E. A. Graviss, T. Chen, E. M. Obasi, and E. E. May, “Compounding Effect of Vitamin D3 Diet, Supplementation, and Alcohol Exposure on Macrophage Response to Mycobacterium Infection,” *Tuberculosis*, Nov. 2018.

[174] N. P. Juffermans, A. Verbon, S. J. van Deventer, W. A. Buurman, H. van Deutekom, P. Speelman, and T. van der Poll, “Serum concentrations of lipopolysaccharide activity-modulating proteins during tuberculosis,” *J. Infect. Dis.*, vol. 178, no. 6, pp. 1839–1842, Dec. 1998.

[175] A. Oeckinghaus and S. Ghosh, “The NF-κB Family of Transcription Factors and Its Regulation,” *Cold Spring Harb. Perspect. Biol.*, vol. 1, no. 4, Oct. 2009.

[176] “SIVABIOCHEM.” [Online]. Available: http://www.sivabio.50webs.com/. [Accessed: 18-Apr-2019].

[177] R. F. Chun, B. E. Peercy, J. S. Adams, and M. Hewison, “Vitamin D Binding Protein and Monocyte Response to 25-Hydroxyvitamin D and 1,25-

Dihydroxyvitamin D: Analysis by Mathematical Modeling," *PLoS ONE*, vol. 7, no. 1, p. e30773, Jan. 2012.

[178] S. Imtiaz, K. D. Shield, M. Roerecke, A. V. Samokhvalov, K. Lönnroth, and J. Rehm, "Alcohol consumption as a risk factor for tuberculosis: meta-analyses and burden of disease," *Eur. Respir. J.*, vol. 50, no. 1, Jul. 2017.

[179] Y. Wang, D. S. Huang, P. T. Giger, and R. R. Watson, "Ethanol-induced modulation of cytokine production by splenocytes during murine retrovirus infection causing murine AIDS," *Alcohol. Clin. Exp. Res.*, vol. 17, no. 5, pp. 1035–1039, Oct. 1993.

[180] Y.-M. Tseng, S.-Y. Chen, C.-H. Chen, Y.-R. Jin, S.-M. Tsai, I.-J. Chen, J.-H. Lee, C.-C. Chiu, and L.-Y. Tsai, "Effects of Alcohol-Induced Human Peripheral Blood Mononuclear Cell (PBMC) Pretreated Whey Protein Concentrate (WPC) on Oxidative Damage," *J. Agric. Food Chem.*, vol. 56, no. 17, pp. 8141–8147, Sep. 2008.

[181] C. M. Mason, E. Dobard, P. Zhang, and S. Nelson, "Alcohol Exacerbates Murine Pulmonary Tuberculosis," *Infect. Immun.*, vol. 72, no. 5, pp. 2556–2563, May 2004.

[182] P. Bifani, S. Moghazeh, B. Shopsin, J. Driscoll, A. Ravikovitch, and B. N. Kreiswirth, "Molecular Characterization of Mycobacterium tuberculosis H37Rv/Ra Variants: Distinguishing the Mycobacterial Laboratory Strain," *J. Clin. Microbiol.*, vol. 38, no. 9, pp. 3200–3204, Sep. 2000.

[183] W. Steenken, W. H. Oatway, and S. A. Petroff, “Biological Studies of the Tubercle Bacillus: Iii. Dissociation and Pathogenicity of the R and S Variants of the Human Tubercle Bacillus (h37),” *J. Exp. Med.*, vol. 60, no. 4, pp. 515–540, Oct. 1934.

[184] W. R. Bishai, A. M. Dannenberg, N. Parrish, R. Ruiz, P. Chen, B. C. Zook, W. Johnson, J. W. Boles, and M. L. M. Pitt, “Virulence of Mycobacterium tuberculosis CDC1551 and H37Rv in Rabbits Evaluated by Lurie’s Pulmonary Tubercle Count Method,” *Infect. Immun.*, vol. 67, no. 9, pp. 4931–4934, Sep. 1999.

[185] S. E. Valway, I. Orme, and H. Westmoreland, “An Outbreak Involving Extensive Transmission of a Virulent Strain of Mycobacterium tuberculosis,” *N. Engl. J. Med.*, p. 7, 1998.

[186] C. Manca, L. Tsenova, C. E. Barry, A. Bergtold, S. Freeman, P. A. J. Haslett, J. M. Musser, V. H. Freedman, and G. Kaplan, “Mycobacterium tuberculosis CDC1551 Induces a More Vigorous Host Response In Vivo and In Vitro, But Is Not More Virulent Than Other Clinical Isolates,” *J. Immunol.*, vol. 162, no. 11, pp. 6740–6746, Jun. 1999.

[187] “BEI Reagent Search.” [Online]. Available: https://www.beiresources.org/Catalog/Bacteria/NR-19025.aspx. [Accessed: 21-Apr-2019].

Appendices

Table 29. In silico reactions

Reaction	Equation
Gqby metabolism	$\frac{d[gqby]}{dt} = 1$
Gqby activated	$\frac{d[gqby_a]}{dt} = k_{100} * [gqby][lam] - k_{101}[gqby_a][plcb]$
Plcb metabolism	$\frac{d[plcb]}{dt} = -k_{101}[gqby_a][plcb]$
Plcb activated	$\frac{d[plcb_a]}{dt} = k_{101}[gqby_a][plcb] - k_{102}[plcb_a][pip2]$
Pip2	$\frac{d[pip2]}{dt} = -k_{102}[plcb_a][pip2] - k_{103}[plcb_a][pip2]$
Ip3	$\frac{d[ip3]}{dt} = k_{102}[plcb_a][pip2] - k_{104}[ip3]$
Dag	$\frac{d[dag]}{dt} = k_{103}[plcb_a][pip2] - k_{105}[ca][dag][pkc]$
Pkc	$\frac{d[pkc]}{dt} = -k_{105}[ca][dag][pkc]$
Mrna_Cyp27b1	$\frac{d[mra_{cyp27b1}]}{dt} = k_{32}[nfkb_p]^{0.5} - k_{33}[mrna_{cyp27b1}]$

Table 30. Kinetic Rates for fully integrated in silico model

Kinetic Rate	
k1	1.00E-05
k2	1.60E-05
k3	1.00E-06
k4	5.28E-06
k5	5.28E-06
k6	1.00E-06
vmax7	3.90E-06
km7	2.70E-05
k8	3.00E-06
k9	1.60E-06
k10	4.00E-06
k11	5.28E-06
k12	5.28E-06
k13	1.00E-06
k14	5.00E-06
k15	1.00E-06
vmax16	1.00E-06
km16	4.00E-06
k17	1.00E-06
k18	1.00E-06
k19	1.00E-06
k019	1.00E-05
k20	1.00E-06
k21	1.00E-06
k22	1.00E-06
k23	3.00E-06
k24	1.00E-06
k25	1.00E-06
km25	1.00E-06
k26	5.00E-06
k27	5.00E-06
k28	2.25E-06
k29	1.85E-06
k30	5.00E-09
k31	2.04E-07
k32	1.70E-06
k33	4.08E-06
k34	1.00E-04

Table 30. continued

k35	1.00E-05
k36	1.00E-05
k38	9.26E-06
k39	9.26E-06
k40	1.00E-06
k41	5.00E-06
vmax42	1.90E-06
km42	1.50E-06
k43	5.00E-06
k100	1.00E-05
k101	2.52E-05
k102	3.00E-06
k103	3.00E-06
k104	2.50E-06
k105	3.50E-06
k106	4.00E-06
k107	1.00E-05
k108	8.20E-06
k109	1.00E-06
k110	1.00E-06
km111	2.00E-06
vmax111	4.00E-06
k112	1.00E-05
km113	1.00E-05
vmax113	2.00E-06
k114	1.00E-06
k115	6.50E-05
k116	1.00E-06
k117	1.00E-06
k118	1.00E-06
k119	1.00E-05
k120	1.00E-05
k121	1.00E-05
k122	3.00E-06
k123	2.00E-06
k124	6.00E-06
k125	3.00E-05
k200	1.00E-06
k201	1.00E-06
k202	1.00E-06

Table 30. continued

k203	1.00E-06
k204	1.00E-06
k205	1.00E-06
k206	1.00E-07
k207	1.70E-06
km207	1.10E-06
k208	1.00E-06
k209	1.00E-06
k210	1.00E-06
k211	1.00E-06
k212	1.00E-07
km212	4.00E-06
k213	1.00E-06
k214	1.00E-05
k215	1.00E-05
k216	1.00E-05
k217	1.00E-06
k218	1.00E-06
km218	4.00E-06
k219	1.00E-06
k220	1.00E-06
k221	1.00E-05
k222	1.00E-06
k223	1.00E-05
km224	4.00E-06
k224	1.00E-06
k225	1.00E-06
k226	1.00E-06
k227	4.00E-06
k228	3.00E-06
k229	1.00E-06
k230	5.10E-06
kts1	100
kts2	50
kts3	20
kts4	20
kts5	40
kts6	200
kts7	5
kts8	8

Table 30. continued

kts9	800
kts10	400
kts11	5
kts12	500
kts13	20
kts14	100
kts15	1
kts16	200
kts17	3
kts18	1
kts19	200
kts20	3
kts21	1
kts22	200
kts23	3
kts24	2.00E-04
kts25	200
kts26	5
kts27	20
kts28	100
kts29	1
kts30	200
kts31	5
kts32	1
kts33	200
kts34	5
kts35	2.00E-04
kts36	200
kts37	50
kts38	10
kts39	400000
kts40	1
kts41	10
kts42	5.00E-01
kts43	5.00E-01
kts44	20
kts45	100
kts46	8
kts47	800
kts48	1

Table 30. continued

kts49	200
kts50	3
kts51	5.00E-01
kts52	1
kts53	200
kts54	8
kts55	800
kts56	1
kts57	200
kts58	3
kts59	5.00E-01
kts60	5.00E-01
kts61	3
kts62	5.00E-01
kts63	20
kts64	100
kts65	20
kts66	100
kts67	20
kts68	100
kts69	20
kts70	20
kts71	100
kts72	50
kts77_1	2500
kts77_1minus	25.1
kts77_2	2.86E-03
kts77_2minus	25.1
kts77_3	2.86
kts77_3minus	25.1
kts80	2.81E-02
kts83	1.05E-02
kts85	16
kts86	7.80E-05
kts87	16
kts89	6.33E-01
kts90	9.00E+00
kts91	1.83E-01
kts92	6.33E-01
kts93	9.00E+00

Table 30. continued

kts94	103830
kts95	590000
kts100	1.60E-02
kts103	1.60E-02
kts104	50
kts105	1.30E+00
kts106	1.60E+00
kts107	50
kts108	1.30E+01
kts109	1.60E+00
kts110	50
kts111	3.40E+00
kts112	10
kts113	1000
kts114	50
kts115	45
kts116	1000
kts117	92
kts118	11
kts119	990
kts120	55
kts121	46
kts122	990
kts123	93
kts125	1.00E-01
kts126	100
kts127	1.00E-08
kts129	0.00185
kts130	12.5
kts131	20.4
kts133	1.00E-08
kts134	8.00E-02
kts135b	30
kts137	10000
kts139	10
kts140	5
kts141	10
kts142	3000
kts143	4000
kts145	10

Table 30. continued

kts146	100
kts147	18.3
kts148	0.35
kts151	100
kts152	100
kts153	100
kts153b	100
ktsiNOS1	22
ktsiNOS2	17
kts154	1
kts155	20
kts156	1
kts157	10
kts158	5.83
kts159	2800000
kts160	86000
kts161	44000000
kts162	171670
kts163	2.00E+08
kts165	1
kts166	4.08
kts167	1.60E-01
kts170	10
kts171	400000
kts172	1
kts173	10
kts77_4	6.47E-03
kts77_4minus	3.65E-01
kts77_5	2.33E-03
kts77_5minus	6.34E+01
kts77_6	4.37E-01
kts77_6minus	4.03E+01
kts79	4.80E-01
kts81	2.82E-01
kts82	7.56E-02
kts84	6.84E-01
kts88	2.08E-01
kts96	3.30E-01
kts97	2.17E+00
kts98	7.40E+00

Table 30. continued

kts99	2.57E-01
kts101	5.64E+00
kts102	2.70E+00
kts124	8.93E-02
kts128	3.96E-01
kts132	2.61E-02
kts135	4.43E+00
kts136	1.94E+03
kts138	1.36E+00
kts144	8.05E-01
kts164	1.47E+01
kts168	1.38E+00
kts169	4.99E+00
kts174	4.60E+00
ktsIirf2	3.64E+05
k231	1.00E+06
k232	1.00E+06
k233	1.00E+06